THE EFFECTS OF PERTURBATION FREQUENCY, MAGNITUDE, AND UNCERTAINTY DURING STATIC AND DYNAMIC TRACKING ON THE ESTIMATED LEVEL OF MUSCLE CO-CONTRACTION

by

Jerry Paul Purswell

Dissertation Submitted to the Faculty of

Virginia Polytechnic Institute and State University

in partial fulfillment of the requirements for the degree of

DOCTOR OF PHILOSOPHY

in

Industrial and Systems Engineering

APPROVED:

Jeffrey C. Woldstad, Co-Chair

John G. Casali, Co-Chair

C. Patrick Koelling

Karl H. E. Kroemer

Daniel J. Schneck

June 1997

Blacksburg, VA

THE EFFECTS OF PERTURBATION FREQUENCY, MAGNITUDE, AND UNCERTAINTY DURING STATIC AND DYNAMIC TRACKING ON THE ESTIMATED LEVEL OF MUSCLE CO-CONTRACTION

by
Jerry Paul Purswell

Co-Chairmen: Dr. Jeffrey C. Woldstad and Dr. John G. Casali
Industrial and Systems Engineering
(ABSTRACT)

Two experiments were performed to investigate the predictability of antagonistic muscle forces during static and dynamic tracking tasks with perturbations. In the first experiment, perturbations to the isometric tracking were effected by sudden momentary changes in the gain. In the second experiment, perturbations to the tracking consisted of momentary changes in the resistance of the lever arm used to track the icons.

In the first experiment with isometric tracking the effects of perturbation frequency, perturbation magnitude, tracking gain, tracking phase and the absence or presence of preview information on the level of antagonistic co-contraction about the elbow were investigated. The effects of these variables on the tracking error were also examined. In the second experiment, the effects of perturbation frequency, perturbation magnitude, tracking phase, and the absence or presence of preview information were

investigated using a dynamic tracking task. Measures of antagonistic co-contraction and tracking error were again computed and used as dependent measures.

Optimization-based biomechanical models have been used by a number of authors to calculate calculate individual muscle forces. The models require that certain lower bounds of the muscle forces be specified. The optimization criteria typically used result in a solution in which the antagonistic muscle forces are at their lower bounds. This lower bound is typically assumed to zero, but could very well be specified at some other nonnegative value.

Two experiments were designed to test whether the level of antagonistic co-contraction varies in a regular predictable way with the factors under study. The aim of the study was to establish a theoretically-derived and experimentally confirmed basis for selecting lower bounds greater than zero for antagonistic muscles.

The two experiments showed that perturbations were effective in impairing tracking performance and subjects evidenced a limited ability to respond to the perturbations by increasing the antagonistic muscle force so that it would minimize the effects perturbations. The study also examined the effects of movement direction, and level of force required on the level of observed antagonistic co-contraction and confirmed the findings of previous authors.

The results of the study do not support different lower bounds for tasks which vary in perturbation frequency, or preview information. The results do indicate significantly different levels of antagonistic activity with tracking gain and direction of exertion in the isometric task. The results also indicate significantly different levels of antagonistic activity with perturbation magnitude in the dynamic tracking task.

DEDICATION

To my wife, Valerie.

ACKNOWLEDGMENTS

This work was made possible by the funds and facilities of the Industrial and Systems Engineering Department at Virginia Tech and specifically, the Industrial Ergonomics Laboratory of the Human Factors Engineering Center. I would like to thank all my committee members for their advice and assistance. I would also like to thank Randy, Jeff, and Bill for their assistance with putting together the apparatus.

I would like to thank all the members of my family whose support and encouragement made the completion of this dissertation possible. Special thanks go to my wife and to my father.

TABLE OF CONTENTS

TABLE OF CONTENTS

(continued)

TABLE OF CONTENTS

(continued)

TABLE OF CONTENTS

(continued)

TABLE OF CONTENTS

(continued)

LIST OF FIGURES

LIST OF TABLES

CHAPTER 1
INTRODUCTION

The Use of Assumptions in Muscle Force Prediction Models

Mathematical modeling of the human body requires many assumptions. In formulating any mathematical model it always wise to identify the assumptions used in formulating the model and if possible, to verify that the assumptions hold. If the assumptions are incorrect, the model will produce false results. The assumptions made in estimating the compression and shear forces between the intervertebral discs of a person holding a symmetric static posture illustrate this problem.

Schulz and Andersson (1981) proposed a cutting plane approach in which the torso is isolated above the L3/L4 intervertebral disc. Figure 1.1 shows a simplified planar model of a person holding a load. Using the principles of statics, any portion of the person may be isolated and a free-body diagram can be used to determine the forces and moments acting on the segment. The cutting plane is also shown in Figure 1.1. A free-body diagram of this posture is shown in Figure 1.2. There are five forces considered in this model. They include the Rectus Abdominus (RA), the Erector Spinae (ES), the compressive reaction force (C), the shear reaction force, and the combined weight of the upper body and the load (G). Distances are indicated by dotted lines. The distance *d1* is the horizontal distance between the center of gravity of the load and upper body to the L3/L4 vertebrae. Distances *d2* and *d3* are the distances between the Erector Spinae and Rectus abdominus respectively to the L3/L4 vertebrae. In this model only the actions of the erector spinae and the rectus abdominus muscles are considered. There are more complex and realistic models of the muscles of the which cross the L3/L4 cutting plane, but

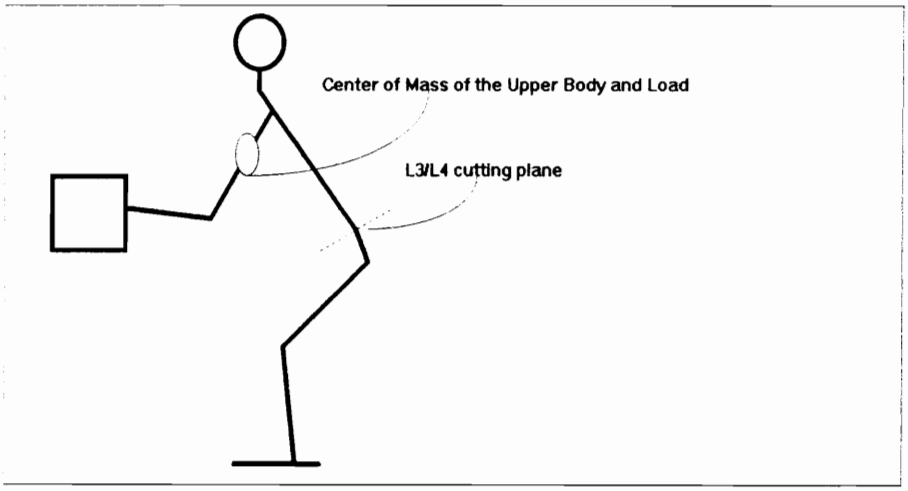

Figure 1.1. Planar analysis of the static posture.

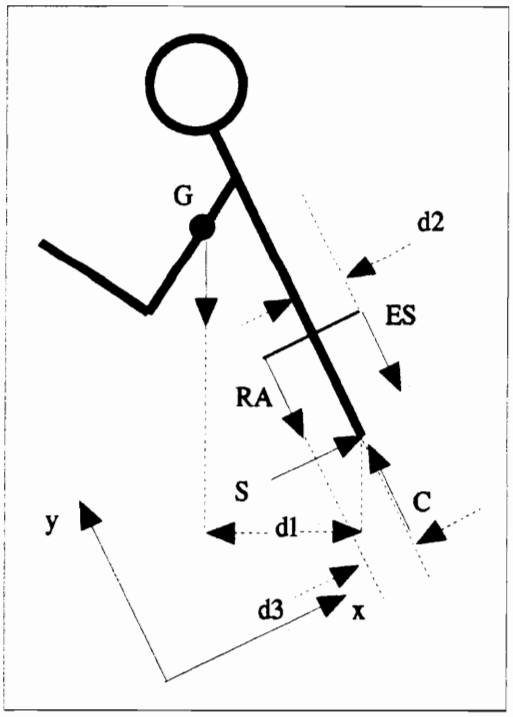

Figure 1.2. Free body diagram of person supporting a load.

the principle concerning predicted levels of antagonistic co-contraction and predicted compression between the L3 and L4 vertebrae is the same.

The lines of action of the rectus abdominus and the erector spinae at the L3/L4 cutting plane are assumed to be parallel to the spine. The modeling process requires that the lines of action be specified in order to calculate forces and moments about the joint. Nussbaum and his co-authors (Nussbaum, Chaffin, and Rechtien, 1995; Nussbaum and Chaffin, 1995) have shown the estimated compression may vary significantly depending on what lines of action are assumed.

Assumptions that have been made in formulating this model include (among others) the following:

1. The lines of actions of the muscles as they cross the cutting plane are known. Though not required, it is often assumed that muscles with several point of attachment can be modeled as a single force with a single line of action.
2. The weights and locations of centers of mass of various body segments are known.
3. It is appropriate to treat the case with rigid body mechanics (i.e., any deformations can be neglected)

It is beyond the scope of this study to examine the validity of each assumption in detail. The point is simply to note that these assumptions are required for several muscle force prediction models (see Bean and Chaffin, 1988 for an example) that have been proposed.

The problem as posed has four unknowns. The unknowns include the force exerted by the erector spinae, the force exerted by the rectus abdominus, and the compression and shear forces between the discs). However, only two independent equations of equilibrium are available for this

planar model. A realistic three-dimensional model would consider the left and right pairs of the rectus abdominus and the erector spinae separately for cases of asymmetric loading. A realistic model of the torso would also include the left and right internal and external oblique muscles and the left and right latissimus dorsi muscles.

The problem as posed is indeterminate but a unique solution can be found by introducing some optimization criterion. Many different optimization criteria have been proposed and evaluated. The general form of the optimization problem is as follows:

Minimize $\Theta(\mathbf{x})$

s.t. 1.1

$$\left\|\mathbf{f}^{i}\right\| \geq \mathbf{L}_i$$

$$\left\|\mathbf{f}^{i}\right\| \leq \mathbf{U}_i$$

The term $\Theta(\mathbf{x})$ is the selected optimization criterion. The term $\mathbf{f}^{i}$ represents the muscle forces multiplied by the appropriate constants. The muscle forces are restricted to be larger than some lower bound and smaller than some upper bound. The solutions identified through the use of optimization models specify the amount of force each muscle is expected to contribute to supporting the load. One method of evaluating the solutions identified by different optimization criteria is the use of electromyographic (EMG) recordings. The EMG levels are measured in a certain posture with no load, and then again in the same posture while holding the load. If the level of activity rises substantially, the muscle is categorized as "on." More precise methods of obtaining a numerical estimate of the force with EMG data are discussed in Appendices A and B, but the EMG recordings can also be used qualitatively to evaluate the predictions obtained by the optimization models.

In one of the first applications of optimization to the solution of muscle forces, Penrod and his co-authors (1974) proposed that the optimal solution

should minimize the total force exerted by all the muscles. The use of this criterion identified the optimal solution as the one in which all the force was generated by the muscles with the longest moment arms. Experimental studies revealed that some of the muscles predicted to be inactive had EMG readings substantially above the baseline levels. Consequently, optimization-based models of muscle and joint forces went through several more refinements. In a more recent article, Bean and Chaffin (1988) suggested that the optimal solution should minimize the maximum muscle stress (estimated muscle force divided by the estimated physiological cross-sectional area of the muscle). This formulation was essentially one which minimized the ratio of predicted muscle force divided by the maximum force that could be generated by that muscle. Hughes (1991) demonstrated that a broad class of optimization-based biomechanical models (including the Bean and Chaffin formulation) cannot predict a phenomenon known as True Antagonism. Different mathematical definitions of antagonistic co-contraction are considered in Chapter 2, but antagonistic co-contraction may be defined as the condition in which one or more muscles oppose the net muscle moment about a joint. Complete definitions of these terms are provided in Chapter 2. This failure to predict antagonistic activity is a serious flaw in biomechanical models, since electromyographic studies consistently demonstrate that at least some antagonistic activity is observed in a variety of tasks.

The failure to predict antagonistic activity may be a result of invalid assumptions used to solve the problem. The use of an optimization criterion requires the following additional assumptions.

1) The body (and specifically the neuromuscular system) behaves in a manner that is optimal.
2) The optimization criterion is known and is reducible to a mathematical expression.

3) The appropriate upper and lower bounds (if any) of the decision variables are known.

The first assumption is certainly reasonable considering that the human body represents millions of years of natural selection and evolution. The validity of second assumption is less certain. Hughes (1991) showed that a broad class of optimization-based force prediction models fail to predict antagonistic co-contraction. It should be noted that other models of human movement do not predict muscle forces. The model of human gait formulated by Beckett and Chang (1968) using a minimum energy criterion is one example of biomechanical model which does not predict muscle forces. These models typically do not address the issue of antagonistic activity because they are cast in terms of net joint torques - not muscle forces. While such models have other uses, it is necessary to estimate the muscle forces in order to calculate compression and shear and shear between joints.

The failure of force-prediction models to predict antagonistic activity may actually be more related to the validity of the third assumption. This third assumption is the focus of this dissertation. The lower bound for muscle force is typically assumed to be constant and fixed at zero. Muscles can only exert force in tension; they cannot push bones apart. Thus, fixing the lower bound at least equal to zero is certainly reasonable. The observation of antagonistic activity suggests that in some circumstances the lower bound should be something greater than zero. This point raises the issue of what the lower bound should be and whether it should change with task characteristics and demands.

This dissertation is an investigation of several factors which may affect the level of antagonistic co-contraction adopted by the body to achieve desired performance. If certain factors can be shown to consistently affect the level of antagonistic co-contraction, then the lower bounds for antagonistic muscle forces can be adjusted accordingly. Several previous articles were reviewed

and a list of factors was developed thought to affect the level of antagonistic co-contraction, including the magnitude and frequency of any environmental perturbations (Hogan 1985a, b, c, d). Hogan (1985c) also predicted a trade-off between the level of antagonistic activity, the error between the commanded and actual position, and the information available to person performing the task. Two tracking tasks were used to examine the effect of several factors on the antagonistic co-contraction and tracking error. Tracking tasks were selected in order to specify a desired position and be able to calculate the position error between the desired and actual position.

Hypotheses Tested

Current optimization-based force-prediction models do not predict true antagonistic co-contraction because the constraints have been incompletely specified. It is hypothesized that some underlying level of antagonistic co-contraction is always present in order for the motor-control system to implement an open-loop disturbance response which assumes the form of an impedance (a force response to a motion input). The level of co-contraction observed should vary in a predictable way with environmental variables which affect the need for joint impedance. A detailed analysis of the factors affecting co-contraction should provide a reasonable mechanical basis for increasing the lower bounds on antagonistic muscle forces. The following hypotheses about the observed level of co-contraction and position error were tested.

1) The level of antagonistic co-contraction increases as the magnitude of the environmental perturbations increases.
2) The level of antagonistic co-contraction increases as the frequency of the environmental perturbations increases.
3) The level of antagonistic co-contraction increases as the information provided about the perturbations decreases.

4) The position error increases as the magnitude of the environmental perturbations increases.
5) The position error increases as the frequency of the environmental perturbations increases.
6) The position error increases as the information provided about the perturbations decreases.

If these hypotheses prove true, the results would provide a first step in specifying the lower bounds on nonbasic variables to be some value greater than zero.[1]

Dissertation Organization

This dissertation is organized into ten chapters. Chapter 2 addresses the "Nonprediction Result" of Hughes (1991) which shows that "true" antagonistic co-contraction (as defined by Hughes) cannot be predicted by optimization models which minimize muscle stresses or spinal compression. Several previous observations of antagonistic activity are then reviewed to indicate what kind of antagonistic activity is observed but not predicted.

The third chapter reviews the arguments that the motor control system modulates joint impedance. It also addresses the idea that this modulation is accomplished via antagonistic co-contraction.

The fourth chapter reviews two previous evaluations of joint impedance or one of its components.

The fifth chapter describes the procedure and methods of the study. The sixth chapter contains the data analysis and results of the isometric study. The seventh chapter contains a discussion of these results.

---

[1] Nonbasic variables are those decision variables which are at either their upper or lower bounds at a particular iteration of the linear programming procedure. Similarly, basic variables are those which are at some intermediate point between their respective upper and lower bounds at a particular iteration.

The eighth chapter contains the data analysis and results of the dynamic tracking study. The ninth chapter contains a discussion of the results. The tenth chapter contains conclusions from these two studies.

Appendix A is devoted to the explanation of how the muscle forces of the biceps and triceps can be accurately estimated for an isometric exertion using electromyographic methods. Appendix B contains the description of how estimates of muscle forces obtained using EMG methods can be adjusted to account for different muscle lengths and shortening velocities.

Appendix C contains the parameter estimates from both tracking studies. Appendix D contains the complete ANOVA summary tables of the experiment. Appendix E contains the informed consent and instructions used for the two experiments.

CHAPTER 2
EMPIRICAL EVALUATIONS OF ANTAGONISTIC CO-CONTRACTION AND THEIR IMPLICATIONS FOR BIOMECHANICAL FORCE PREDICTION MODELS

Introduction

This chapter consists of four sections. A definition of "true" antagonistic co-contraction proposed by Hughes (1991) is reviewed and the "Nonprediction Result" of Hughes is also discussed. In the second section of this chapter, several empirical observations of antagonistic co-contraction are reviewed and some possible explanations for this phenomenon are explored. In the third section, some optimization-based biomechanical models that incorporate antagonistic activity are discussed. In the final section, some theoretically based antagonistic muscle models proposed by Winters are reviewed.

True Antagonism and the Nonprediction Result

The determination of which muscles are agonists and which are antagonists is fairly straightforward in a simple single degree-of-freedom joint. An agonist or prime mover is defined by Gray's Anatomy (1985) as "one or more muscles (which) are constantly active during the initiation and maintenance of a particular movement." The same source defines an antagonist as "one or more muscle or muscles that can wholly oppose such a movement or initiate and maintain its converse." For instance, consider the case of a person assuming a posture in which the upper arm is at the person's side and the forearm is outstretched and supporting a load, as shown in Figure 2.1.

The biceps is the agonist and the triceps is the antagonist in this simple example. However, for a more complex joint such as the L3/L4 intervertebral

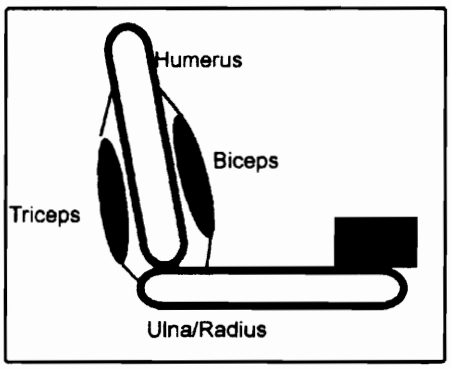

Figure 2.1. Schematic of arm muscles supporting a load.

joint, the determination of which muscles crossing the joint are actually acting as agonists and which are acting as antagonists is less obvious.

There are three possible motions about L3/L4 joint: torso flexion/extension, lateral bending of the torso, and torso rotation. For this three degree-of-freedom (D-0-F) joint, the definition of which muscles are agonist-antagonist pairs depends on the net muscular moment about the joint (i.e., pairs of muscles which may be rightfully designated as agonist-antagonist pairs in flexion/extension may not constitute an agonist-antagonist pair for lateral bending).

Hughes (1991) examined the problem of how to define mathematically antagonistic muscle activity. He noted that "the ability to oppose the action of prime movers is fundamental to the definition of antagonistic muscles." Hughes then critiqued two mathematical statements of antagonism proposed by Andrews and Hay (1983). The component sign definition is to label a muscle as an antagonist for each of three different motions (flexion/extension, abduction/adduction, and rotation) about the L3/L4 joint. According to Andrews and Hay, if the cross product of the unit vector in the line of action of the muscle, τ^i, with the moment arm of the muscle, r^i, dotted with the net moment vector generated by the muscles $\mathbf{M}^M$, about a particular axis is positive, the muscle is designated the agonist. If this product is negative, the muscle is designated the antagonist. The mathematical statement of agonist-antagonist designation is shown for each of the three cases in the following three equations.

$$(\mathbf{r}^i \times \tau^i)_x \cdot \mathbf{M}_x^M \begin{cases} > 0 \Rightarrow \text{flexion / extension agonist} \\ < 0 \Rightarrow \text{flexion / extension antagonist} \end{cases} \qquad 2.1$$

$$(\mathbf{r}^i \times \tau^i)_y \cdot \mathbf{M}_y^M \begin{cases} > 0 \Rightarrow \text{abduction / adduction agonist} \\ < 0 \Rightarrow \text{abduction / adductionantagonist} \end{cases} \qquad 2.2$$

$$(\mathbf{r}^i \times \tau^i)_z \cdot \mathbf{M}_z^M \begin{cases} > 0 \Rightarrow \text{ axial rotation agonist} \\ < 0 \Rightarrow \text{ axial rotation antagonist} \end{cases} \quad 2.3$$

The second definition of antagonistic activity considered by Andrews and Hay (1983) was the Inner Product Definition shown in the following two equations. In this definition the term $\mathbf{M}^M$ is defined as the net muscle moment about the joint rather than the muscle moment about one of the three axes. A muscle is designated an agonist if the following equation holds.

$$(\mathbf{r}^i \times \tau^i) \cdot \mathbf{M}^M > 0 \quad 2.4$$

Alternatively, a muscle is designated an antagonist if the following equation holds true.

$$(\mathbf{r}^i \times \tau^i) \cdot \mathbf{M}^M < 0 \quad 2.5$$

Hughes (1991) argued that a true agonist should be able to generate the opposite of the net muscle moment, $-M^M$. While the inner product definition is better than the component sign in that it considers the net muscle moment, it is does not explicitly incorporate the ability to generate $-M^M$ as a requirement for an antagonist. Consequently, Hughes formulated a new definition of antagonism which explicitly incorporated the ability to oppose the net muscle moment about the joint as the essential characteristic of an antagonist which he termed "true antagonism." True antagonism occurs if there exists at least one active muscle whose contribution to the torque about the joint opposes the net muscle moment. This condition is stated mathematically in equation 2.1. True antagonism occurs if there exists at least one x_i which satisfies the following condition.

$$\sum_{i \in I} (\mathbf{r}^i \times \tau^i) \mathbf{x}^i = -\mathbf{M}^M \qquad 2.6$$

$x_i \geq 0$ for all $i \in I$

where r^j = moment arm of muscle i,
t^i = unit vector in the direction of the line of action of muscle
x_i= tension in muscle i
M^M = net muscle vector generated by muscles.

Hughes also defined a second condition that he termed "equipoise contraction" shown in equation 2.7. Hughes showed that the muscles which satisfy the true antagonism definition necessarily satisfy the conditions for equipoise contraction.

$$\sum_{i=1}^{n} (\mathbf{r}^i + \tau^i)(x_i + v_i) = \mathbf{M}^M \qquad 2.7$$

$x_i + v_i \geq 0 \; \forall \; i = 1,\ldots,n$
$v_i \leq 0 \; \forall \; i = 1,\ldots,n$
$v_k \neq 0$ for at least one k

The terms **r**, τ, and x, are as defined above. The term v_i indicates a slack variable. Thus, equipoise contraction consists in a situation where at least one muscle force can be decreased without violating the moment equilibrium or the nonnegativity constraints and without increasing any other muscle forces. Consider again the case of a person standing with the upper arm at the side and the forearm parallel to the ground with a five kilogram mass in the hand as shown in Figure 2.2. Assume for the sake of simplicity that the only contributions to the net torque about the elbow come from the biceps and the triceps. The person must exert some force with the biceps muscle to resist the torque about the elbow arising from the weight of the load and the forearm. In addition, the biceps must exert enough torque to

overcome any torque applied by the triceps. If the triceps exerts 5 Nm, then the torque exerted by the triceps and the biceps could each be reduced by up to 5 Nm. While static equilibrium is maintained, no muscle forces would required to be less than zero, and no other muscle force would need to be increased. Consequently, this situation would satisfy the conditions of equipoise contraction.

Hughes considered whether a model of the general form shown below could predict equipoise contraction as defined above.

Minimize $\Theta(\mathbf{x})$

s.t. 2.8

$$\left\|\mathbf{f}^{i}\right\| \geq \mathbf{L}_i$$

$$\left\|\mathbf{f}^{i}\right\| \leq \mathbf{U}_i$$

Hughes makes no assumptions about the form of the objective function designated as $\Theta(\mathbf{x})$ except that it be continuous in the neighborhood of **x** so that $\nabla\Theta(\mathbf{x})$ exists. The objective function may be nonlinear or even nonconvex.

The constraints state that muscle forces, f^i, are restricted to be greater than some lower bound and smaller than some upper bound. Several additional constraints may also be incorporated in a model. The constraints may be nonlinear or nonconvex. Regardless of the shape of the feasible solution space, Hughes observed that a necessary condition for an optimum is that $\nabla\Theta(\mathbf{x})$ exists and is strictly positive in all directions. However, by definition, if the condition of equipoise contraction is satisfied, there must be an improving direction (i.e., $x_i + v_i \geq 0$, and $v_i \leqq 0$ with at least one nonzero v_i).

Thus, the point cannot be a local optimum and must therefore not be a global optimum.

Consequently, Hughes observed that the vector of muscle forces, **x,** is not an optimal solution if it in fact satisfies the conditions of equipoise contraction. Further, since the conditions which satisfy Hughes' definition of true antagonism are a subset of those which satisfy equipoise contraction, optimization-based models cannot predict antagonism by this definition.

In summary, a large class of optimization models of the lower back cannot predict "true" antagonism as defined by Hughes. However, certain minimum levels of antagonistic co-contraction in the solution could be ensured by increasing the lower bound on antagonistic muscle forces. This would still not yield solutions which "predict" true antagonism as defined by Hughes, since the solution to the optimization model would necessarily be (at least) a local minimum. However, this approach could be used to ensure that some antagonistic muscle activity is incorporated into the solution.

If this approach were adopted, the problem would be to determine some reasonable estimate of antagonistic muscle activity for the circumstances under study.

Empirical Observations of Antagonistic Co-contraction

Woldstad, Chaffin and Langolf (1988) note that explanations for antagonistic co-contraction can be roughly divided into three categories. Karst et al. (1987) and Marsden et al. (1983) proposed that antagonistic co-contraction facilitates braking of dynamic movements. Smith (1981) and Ghez et al (1987) suggested that co-contraction might occur to facilitate precise control of position. A third explanation is that antagonistic co-contraction occurs in order to modulate the impedance of the joint. By tensing the muscles on both sides of a joint, the body effectively increases the restoring force produced in response to any subsequent imposed motion on the limb.

According to the impedance control explanation for antagonistic muscle activity, the antagonist muscles are tensed *in advance* of any actual perturbation.

Note that these three explanations need not be mutually exclusive. Antagonistic activity may occur for all three reasons concurrently. However, Woldstad et al. (1988) noted while that the first two explanations could account for antagonistic activity with dynamic movements, only the impedance modulation hypothesis could explain antagonistic activity for an isometric task. Thus, several observations of isometric co-contraction are reviewed. Since the experiment proposed for the current study involves a dynamic component, some observations of antagonistic co-contraction under dynamic conditions are also discussed.

Hogan (1984a) performed a simple qualitative experiment designed to test whether more electromyographic activity of an agonist-antagonist pair was observed when the need for impedance was increased. He considered the simple task of maintaining the forearm in an upright position with the elbow supported as shown in Figure 2.2.

If the forearm is perfectly balanced and no perturbations are present, no muscle force would need to be exerted by the biceps or triceps to maintain the arm in this posture. However, in such an arrangement, the forearm is essentially an inverted pendulum and any displacement from the upright position will be quickly amplified in the absence of any restoring force.

Hogan noted that the upright position could be maintained by feedback control, by the incorporation of an impedance response, or by some combination of the two. The term impedance response as used by Hogan is intended to mean a restoring force produced in response to an imposed displacement.

In the simple model used by Hogan, only the biceps and triceps were considered and a large number of simplifying assumptions were made. For instance, the moment arms of the two muscles were assumed equal.

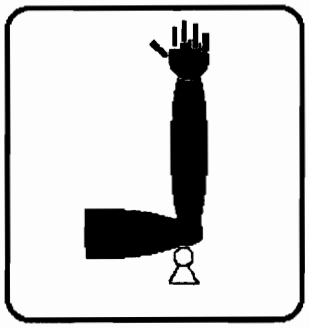

Figure 2.2. Posture of forearm analyzed.

The maximum force and the power consumed by each muscle were also assumed equal. As a consequence of these assumptions, the predictions derived by Hogan are necessarily qualitative in nature. Even so, the analysis is instructive.

Hogan formulated a cost function comprised of the position error and the power consumed by the biceps and the power consumed by the triceps over time as shown in equation 2.9. As a consequence of some simplifying assumptions, the power consumed by the biceps, Pu_b^2, and the power consumed by the triceps, Pu_t^2, were equal in the analysis. The squared position error, θ^2, is weighted by coefficient, Q . The term *u* itself is a dimensionless control input ranging from zero to one.

$$C = \int (Pu_b^2 + Pu_t^2 + Q\theta^2)dt \qquad 2.9$$

If no disturbances are present and the system is initially in balance (θ= 0), then the cost function may be minimized by setting both the power to the biceps and triceps equal to zero. However, if, as in the natural environment, perturbations are present, then the optimal solution determined by Hogan was to involve some contraction of both the biceps and triceps. Specifically, these muscles should contract by an amount proportional to the strength of the perturbations and the moment of inertia of the forearm. The optimal level of activation for both is as follows:

$$u^o = mgl/2K + S/4BK\theta^2_{avg} \qquad 2.10$$

The *mgl* term is the moment-of-inertia, *K* and *B* are the stiffness and viscous components of the impedance, and θ^2_{avg} is the average squared deviation. The term *S* is the mean magnitude of the environmental perturbations. The control input u^o is a dimensionless quantity. The two right-hand side terms are also dimensionless. This result predicts that the motor control system must

trade-off position error and power consumption. It also indicates that as the moment of inertia of the forearm is increased or as the mean strength of the perturbations is increased, the effect is to increase the optimal level of control input, and thereby raise the level of agonist-antagonist co-contraction.

Hogan performed a simple qualitative test of one of these predictions. Specifically, he tested the effect of changing the forearm moment of inertia. He measured the unintegrated EMG of the biceps and triceps in the position described above (forearm upright, elbow supported) with and without the subject holding a five pound mass. Hogan found that the level of (unintegrated) EMG activity in fact increased when the subject held the mass in his hand. Since no attempt was made to calibrate the force-EMG relation, no statement can be made regarding how much the level of antagonistic co-contraction was affected. Even so, this study provides an observation of antagonistic co-contraction. Perhaps more importantly, it predicts that antagonistic co-contraction should increase as the moment of inertia increases or as the strength of environmental perturbations increases.

Woldstad et al. (1988) designed an quantitative test of whether they could obtain antagonistic activity in an isometric test. The experiment they conducted required a subject to track a slow sinusoidal reference signal using an isometric force control. The subject was seated in a chair with the shoulder posture at 90 degrees abduction and zero degrees flexion. The elbow angle was set at approximately 100 degrees. In this posture the subject exerted force on an isometric control at the wrist. The primary flexors of the elbow in this posture are the biceps brachii and the primary extensors are the triceps. The EMG activity of the muscles were monitored during the tracking task. The EMG signals were calibrated in terms of torque using the methods of Redfern (1988) discussed in Appendix A. The authors found significant levels of antagonistic co-contraction in this task. The antagonistic muscle force of the

biceps in the extension phase was 36.6% of the force in the triceps.[1] The antagonistic force of the triceps during the flexion phase was 16.7% of the biceps force. Clearly, substantial levels of force were exerted by the antagonistic muscle during this tracking task.

Redfern (1988) also found substantial levels of co-contraction during isometric tracking of a slow sinusoid with an isometric foot pedal control. Redfern asked subjects to perform an isometric tracking task. The principal muscle exerting torque in dorsiflexion of the ankle is the tibialis anterior. The principal muscles exerting torque in the plantar flexion of the ankle are the soleus and gastrocnemius. Redfern attempted to isolate the contribution of the soleus from the gastrocnemius by the selection of knee and ankle angles that would minimize the moment arm of the gastrocnemius. Using these methods with EMG collection and processing techniques detailed in Appendices A and B, Redfern found that he could predict 99% of the variation in the observed torque from the tibialis and the soleus. Thus, the model used to predict the net torque produced by the two muscles worked quite well. Redfern's model showed that, under the conditions tested, the torque contribution of the (antagonist) soleus during dorsiflexion was about one sixth of that of the tibialis. Consequently, the results of Redfern in this study of isometric tracking also show that significant levels of antagonistic activity are observed which could only be explained by the impedance modulation hypothesis. It is also noteworthy that both studies found higher levels of co-contraction when the net muscle moment was in the extension direction.

A third study in which significant levels of antagonistic co-contraction were found was reported by Rockwell (1992) that extended an earlier tracking

[1]The authors labeled the phase during which the torque applied to the isometric control was acting in the direction of extension as the extension phase, and the phase during which the net torque was acting in the direction of flexion as the flexion phase. It is important to note that although the two alternating phases of the tracking were called the extension and flexion phases, no actual movement of the forearm occurred.

study by Berkowitz (1990). Berkowitz sought to determine the optimum gain (i.e., force-displacement ratio) for a one dimensional zero-order isometric tracking task. Specifically, Berkowitz examined the effect of varying the gain of the isometric control and frequency of the target on the observed error. Berkowitz found that the optimal gain (i.e., the one which minimized tracking error) was one in which approximately 65% of the maximum voluntary contraction was required to obtain the maximum excursion of the controlled object.

Rockwell (1992) extended this work by investigating how the level of force of each muscle varied with tracking parameters. Rockwell again varied the level of force required as a percentage of EMG and the frequency of the sinusoidally varying target. He also considered the effect of gender. Rockwell monitored the absolute tracking error as a proportion of the required force (PE), the absolute antagonist muscle force (AAF), and the ratio of the antagonist to agonist force (co-contraction ratio, CR). The maximum muscle force (MMF) of the biceps and triceps required to track in each condition was also determined. Rockwell confirmed the finding of Berkowitz that the PE ratio increased linearly with frequency while the effect of force required was quadratic in nature. He further confirmed that the minimum PE corresponded to about 66% of the biceps and 65% of the triceps maximum muscle force (MMF). This finding would be expected since the MMF is basically the same measure of muscle strength as the maximum voluntary contraction. Among the important results of this study is the finding that no significant difference was found between levels of absolute co-activity due to required tracking force or frequency of the target. However, the effect of both factors on the co-contraction ratio was significant. Another interesting result is that the CR was higher during decreasing force production than during increasing force production.

These studies documenting the occurrence of antagonistic activity for isometric exertions around the knee, elbow and ankle joint are important because they indicate that it is not appropriate to assume that the lower bound of the antagonist muscle should be fixed at zero. Since each of the instances noted here involved isometric conditions, the co-contraction cannot be due to braking of the movement or to facilitate precise control of the end-point position. Of the three explanations developed by Woldstad and his colleagues for the occurrence of antagonistic activity, the only one which could explain the occurrences noted is the impedance modulation hypothesis.

When optimization models were first employed to find a unique solution to muscle forces crossing a joint (Serig and Avikar, 1973; Penrod, Davy, and Singh, 1974), the theory of reciprocal innervation proposed by Sherrington (1905) was favored among researchers in motor control. This theory held that only one of the agonist/antagonist pair could be active at once. Although there were some dissenting opinions in the matter (Tinley and Pike, 1925; Wachholder and Atenberger, 1926), Sherrington's view that only one of the agonist/antagonist pair could be active at once was generally accepted. Smith (1981) summarized the work of several authors and drew some conclusions about which circumstances favored reciprocal inhibition and which favored antagonistic co-contraction. Smith generalized that reciprocal inhibition was observed with rhythmic motor processes such as locomotion, mastication, respiration, and with low velocity limb movements without load. Antagonistic co-contraction was observed when precise adjustment of muscular tension or limb position without a load was needed. Co-contraction was also favored with higher velocity limb displacements and with the grasping and holding of objects. DeLuca and Mambrito (1987) observed that antagonistic co-contraction was favored in a control task when there was more uncertainty or when the fast compensatory generation of force was needed.

Thus, reciprocal inhibition is sometimes observed and sometimes antagonistic co-activation is observed, depending on the circumstance. The observations of antagonistic co-contraction found in the literature are in line with the explanations by Woldstad et al. (1989). These studies demonstrate that antagonistic co-contraction occurs and is not incorporated into the current formulations of muscle force models. Given the observations of antagonistic activity, it is appropriate to consider how one might predict the level of antagonistic muscle activities depending on the goals of the person, the characteristics of the environment and the task requirements.

Optimization-Based Biomechanical Models which can Predict Antagonistic Activity

Several authors (Hogan, 1985: Hasan, 1986; Winters, 1988) have formulated models of joints in which one or more of the components of a joint impedance are modulated to minimize actual or "virtual" accelerative transients. The ratio of agonist to antagonist force is considered to specify some virtual position to which the unconstrained joint would eventually come to rest. "Virtual" velocity and virtual acceleration are the first and second derivatives of this virtual position. The results of these models are predictions of joint stiffness and viscosity, peak velocity, and peak acceleration. Some level of antagonistic co-contraction is presumed in order to generate the required joint impedance. Thus, while these models incorporate some antagonistic activity, the antagonism is assumed rather than predicted. In addition, these formulations do not yield predictions of muscle forces and consequently, and thus it is not possible to estimate joint compression with these models.

In contrast, Crisco and Punjabi (1990) obtained a prediction of bilateral antagonistic co-contraction by torso models using an approach based on Euler buckling. The authors modeled the spine as a Euler column and examined the

role that co-activation of bilateral muscles might play in increasing the so-called "critical load." The critical load of an Euler column is that load at which a slender column will become unstable and buckle. This critical load level is significantly smaller than the actual failure stress of the material. The critical load may be substantially increased by incorporating balanced support cables acting in tension on the column. Even though these cables have the effect of increasing the force acting downward through the column, the net effect is to raise the critical load. Chapter Eleven in *Mechanics of Materials* by Gere and Timoshenko (1984) discusses slender columns and Euler buckling.

Crisco and Punjabi (1990) investigated the implications of Euler buckling and critical loads in a model of the spine. The authors performed two comparisons of muscle-spine architectures which are illustrated in Figure 2.3, (redrawn from the cited article).

In architecture 1, each vertebrae is fixed to the one immediately below by a pair of muscles. In architecture 2, the stabilizing muscles skip a vertebrae. Crisco and Punjabi stated that the critical muscular stiffness required to stabilize the spine is 70% less in Architecture 2 as compared to Architecture 1. In addition, they note that the efficiency of stabilization increases as the number of vertebrae spanned by the muscles increases. The comparison between architecture 3 and 4 is also instructive. In this comparison, the origin of each of the muscles is the pelvis. However, note that in architecture 4, the L3 vertebra is unconnected to any stabilizing muscles. The authors report that this architecture is unstable regardless of the muscular stiffness. Thus, this work supports the notion that there are in fact valid physical reasons for antagonistic (and specifically bilateral) co-contraction. This work is particularly interesting in that it provides a sound physical reason for the muscles of the torso to co-contract during lifting. It also suggests that as the load is increased, the torso muscles should co-contract more to

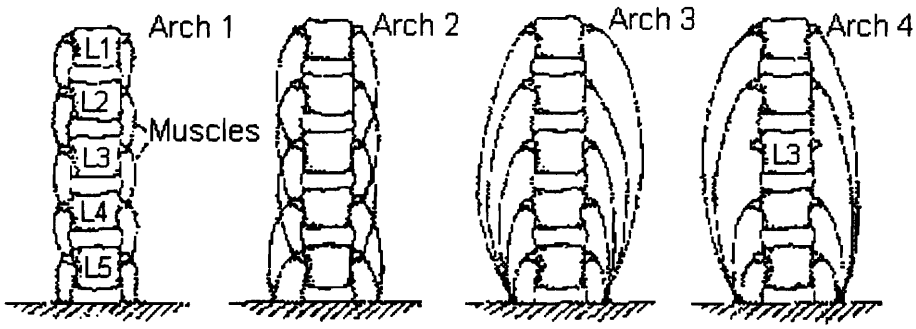

Figure 2.3. The four muscle spine architectures.

increase the amount of compressive force that can be borne before the critical loading of the spine is reached.

There are some limitations to this approach. The spine is not in fact a slender column of uniform composition, but several irregular shaped bones stacked between the softer intervertebral discs. To the extent that the spine behaves as an Euler column, the analysis of Crisco and Punjabi is valid. However, the spine deviates from the required assumptions in two important respects. One problem with this approach is the thickness of the spine. Gere and Timoshenko (1984) state that only extremely slender columns behave elastically, which is a requirement for Euler-like behavior. Thicker columns behave inelastically and consequently have a much smaller critical load. The compressible discs between the vertebrae may make the spine sufficiently elastic to satisfy the assumptions, but no supporting data is presented. A second problem has to do with the natural curvature in the spine. Any initial curvature in the column will result in a departure from Euler-like behavior (Gere and Timoshenko 1984). Again, no consideration of the assumption is made. Thus, while the Euler-based approach arrives at predictions of bilateral co-contraction, it does so with some questionable assumptions. This approach is also limited; while it provides an explanation for co-contraction in the torso, it does not offer any rationale as to why antagonistic activity should be observed in limb movement. The cause may be different, but it would seem appropriate to first look for one explanation that would explain both cases.

Thus, with the exception of Crisco-Punjabi model, optimization-based biomechanical models of the lower back do not predict antagonistic co-contraction. Other models such as those of Hogan (1985d) and Hasan (1986) assume some co-contraction but do not predict it as such. Finally, none of these models consider how the optimal level of co-contraction might be affected by environmental considerations.

The Antagonistic Muscle Models of Winters

Winters and his colleagues (Winters, 1985; Winters and Stark, 1987; Winters, 1988) developed a model of a simple hinge joint that incorporated an eighth-order nonlinear model of two antagonistic muscles about a joint. The model incorporates several important, well-documented muscle properties. These features include the torque-angle relation, the torque-velocity relation, and nonlinear elastic elements in series and in parallel with the contractile elements. The inputs to the model include the empirically determined relations cited above, individual muscle material properties, and anatomical and geometric information, and some hypothesized level of neural input to the two muscles. Unfortunately, few details of this model are available in the open literature. On the basis of his model, Winters (1988) asserts that three conditions must be met in order for the impedance of a joint to be modulated via antagonistic co-contraction. These conditions are listed below.

1. There must be a minimum of two muscles surrounding a joint.
2. There must be an element in series with the contractile element which has a compliance that is not negligible.
3. The series element must be nonlinear with a concave upward shape.

The first condition simply states that there must be an agonist-antagonist pair about the joint. This condition can be verified anatomically for each joint.

The second condition asserts that muscles must behave as if there were an element in series with the contractile element having a characteristic force-displacement relation with a nonzero slope. The final condition simply asserts that the force displacement relation of this element in series with the idealized contractile element must be nonlinear with a concave upward shape.

The nonlinear, concave-upward compliance relation for the elastic element in series with the contractile element could presumably be verified experimentally. However, such a study would show only that impedance modulation via antagonistic co-contraction was possible with the Winters model. It would not provide a rational basis for predicting the antagonistic activity in terms of environmentally observable factors. Thus, while the work of Winters and his colleagues is of some theoretical importance, it does not appear to be helpful in answering the question of why antagonistic muscles co-contract under certain circumstances and how one might go about determining how much co-contraction one might expect. These considerations are addressed in the following chapter.

Summary

Popular optimization-based force prediction models can not predict equipoise contraction. The set of conditions which satisfy true co-contraction is a subset of those which satisfy equipoise contraction. Consequently these models cannot predict true antagonistic co-contraction. Valid empirical observations of co-contraction were shown to exist. Models can predict true antagonism albeit with different optimization criteria.

CHAPTER 3
IMPEDANCE CONTROL CONCEPTS AND THEIR IMPLICATIONS FOR OPTIMIZATION-BASED MUSCLE FORCE PREDICTION MODELS

Introduction

This chapter presents the theoretical background developed by Hogan (1985a, b, c) for the implementation of an open-loop impedance control strategy. Definitions and distinctions of what constitutes an impedance and what constitutes an admittance are discussed. The reasons underlying the use of impedance control rather than admittance control are also addressed. An overview of an open-loop impedance control law developed by Hogan (1985b) is presented. The following section consists of a discussion of how an optimal impedance for a given set of circumstances might be selected. The implications of impedance modulation for the trade-off between energy expenditure and position error are revisited in more detail. The role that information about environmental perturbations might play is also considered. Finally, an idea proposed by Hogan (1985b, d) is noted which suggest that "redundant" muscles may not actually be redundant because they are needed by the motor-control system to independently modulate torque and the end-point impedance.

Introductory Concepts and Definitions

An impedance is a transfer function which relates an output "effort" variable such as force or voltage to an input "flow" variable such as velocity or amperage (Karnopp and Rosenberg, 1975). An admittance is the inverse relationship; that is, the "flow" variable is considered to be the input, while the effort variable is output. Although the concept of impedance is used in several

fields, the term will be used here to mean specifically mechanical impedance, i.e., the relationship between an imposed motion and the resulting force.

A few examples of mechanical impedances and admittances help to clarify what these two transfer functions are and how they differ. The impedance of a spring relates a displacement to a force. The impedance of a viscous element relates a force to a velocity. In both cases, causality requires that the fundamental relationship be written with the motion as the input and force as the output. The force-displacement relationship for a linear spring can be written with either force or motion as the input and the remaining quantity can be computed. As Hogan (1985a) points out, the force-displacement relation of a spring need not be linear, continuous, or even monotonic. Examples of these characteristics are discussed below.

Figures 3.1 through 3.3 illustrate several possible relationships between force and displacement for springs. In Figure 3.1, the relation for a simple linear spring described by the equation $F = 6x-4$ is shown.

A unit displacement in either direction results in the same change in the force regardless of the starting displacement. A displacement twice the size of another results in exactly twice the force. Given the spring constant (i.e., the slope) and either the force or the displacement, one can compute the remaining quantity.

Figure 3.2 shows the relation for a nonlinear but monotonic spring described by the equation $F = .07 x^3-1.4 x^2+10x+15$. The force and the displacement are related not by a single constant, but by a relation which must be known over the region of interest. However, if this relation and either the force or the displacement are known, then the remaining quantity can still be computed. Figure 3.3. shows a nonlinear, nonmonotonic spring described by the equation $F = .09 x^3 -1.4 x^2 + 5x + 25$. Note that while a particular

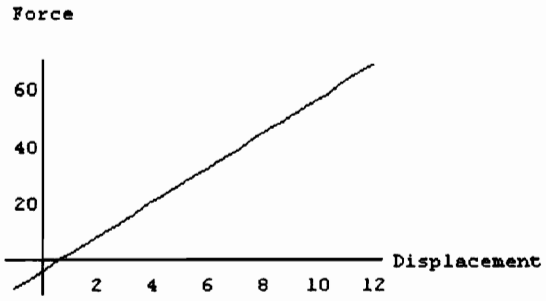

Figure 3.1. Force-displacement relation for a linear spring.

Figure 3.2. Force-displacement relation for a nonlinear monotonic spring.

Figure 3.3. Force-displacement relation for a nonlinear nonmonotonic spring.

displacement determines a unique force, the converse does not hold; however, zero force defines a unique position.

Thus, the relationship for a nonmonotonic spring can only be written with the displacement as the input. Knowledge of the force exerted by a spring does not in general uniquely determine a displacement. Similar arguments hold for a viscous element. The relationship between a force and an imposed motion for spring and damper elements must also be written as impedances.

On the other hand, the force-motion relationship of an inertial element is fundamentally an admittance (i.e., the applied force causes the element to accelerate or decelerate).

Open-Loop Impedance Control

The concepts of impedance control are important for biomechanical modeling because these concepts have implications for the formulations of the constraints used in biomechanical models. Hogan (1985a) observed that control of a single vector quantity such as the position of a general manipulator or the force exerted by it is insufficient for a manipulator which must exchange work with its environment. The manipulator is no longer an isolated system; any control strategy must account for the fact that mechanical work is exchanged.

This observation holds true regardless of whether the exchange of work is required by the nature of the task or is due to unpredictable perturbations. Regardless of whether the environment exerts a force which displaces the manipulator or vice versa, if work is exchanged at the manipulator-environment interface (i.e., $\mathbf{F} \bullet d\mathbf{x} \neq 0$), then a disturbance response is needed.[1]

---

[1] An illustration involving the control of a robot manipulator by Hogan (1985a) is helpful in understanding why this is true. The most common use of robots in industry is restricted to situations in which the interaction forces between the robot and its environment are zero or negligible. Cases such as spray-painting and welding are good examples of situations in which robots which apply either zero or negligible force on the environment. No work is

This disturbance response could be implemented simply as a feedback control response. When sensors on the manipulator indicated that the manipulator had been displaced, the information could be relayed to the manipulator controller and it could implement a correction. This is the principle upon which a direct current electric motor with position control is based. However, for humans as well as for robot manipulators, a feedback control strategy necessarily involves a transmission delay between the disturbance and the onset of the response. Hogan (1985b) noted that humans excel at fine motor tasks that involve the exchange of work with the environment. At the same time he pointed out that time delays of up to 250 milliseconds for reflex loops are common. Taken together, these observations suggest some open-loop form of a disturbance response is used for the control of human movement.

Of course, the use of some form of open-loop control does not preclude the incorporation of some feedback-based control strategies employed in parallel. The stretch reflex is a clear example of feedback control of movement. When the muscle is stretched, γ motoneurons respond and send signals which are sensed and generate some degree of muscle contraction. In addition, Marsden, Merton, and Morton (1972) documented that the effective gain of the stretch reflex can be adjusted by setting the γ motoneurons in the

---

exchanged between the manipulator and its environment because no force is applied on or by the manipulator.

A second class of robot applications involves situations in which the forces between the robot and its environment are nonzero, but no work is done. The direction of motion and the direction of force are orthogonal, so the dot product of force with displacement is still zero. In neither of these two cases is the manipulator displaced from its position and consequently no disturbance response is needed.

The most general class of robot applications is that in which the dot product of the force and the motion is not zero. Work is done on or by the manipulator and power (work per unit time) flows from the manipulator to the environment or vice versa. Because the manipulator may be displaced from the desired position due to the exchange of work with the environment, a disturbance response is needed for the manipulator. Hogan cites several examples of manufacturing processes in which such a disturbance response is required, including "drilling, reaming, routing, counterboring, grinding, bending, chipping and fettling."

muscle. Thus, the use feedback loops in motor control is well documented. However, the use of feedback loops does not preclude other forms of control also being used which are effectively open-loop. Control of a manipulator's impedance provides a means of implementing an open-loop control strategy for the manipulator. If the manipulator is provided with certain stiffness and viscous characteristics, then the response is immediate and no feedback response is needed. The springs and shock absorbers of a car are a simple example of this type of impedance control. The springs and shocks are stretched or shortened by the vertical displacement of the tires. In response, these elements exert force to damp out the vertical motion. No feedback control is required because the force produced by these elements in response to the imposed motion is inherent in the nature of the elements.

A second important observation made by Hogan was that the open-loop disturbance response of the manipulator must assume the form of an impedance rather than an admittance (i.e., a motion input to the manipulator and a force output from it rather than vice versa). Either a motion or a force could serve as the input to the transfer function. However, Hogan noted that implementation of the disturbance response as an admittance would require that the manipulator displace an object in response to an imposed force. In contrast, impedance control requires only that the manipulator exert a force on the object in response to an imposed displacement of the manipulator. The difference may seem trivial, but Hogan pointed out that while the manipulator can always impress a force upon some object in the environment, it is not generally true that the manipulator could displace it. Consequently, the disturbance response for the manipulator should take the form of an impedance.

From the perspective of the environment, physical systems come in only two forms. They are either impedances or admittances. If power flows between two physical systems, one must be an impedance and one must be

an admittance. An interesting consequence of this observation is that if the manipulator is considered to be an impedance, the environment must be an admittance. Hogan (1985a) noted that one could consider the manipulator and the environment to be two separate physical systems. One can then analyze the power flows between these two systems using standard solution approaches such as Norton and Thevenin networks. The power flows are described by conjugate variables between the two systems such as force and velocity. The product of the two conjugate variables has units of power. Secondly, each of the two physical systems can determine only one of the two conjugate variables. The remaining variable is determined by the second system. For instance, one can push against an object with a certain force, but the resulting motion of the object is determined by the characteristics of the object itself. Alternatively, one can attempt to impose a certain motion on an object, but then the force required is determined by the physical characteristics of the object.

Using Norton and Thevenin networks, Hogan (1985a) showed that if one can assume that a manipulator controller is capable of determining an equilibrium position of an unconstrained inertial object, then certain desirable control properties are preserved. The controller must be able to determine a "virtual" position that would correspond to any given set of interface forces. This virtual position need not lie within the actual workspace of the manipulator. At this virtual position, there is zero power flow between the manipulator and its environment. The differential equation which relates the port variables under these conditions is the impedance or the admittance. Thus, the use of a virtual position is simply a convenient fiction which allows one to write the relationship between motions imposed upon the manipulator and restoring force which is produced in response as an impedance (hence the name impedance control).

A central difficulty in determining how to specify the force produced in response to an imposed motion is that the overall response may be composed of several possibly nonlinear elements. However, in Hogan's analysis, there is only a single port across which work is exchanged. In such a case, the environmental admittance sums all the forces applied to it and determines a motion in response. Mathematically, the environmental admittance sums all the impedances applied to the admittance in a linear fashion regardless of whether the individual elements are linear in nature.

A second assumption required in Hogan's analysis is that zero force at the interface must define a unique position. This assumption is needed to provide a reference point for the controller from which to judge the location in space where the virtual position lies. All other positions are stated relative to this position.

Figure 3.4 shows the same curve plotted in Figure 3.3, but shifted downward slightly. Note that zero force does not define a unique position.

While both figures show a nonlinear, nonmonotonic relation between force and displacement, the relation shown in Figure 3.4 does not define a unique position for zero force.

This point leads to the third assumption required, that it is sufficient to consider only the "nodic" components of the impedance and to disregard the non-nodic components. According to Hogan (1985a), "Nodicity refers to the invariance of the constitutive equation of an element under a change in the reference value (origin) of its argument." Stated another way, nodicity means that regardless of where the manipulator is located in the workspace, the amount of force produced in response to a particular imposed motion is the same. This is so commonly true that it is somewhat difficult to think of exceptions. For instance, in the case of a spring element, the force produced depends only on the change in the length of the spring. The location of the spring in relation to some absolute reference frame is immaterial to the force

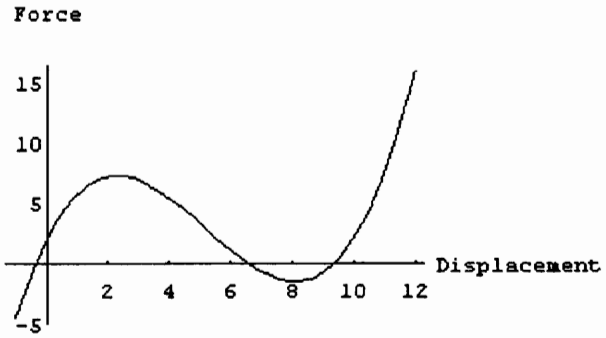

Figure 3.4. Force-displacement relation for a nonlinear nonmonotonic spring where zero force does not define a unique position.

produced. The same holds true for a viscous element. The force produced depends only on the imposed velocity. Again, the location of the element in some absolute reference frame is of no relevance.

One example of a situation in which the non-nodic component would be important is a nonmobile manipulator operating at the boundaries of its workspace. If one displaces the manipulator beyond the workspace boundary, thereby causing physical damage to it, one could certainly not expect the manipulator to generate the expected restoring force.

There had evidently been some considerable degree of confusion regarding the distinction between admittance and impedance prior to the publication of this series of papers by Hogan. According to Hogan (1985b), impedance and admittance are in fact interchangeable representations *only* for linear systems operating at finite frequencies. Researchers in both the areas of human motor control and robot control had treated the problem as if there were no distinction between implementing a disturbance response as an impedance or an admittance (Weineke and van der Gon, 1973, Lacquaniti et al. 1982). However, Hogan noted that manipulation is fundamentally a nonlinear problem and hence the distinction between impedance and admittance does matter. Consequently, the correct formulation of a control law is critical to a successful control strategy.

The implication of these observations about impedance and admittance control for biomechanical models is that the human motor control system seems to implement some sort of open-loop disturbance response. A second observation is that this disturbance response must be implemented as an impedance rather than an admittance. Finally, the impedance should be tunable in order to explain how the human motor control system seems to adapt to a wide variety of situations. In the section that follows, an overview of a general impedance control law derived by Hogan (1985b) is presented.

Development of a General Impedance Control Law

Hogan (1985b) adopted a very general approach to the development of an impedance-based control law. He attempted to develop a framework within which a control system could implement an open-loop for a manipulator. His analysis is based upon the result noted in the previous section that the individual impedances at the point of contact are summed by the environmental admittance, even if the individual elements are nonlinear in nature.

Hogan began by considering the lowest order term of an impedance, the stiffness. The relationship between the restoring force and the imposed displacement (which need not be linear or even continuous) is described by equation 3.1. Thus, the *K* term is intended to represent the force displacement relation and not necessarily a single ratio. The Jacobian (Eq 3.2) describes the relationship between the displacement of the end-point and the angular displacement of the actuator. Note that the position of the endpoint (for instance the hand) can be expressed in terms of the angular positions of the more proximal links as shown in equation 3.3 (e.g., the elbow angle). Hogan used the principle of virtual work as shown in equation 3.4 to describe the restoring forces to be generated at the interface (e.g., the hand) in terms of actuator torques (e.g., the triceps and biceps). Finally, by simple substitution, Hogan related the imposed displacement to the actuator torques to be produced in response. Notice that the response to the imposed displacement is entirely open-loop in that the restoring force is generated by the relative spring settings of the two actuators and not by feedback control.

$$\mathbf{F}_{int} = K(\mathbf{X}_0 - \mathbf{X}) \qquad 3.1$$

$$d\mathbf{X} = \mathbf{J}(\theta)d\theta \qquad 3.2$$

$$\mathbf{X} = L(\theta). \qquad 3.3.$$

$$\mathbf{T}_{act} = \mathbf{J}_t(\theta)\,\mathbf{F}_{int} \qquad 3.4$$

$$\mathbf{T}_{act} = \mathbf{J}(\theta)K(\mathbf{X}_0 - L(\theta)) \qquad 3.5$$

The term $\mathbf{F}_{int}$ is the vector of interface forces to be exerted by the manipulator; $\mathbf{X}_0$ is the commanded end-point position and $\mathbf{X}$ is the actual end point position. The term $\mathbf{T}_{act}$ refers to the actuator torques and $\mathbf{J}(\theta)$ is the Jacobian.

Hogan proceeded to show a very similar derivation of the implementation of impedance control for the next higher order term of the impedance, the viscous term. The equations relating an imposed velocity on the force produced follow. Note again that the viscosity need not be linear or monotonic.

$$\mathbf{F}_{int} = B(\mathbf{V}_0 - \mathbf{V}) \quad 3.6$$

$$\mathbf{V} = \mathbf{J}(\theta)\omega \quad 3.7$$

$$\mathbf{X} = L(\theta). \quad 3.8$$

$$\mathbf{T}_{act} = \mathbf{J}_t(\theta)\,\mathbf{B}_{int} \quad 3.9$$

$$\mathbf{T}_{act} = \mathbf{J}^t(\theta)B(\mathbf{V}_0 - \mathbf{J}(\theta)\omega) \quad 3.10$$

Because the environmental admittance sums all the impedances applied to it, the interface forces arising from these two impedances sources can simply be summed.

This accounts for the dynamics of the manipulator arising from stiffness and viscous effects. However, the manipulator itself has mass and thus the inertial dynamics must be considered. Hogan (1985b) devised an analysis approach whereby the nonlinear, configuration-dependent inertia of the manipulator is lumped with environmental admittance. Thus, the apparent inertia seen by the manipulator at the end-effector is assumed to be that of a rigid body whose inertia tensor is invariant under translation. This inertia tensor of such a rigid body, designated M, is shown in equation 3.11.

$$M = \begin{bmatrix} m & 0 & 0 & 0 & 0 & 0 \\ 0 & m & 0 & 0 & 0 & 0 \\ 0 & 0 & m & 0 & 0 & 0 \\ 0 & 0 & 0 & I & 0 & 0 \\ 0 & 0 & 0 & 0 & I & 0 \\ 0 & 0 & 0 & 0 & 0 & I \end{bmatrix} \qquad 3.11$$

Thus, the interface forces may be expressed as follows.

$$\mathbf{F}_{int} = F(\mathbf{X},\mathbf{V}) - M d\mathbf{V}/dt \qquad 3.12$$
$$\mathbf{F}_{int} = F(\mathbf{X}_0-\mathbf{X},\mathbf{V}_0-\mathbf{V}) - M d\mathbf{V}/dt \qquad 3.13$$
$$\mathbf{F}_{int} = K[\mathbf{X}_0-\mathbf{X}] + B[\mathbf{V}_0-\mathbf{V}] - M d\mathbf{V}/dt \qquad 3.14$$

Now if the environment can be considered to be a simple rigid body acted upon by unpredictable forces, then it has only inertial characteristics and Newton's Second Law holds ($\Sigma\mathbf{F} = m\mathbf{a}$).

$$\mathbf{M}_{env} (d\mathbf{V}/dt) = \mathbf{F}_{int} + \mathbf{F}_{ext} \qquad 3.15$$

As Hogan notes, the manipulator and the environment are coupled, so that $\mathbf{F}_{int}$ term equation 3.14 may be replaced by the difference of the two terms, $\mathbf{M}_{env} (d\mathbf{V}/dt) - \mathbf{F}_{ext}$. Hence, we have the following result.

$$(\mathbf{M}_{env} + M) (d\mathbf{V}/dt) = K[\mathbf{X}_0-\mathbf{X}] + B[\mathbf{V}_0-\mathbf{V}] + \mathbf{F}_{ext} \qquad 3.16$$

After several more lines of algebraic manipulation and substitution (the reader is referred to appendix I of the cited article), Hogan arrived at the expression for the torques required of the manipulator actuator shown below. The terms $S(\theta)$, $V(\omega)$, $G(\theta,\omega)$, and $C(\theta,\omega)$ represent the position and velocity

dependent torques respectively. The terms $G(\theta,\omega)$, and $C(\theta,\omega)$ represent the accelerative and inertial coupling terms respectively. All other terms have been previously defined.

$$\begin{aligned}\mathbf{T}_{act} = {} & I(\theta)\,\mathbf{J}^{-1}(\theta)\mathbf{M}^{-1}\,K[\mathbf{X}_0-\mathbf{X}] + S(\theta) + \\ & I(\theta)\,\mathbf{J}^{-1}(\theta)\mathbf{M}^{-1}\,B[\mathbf{V}_0-\mathbf{V}] + V(\omega) + \\ & I(\theta)\,\mathbf{J}^{-1}(\theta)\mathbf{M}^{-1}\,\mathbf{F}_{int} - \mathbf{J}^{-1}(\theta)\,\mathbf{F}_{int} + \\ & I(\theta)\,\mathbf{J}^{-1}(\theta)\,G(\theta,\omega) + C(\theta,\omega). \end{aligned} \qquad 3.17$$

The point of all this algebra is simply to demonstrate that it is possible to formulate a control law capable of modulating the end-point impedance of the manipulator. The stiffness and viscosity of the manipulator can be varied to produce different amounts of actuator torque in response to an imposed motion.

The Choice of an Optimal Impedance

In the third paper of the series, Hogan (1985c) considered how a controller might choose an impedance appropriate for a given task. In biological systems, there is some energy cost incurred to maintain a given stiffness and viscosity about a joint by muscular contraction. For instance, in order to stiffen the elbow joint (i.e. raise the joint impedance), one must co-contract the triceps and biceps. On the other hand, sustaining a muscular exertion incurs a metabolic cost. Thus, there are competing costs to be balanced. Hogan (1985c) performed an analysis which suggested that an optimal controller should be able to trade off energy costs and end-point position error given some weighting of the two costs. An additional wrinkle revealed by his analysis was that the manipulator might be able to trade off information about the environment with these other two costs. That is, greater uncertainty about potential environmental perturbations to the task would

necessitate the maintenance of a higher impedance. These results are discussed in this section.

The control of a general manipulator such as the human hand requires a disturbance response for all available degrees of freedom. Consequently, a completely general control law would specify a restoring force for any translational or rotational motion that is imposed, i.e., the problem involves six degrees of freedom. Hogan noted that the six degree-of-freedom problem could be decomposed into six one-degree-of-freedom problems if the stiffness and viscosity tensors were assumed to be symmetric and if the eigenvectors of these tensors were assumed to be collinear with the inertia tensor.[2] Hogan then considered the problem of maintaining a stable position of the manipulator end-point in the presence of environmental perturbations. He assumed that the magnitude of perturbations would be normally distributed with a mean of zero and an unspecified magnitude, *S*. Since the original six degree of freedom problem has been decomposed in six one dimensional problems, the direction of the disturbance is limited to one degree of freedom. Hogan formulated a cost function, *Q*, that consisted of the integral with respect to time of a force term and a position error term, shown in equation 3.18.

$$\text{Minimize } Q = \int_0^\infty \{(F / F_{tol})^2 + [(X_0 - X) / X_{tol}]^2\} dt \qquad 3.18$$

[2]An experimental investigation by Hogan and his colleagues of the validity of these two assumptions for humans is discussed in the following chapter (Mussa-Ivaldi, Bizzi and Hogan, 1984). To briefly summarize the results, the two dimensional stiffness tensor (describing the end-point stiffness in the transverse plane) is predominantly, although not entirely, symmetric. The assumption of the collinearity of the eigenvectors is somewhat more questionable. The experimental evaluation indicated that the eigenvectors of the stiffness and inertial tensors were consistently 20 to 40 degrees off axis from each other. The reader is referred to the following chapter and the cited article for further details. Consequently, the needed assumptions are not entirely valid for the human body, but in order to examine Hogan's results, the required assumptions will be granted.

Note that both the force and position errors are scaled by the tolerance limits on these terms. Incidentally, the "tolerable" force level specified by Hogan does not necessarily correspond to a maximal voluntary contraction. Clearly, the tolerable force cannot be any larger, but as Hogan used the term, the tolerable force may be a level of exertion that the body does not wish to exceed for other reasons, such as fatigue.

The solution obtained by Hogan for the decision variables is as follows.

$$k_{opt} = F_{tol}/X_{tol} \qquad 3.19$$

$$b_{opt} = (2(k_{opt} \cdot m))^2 \qquad 3.20$$

According to Hogan(1985c), this result is simply the solution to the second-order regulator problem. Hogan remarked that this solution is particularly important in two respects. First, it shows that the minimization of the weighted sum of the expenditure of effort and position error can be used to derive an impedance appropriate for the task. Second, the results are expressed in terms of the mechanical behavior of the end-point. Consequently, there is no restriction on how the impedance must be implemented. It could be done using feedback control or it could be accomplished using the intrinsic characteristics of the manipulator.

On the basis of this analysis, Hogan noted that even if very little is known about the magnitude or distribution of the disturbing forces, the manipulator-environment interaction may be specified so that task requirements are met (i.e., the manipulator position error remains within a specified tolerance range). Hogan also posed the question of whether the manipulator controller might be able to use information about the distribution and/or magnitude of the disturbances to reduce the weighted sum of the force exerted over time and the position error. Although Hogan posed this question he did even not begin to answer it.

Impedance Considerations and Indeterminacy in Biomechanical Models

There is one additional implication of impedance control for biological systems that deserves mention. From the standpoint of biomechanical models of the lower back, so many different muscles crossing the L3/L4 joint is a problem to be solved by the introduction of optimization (i.e., the problem is indeterminate). There are several more muscles which cross the joint vertically than available equations from statics. Consequently, there is no way to uniquely solve for the muscle forces without introducing some optimization criteria. Hogan (1985b) observed that from the framework of impedance control, the fact that the musculoskeletal system is statically indeterminate is not a problem to be solved but a means by which to independently modulate the torque and the impedance of a joint. By co-contracting the muscles around a joint, the same net torque can be generated for a wide range of end-point stiffness. Hogan showed that polyarticular muscles (muscles which cross two or more joints) are particularly useful for generating the same net joint torque over a range of stiffness.

Hogan employed a simplified model of the arm in which muscles were modeled as springs. In the monoarticular case, the springs spanned only the elbow joint. In the case where polyarticular muscles were included, the springs spanned the elbow and shoulder joint. Using this model, Hogan showed that the ability of the neuromuscular system to generate equal stiffness contours of the hand in the transverse plane is greatly enhanced by the inclusion of polyarticular muscles. The term "equal stiffness contours" was used by Hogan to mean that the force produced at the hand in response to a small displacement is the same in all directions. The details of this derivation are contained in another article by Hogan (1985e) and the reader is referred to the article for further details.

This analysis indicates that rather than presenting the CNS with an indeterminate problem that must be solved, redundant muscles actually

provide a means to independently modulate the output torque and the stiffness of the end-point at the same time. The experimental evaluation of such stiffness contours by Hogan and his colleagues (Mussa-Ivaldi, Hogan and Bizzi, 1985) is discussed in the following chapter.

Summary

The literature reviewed in this chapter reveals several important results. Perhaps the most important observation is that control of a single vector quantity such as force or position is insufficient for a manipulator which must exchange work with its environment. Control of single vector quantity is also insufficient if the manipulator must operate in the presence of unpredictable disturbances. A disturbance response is needed. The response could be implemented using feedback control. However, as Hogan pointed out, manipulation tasks require a response time that would preclude the exclusive use of feedback control because of the transmission delays. One method of implementing an open-loop disturbance response is impedance control, which relies on the pre-setting of the response to a perturbation through control of the joint stiffness and viscosity. Hogan demonstrated that such an impedance control law can be formulated with a minimum of assumptions. In particular, it is not necessary to assume that the force-displacement relations of the impedance components are linear, continuous, or monotonic. The theoretical results of Hogan with which the current work is particularly concerned involve the predicted trade-off between position error, force exerted, the magnitude of the disturbance, and the amount of information provided about the disturbance. It is the relationships between these variables that will be explored in the current work.

In summary, the theory presented in Hogan's three papers (1985a, b, and c) concerning the theory, implementation, and optimization of impedance control offers some real insights into the problem of why antagonistic co-

contraction occurs and how its magnitude might be predicted. The role of co-contraction in braking movements is well established, but both Hogan (1985) and Woldstad, Chaffin, and Langolf (1989) demonstrated that co-contraction occurs under isometric conditions. Thus, the evidence indicates that muscles are activated by the body for reasons other than to exert force against external torques, as many biomechanical models of the lower back implicitly assume.

CHAPTER 4
EMPIRICAL EVALUATIONS OF JOINT STIFFNESS AND JOINT IMPEDANCE

Introduction

This chapter contains a review of two studies in which the stiffness or impedance (stiffness and viscosity) of one or more joints was measured. These two studies illustrate how to measure the end-point stiffness of a multi-joint system or the end-point impedance of a single joint. They also demonstrate the experimental difficulties in obtaining accurate measurements of these quantities. The evaluation of the multi-joint end-point stiffness also shows that the behavior of the neuromuscular system is predominantly, although not entirely, spring-like (i.e., it stores elastic potential energy). The study by Mussa-Ivaldi, Bizzi and Hogan (1985) also demonstrates that the end-point stiffness of the hand is regulated in a systematic manner and in coordination with the apparent end-point inertia. This stiffness regulation must be accomplished via antagonistic co-contraction.

Also included in this chapter is a review of an experimental evaluation of the impedance of the human elbow joint in response to high frequency, small amplitude perturbations (Lanman, 1980). A review of this study is instructive for two reasons. The study illustrates some of the difficulties of measuring the impedance of a joint. A discussion of the experimental methods makes apparent some of the limitations that the measurement of the impedance of a joint places on other experimental manipulations. The importance of this experiment is that it demonstrates that under the conditions tested, the modulation of the impedance occurs principally through the variation of the joint stiffness.

Definition of "Spring-Like" Behavior

A linear spring is described by a linear relationship between an imposed displacement and the resulting force. Since the ratio of force to distance is constant, the stiffness of the spring may be expressed in terms of a single ratio. Hogan (1985a) noted that the general definition of a spring is much less restrictive. The displacement-force relation may be nonlinear, nonmonotonic, and even discontinuous. The single defining characteristic of a spring is that the force-displacement integral, the stored elastic energy, must be defined (Mussa-Ivaldi, Bizzi, and Hogan 1985). By definition (Rosenberg and Karnopp, 1983), a potential function such as the stored elastic energy is one for which the curl of the gradient of that function must be zero (i.e., curl grad $E_p = 0$). The curl of a vector **v** is defined as shown in equation 4.1 (Salas and Hille, 1982)

$$\text{curl } \mathbf{v} = \left(\frac{\partial v_3}{\partial y} - \frac{\partial v_2}{\partial z}\right)\mathbf{i} + \left(\frac{\partial v_1}{\partial z} - \frac{\partial v_3}{\partial x}\right)\mathbf{j} + \left(\frac{\partial v_2}{\partial x} - \frac{\partial v_1}{\partial y}\right)\mathbf{k} \qquad 4.1$$

In two dimensions this reduces to the following relation

$$\text{curl } \mathbf{v} = \left(\frac{\partial v_2}{\partial x} - \frac{\partial v_1}{\partial y}\right)\mathbf{k} \qquad 4.2$$

Hogan observed that the gradient of the stored elastic energy is just the force produced by the element in response to an imposed displacement. In order to prove that the behavior of an element is spring-like, one need only establish that the restoring force of the element is without curl.

Derivation of the Test of Spring-Like Behavior for the Neuromuscular System.

Mussa-Ivaldi, Bizzi, and Hogan formulated a test of the spring-like behavior for the neuromuscular system. For practical reasons associated with

the design of the apparatus, Mussa-Ivaldi, Hogan and Bizzi (1984) restricted the test of spring-like behavior to two dimensions. Specifically, they measured the force produced at the hand in response to a small imposed displacement in the transverse plane. The test proposed by Hogan (that the curl of the force should be zero) was implemented in two dimensions rather than three. The test requires that at least two dimensions be used. The use of a two rather than a three dimensional test is a result of experimental rather than theoretical limitations.

The gradient of a potential function in two dimensions is shown in equation 4.3

$$-grad\,E(x,y) = \begin{bmatrix} \dfrac{-\partial E_p}{\partial x} \\ \dfrac{-\partial E_p}{\partial y} \end{bmatrix} = \begin{bmatrix} F_x(x,y) \\ F_y(x,y) \end{bmatrix} \qquad 4.3$$

The curl of a vector field in two dimensions (as given by a calculus text) is shown by equation 4.4 (Salas and Hille, 1986)

$$curl\,\mathbf{F}(x,y) = \frac{\partial F_x}{\partial y} - \frac{\partial F_y}{\partial x} \qquad 4.4$$

Thus, for the curl of the force to be zero, equation 4.5 must hold.

$$\frac{\partial F_x}{\partial y} = \frac{\partial F_y}{\partial x} \qquad 4.5$$

The vector field of forces may be nonlinear in general, but for sufficiently small displacements the relation may be assumed to be linear. Hogan

illustrated this by expressing the force in the *x* and *y* directions as Taylor series expansions (see equations 4.6 and 4.7). Feeman and Grabois (1970) and Kaplan (1984) present examples of Taylor series expansions in several variables.

$$F_x = F_x(x_o y_o) + \delta F_x/\delta x\,(x_o y_o)\,dx + \delta F_x/\delta y\,(x_o y_o)\,dy + \text{higher order terms} \qquad 4.6$$

$$F_y = F_y(x_o y_o) + \delta F_y/\delta x\,(x_o y_o)\,dx + \delta F_y/\delta y\,(x_o y_o)\,dy + \text{higher order terms} \qquad 4.7$$

The expression of the force in these terms assumes that the force-displacement relation is differentiable in the neighborhood of the equilibrium point, but does not require that the relation be differentiable throughout. The force at the equilibrium position (x_o, y_o) is zero and as the displacements become small, the higher order terms vanish. As discussed below, Mussa-Ivaldi, Hogan, and Bizzi took care in the design of their experimental evaluation making the displacement small (5-8 mm). The force can then be expressed as shown in equations 4.8 and 4.9.

$$F_x = \delta F_x/\delta x\,(x_o y_o)\,dx + \delta F_x/\delta y\,(x_o y_o)\,dy \qquad 4.8$$

$$F_y = \delta F_y/\delta x\,(x_o y_o)\,dx + \delta F_y/\delta y\,(x_o y_o)\,dy \qquad 4.9$$

The partial derivatives in the two equations may be recognized as the stiffness coefficients and the relationship between force and displacement and can be rewritten as follows.

$$\begin{bmatrix} F_x \\ F_y \end{bmatrix} = \begin{bmatrix} -K_{xx} & -K_{xy} \\ -K_{yx} & -K_{yy} \end{bmatrix} \begin{bmatrix} dx \\ dy \end{bmatrix} \qquad 4.10$$

The various stiffness coefficients are defined as follows.

$$K_{xx} = -\delta F_x/\delta x \qquad 4.11$$

$$K_{xy} = -\delta F_x/\delta y \qquad 4.12$$

$$K_{yx} = -\delta F_y/\delta x \qquad 4.13$$

$$K_{yx} = -\delta F_y/\delta y \qquad 4.14$$

Thus, the requirement of equation 4.5 may be restated as requiring that the off-diagonal elements of the stiffness components be equal. Hogan (1985d) showed that the stiffness matrix shown in equation 4.10 can be partitioned into a symmetric component and an anti-symmetric component as shown in equations 4.15 and 4.16. Note that $\mathbf{K} = \mathbf{K_s} + \mathbf{K_a}$.

$$\mathbf{K_s} = (\mathbf{K} + \mathbf{K}^t)/2 = \begin{bmatrix} K_{xx} & \frac{Kxy+Kyx}{2} \\ \frac{Kxy+Kyx}{2} & -K_{yy} \end{bmatrix} \qquad 4.15$$

$$\mathbf{K_a} = (\mathbf{K} - \mathbf{K}^t)/2 = \begin{bmatrix} 0 & \frac{Kxy-Kyx}{2} \\ \frac{Kxy-Kyx}{2} & 0 \end{bmatrix} \qquad 4.16$$

The approach adopted by the Mussa-Ivaldi, Bizzi, and Hogan (1985) was to displace the hand from an equilibrium position and measure the restoring force. The parameters of the stiffness matrix were then fit using a simple least-squares regression. The stiffness was also represented graphically as an ellipse. The directions of minimum and maximum stiffness were represented as the minor and major axes of the ellipse. The ellipse was characterized by a magnitude (area), shape (ratio of the axes) and orientation (direction of the major axis).

Methods Used to Measure the Stiffness

Apparatus. A special apparatus was used for the hand displacement and force measurement. Subjects were seated in a chair with the shoulder restrained by a shoulder harness belt. Only subjects whose dominant hand was the right hand were used. The subject's right hand was extended a handle connected to a two-link planar extension. This authors called this device a manipulandum. The subject's wrist and palm were wrapped to the handle using calcium-impregnated gauze to create as firm a connection as possible. The subject's right elbow was supported by a rope attached to the ceiling.

A piece of clear plexiglass, on which a set of light-emitting diodes (LEDs) was mounted, was positioned above the handle which moved only in the horizontal plane. The authors called the handle a manipulandum. Each subject was instructed to move the hand to a position underneath an LED which was lit. This allowed the investigators to direct the subject to place his or her hand at a specified location in turn. The design of the apparatus allowed the investigators to apply a force of known magnitude and direction to the hand, and to displace it by a small set amount. The purpose of having the LEDs was to specify an exact resting position for each location tested. Displacements of either five or eight millimeters were used. Since the manipulandum only moved horizontally, all displacements and stiffness measurements occurred in the horizontal plane.

The authors did not report any details of differences found of the hand stiffness due to displacement magnitude. According to the authors, the direction of displacement ranged from 0 to 325 degrees in step sizes of 45 degrees. However, as is readily apparent, 325 is not a whole number multiple of 45. It appears that the authors intended to state that the range employed was 0 to 315 degrees. This interpretation is consistent with the rest of article and thus it will be the one adopted for the purposes of discussion.

In order to move the subject's hand by the desired amount, the direction and magnitude of the displacement were first selected in the subject's coordinate system and then transformed into the coordinates of the apparatus. The force required to displace the hand was then computed and implemented with the apparatus. The origin of the subject's coordinate system was selected to be the subject's right shoulder. The origin of the apparatus was the point of attachment of the manipulandum to the wall. The x and y axes of the two systems were parallel to each other but pointing in opposite directions.

In order to compute the force needed to displace the hand by the desired amount, the authors used the feedback control law shown in equation 4.18 which specified the force to be generated by the manipulandum in terms of the position and velocity. In order to accurately measure the displacement of the hand, two high resolution potentiometers were mounted on the axes of the mechanical joints of the manipulandum so that the position of the endpoint of the apparatus (and thus the hand) could be determined.

$$T = a(\theta_d - \theta_a) - b(\omega_d) \qquad 4.17$$

The term *T* represents the torque to be generated by the manipulandum on the hand. The terms θ_d and θ_a represent the actual and desired hand positions. The term ω_a is the actual angular velocity of the manipulandum. The terms *a* and *b* determine the effective stiffness and viscosity of the apparatus.

Experimental procedure. During the actual test, the subject was instructed to move his or her hand to a position underneath the plexiglass. The desired location was indicated by lighting one of the LEDs. While the hand was under one of the targets, a random sequence of displacements was applied. The displacements were varied both in magnitude and direction. As described above, the directions of the displacements were selected from whole

number multiples of 45 degrees. The movement time in which the hand was displaced was 120 msec in duration. A holding phase of 1.5 seconds followed the displacement during which the force applied by the subject to the apparatus was monitored. The authors attempted to minimize the contribution of any voluntary response during the displacement and holding phase. They did this by asking the subjects to focus on perceiving the direction of the displacement, to say aloud "one-two," and finally to move the manipulandum rapidly in the direction opposite the imposed displacement. The rationale for giving the instruction was to increase the reaction time and be able to observe the onset of the voluntary response. The authors measured the EMG activity of the biceps, triceps, and the pectoralis major to verify the absence of significant voluntary response during the holding period. They reported that some EMG activity was present during the displacement of the hand, but that the EMG levels returned to base line levels during the holding phase. Since the hand was at rest for several hundred milliseconds, the force exerted by the subject on the handle must consist only of a static restoring force with no viscous or inertial components.

Evaluation of the Curl

The authors computed the curl using the analysis procedure described previously and performed a t-test to determine if the curl was significantly different from zero. The curl was significantly different from zero for two of the four subjects at all the locations tested ($\alpha = 0.01$), for a third subject at two of the five locations tested and at only one location for the fourth subject. These findings indicate that the neuromuscular behavior was not consistently spring-like. However, a finding of a curl that is reliably different from zero does necessarily imply that the magnitude of the curl is large in relation to the force which is spring-like (i.e., exerted parallel to the displacement). The authors also reported statistics for the mechanical apparatus which, by design, had no

curl. Any finding of a curl component for the apparatus must be artifactual and thus indicates the presence of measurement error in the values of the force and the displacement. The authors reported that for two of the five workspace locations tested, the curl of the apparatus was found by the t-test to be non-zero.

Consequently, the authors compared the force due to the curl alone to that due to the maximum and minimum spring-like stiffness. The comparison was done by forming the ratio of force produced in a direction normal to the displacement with that produced along the line of the displacement. Since the stiffness of the hand in the transverse plane was found to be substantially anisotropic, the ratio of curl to spring-like force was necessarily dependent upon the direction selected. The authors described the restoring force graphically as an ellipse for each subject at each location. They reported the ratio of the curl to the spring-like stiffness along the major and minor axes, Z_{max} and Z_{min} of the stiffness ellipse respectively. The authors computed the geometric mean of these two ratios as well and called this Z_{mean}. The maximum value of Z_{mean} for a particular subject and orientation was found to 14%. However, Z_{mean} exceeded 10% in only a quarter of the cases and was often in the range of less than four percent. Values of Z_{mean} were an order of magnitude smaller for the apparatus than for the subjects, with the largest value being 1.7. On the basis of these results, the authors concluded that the behavior of the neuromuscular system is predominantly but not entirely spring-like.

Other Important Findings

As part of this study, the authors investigated how the stiffness varied over the course of several days and whether the subjects were capable of modifying the shape and orientation of the ellipse. The authors found that while the subjects were capable of varying the size of the ellipse over time, the

shape and orientation were essentially unchanged over time. The authors did not report any statistical tests of changes in the stiffness, but they were evidently not very large.

Mussa-Ivaldi, Hogan, and Bizzi also found that the subjects were capable of modulating the magnitude of the stiffness in response to perturbations. They perturbed the arm position prior to the stiffness measurement in three different ways. The first perturbation consisted of a force of rotating direction and constant magnitude (5 Hz, 8N). The second perturbation was the application of force along the x axis of varying amplitude (1 Hz, $\pm$10N). The remaining perturbation was a force of the same magnitude and frequency along the y axis. The authors found that the result of all the perturbations was to effect a global increase in the stiffness. When the force was applied only in the x or y direction the stiffness pattern was essentially the same as when the direction of the force varied.

One final manipulation was the investigation of the effect of shoulder abduction angle. The authors found that changing the shoulder angle altered the pattern of stiffness substantially.

The authors were intrigued by the fact that the stiffness ellipse seemed to vary in a regular fashion throughout the workspace. The stiffness ellipse at intermediate locations seemed to be a hybrid of those at more extreme locations. Consequently, the authors performed an added calculation. Modeling the arm as two rigid body links, they computed the inertia of the hand at each location and represented it as an ellipse. The major and minor axes of this inertia ellipse correspond to the directions of greatest and least apparent mass. They found that the angles between the long axis of the stiffness ellipse and the long axis of the inertia ellipse were consistently 20-40 degrees. This finding indicates that the neuromuscular system regulates joint stiffness in conjunction with the inertia of the end-point.

These findings show that the stiffness of the neuromuscular system is modulated in a coherent fashion and that the magnitude of the stiffness can be increased to compensate for environmental perturbations. The stiffness of the system also changed in a coordinated fashion with the apparent inertia of the end-point, changes in arm configuration. Thus, as the articles discussed in the previous chapter suggest, the human body incorporates a spring-like disturbance response. This spring-like response occurs as a result of an ongoing force exertion. Clearly, regulation of hand stiffness requires that torque be generated about the elbow and this must be accomplished by antagonistic co-contraction.

An Experimental Determination of Joint Impedance

Several studies have been reported in the literature which purport to measure the impedance of muscles and joints. However, as Hogan (1985a) noted in the series of articles discussed in the previous chapter, a mechanical impedance describes the relationship between an input motion and an output force. The converse relationship of an input force and an output motion is properly described as an admittance. The literature contains several reports labeled by their authors (Weineke and Dernier van der Gon, 1973; Lacquaniti et al., 1982) as measurements of impedance which are actually measurements of the motion response of a human limb to a force input.

Background. Lanman (1980) correctly measured the impedance of the elbow joint under the conditions of isometric contraction, voluntary movement, and passive movement. The results of the experiments were used to develop a model to explain differences in the short-range stiffness under passive movement, voluntary movement, and isometric contraction conditions. Short-range stiffness was defined as the range of muscle stretch for which the bond bridges between actin and myosin are not severely disrupted, which Lanman assumed to be about 100 angstroms per half sarcomere. While the

dissertation was not directed toward the investigation how the components of elbow impedance change with measurable variables, some environmental factors were varied. These factors and their effects are discussed below.

In addition to measuring the impedance of the elbow joint, Lanman concurrently measured forearm position and iEMG activity of the biceps and triceps. In all cases, the position of the elbow was fixed. As part of the design of his experiment, Lanman attempted to exclude the reflex portion of the response by the use of high frequency sinusoidal perturbations. This particular feature is important because the force must be due to an ongoing level of muscle contraction, and not simply the force resulting from the stretch reflex.

The results of Lanman's study have implications for the control of movement and tend to support the hypothesis of Hogan that antagonistic co-contraction occurs to modulate the impedance of the limb. Lanman found that the measured stiffness and viscosity of the elbow joint increased with increasing iEMG of the triceps and the biceps. While no efforts were made by Lanman to develop a quantitative relationship between the level of electrical activity of the two muscles and the measured impedance, these results show that iEMGs of the two muscles are positively correlated with the stiffness and viscosity of the elbow joint. Thus, these results are consistent with the conclusions of Hogan that the antagonistic muscle activity occurs at least in part to modulate impedance. One source of possible confusion for the reader in the following discussion is how the force that results from an imposed motion can be measured. Specifically, how does one impose (or superimpose) a motion on the arm? The obvious answer is that one applies a force to the arm. However, since an impedance relates a *motion* input to a *force* output, this may appear to be a source of difficulty.

The solution developed by Lanman was to find the (output) force indirectly. An accurately known force was applied to the forearm with a fixed elbow position. He then computed the rotational acceleration that should occur

as a result of the applied force alone. Finally, he measured the actual acceleration and noted the difference. Assuming that the applied force, the resulting motion, and the moment of inertia were all known, he could find the torque exerted by the arm muscles by subtraction. This is shown in the following two equations. The term τ_s represents the torque applied to the forearm by the shaft while τ_j is the torque due muscle and tendons. The term I is the inertia of the forearm and α is the measured angular acceleration of the forearm about the elbow.

$$\Sigma M = I\alpha = \tau_s + \tau_j \qquad 4.17$$

$$\tau_j = I\alpha - \tau_s \qquad 4.18$$

Experimental Methods used to Measure the Elbow Impedance

Lanman used a torque motor to apply a known, sinusoidally varying torque to the forearm. The torque was measured with an axial strain gauge and the resulting acceleration was monitored using high resolution potentiometers (i.e., the position data were differentiated twice to obtain angular acceleration). Lanman did not mention any filtering of this position data nor did he consider measuring the acceleration directly

The inertial effects were then subtracted. In order to be able to subtract out the inertial effects, it was necessary to accurately know the moment of inertia about the instantaneous point of rotation. Lanman determined the moment of inertia by carefully fixing the point of rotation and maintaining a constant moment of inertia about that point. A concrete footing was used to support the elbow on the point of rotation. The forearm of each subject was placed in an individually fitted fiberglass cast and this cast was fixed in a brace on the concrete footing. These precautions assured a constant point of rotation. A sketch of the apparatus from Lanman's thesis (Lanman, 1980) is shown in Figure 4.1.

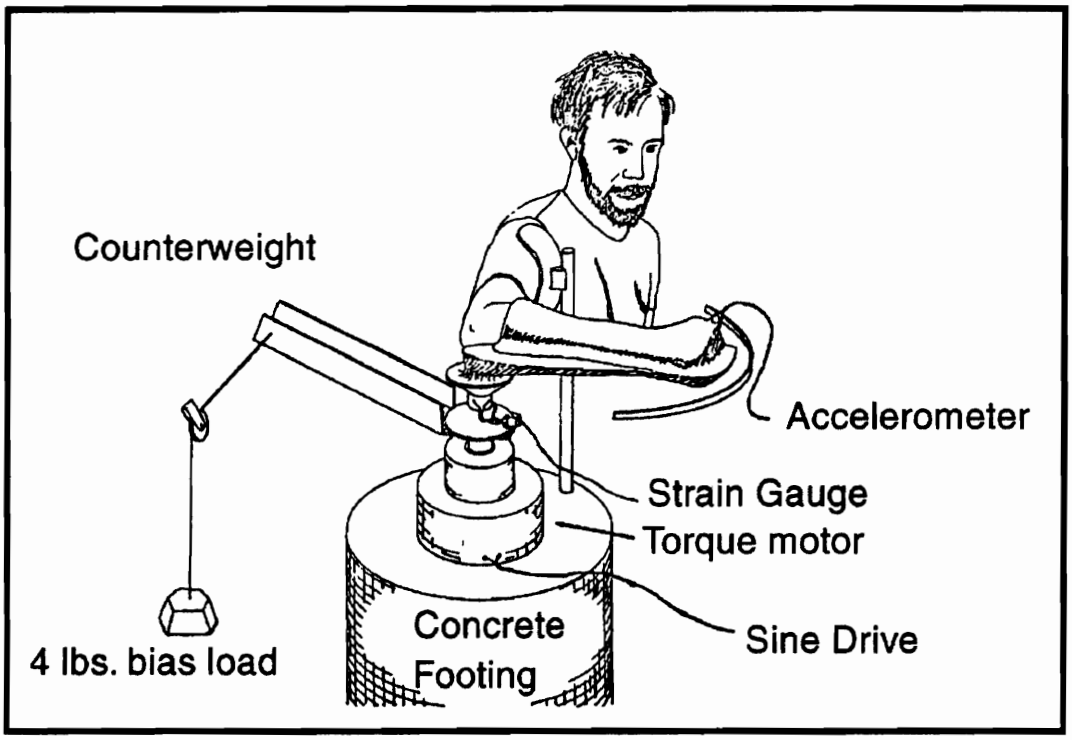

Figure 4.1. Lanman's apparatus (Copyright © 1980 MIT, reprinted with permission).

In order to maintain a constant moment of inertia of the forearm-cast system, any residual spaces in the forearm casts were filled with a viscous solution of corn starch and water. The forearm-cast system was then sealed so that the arm could not be pushed in or withdrawn without creating a bubble. No such bubbles were observed and since any movement of the forearm *within* the cast would displace an equivalent volume of the corn starch mixture, the experimental apparatus ensured a constant moment of inertia of the arm/cast system.

After finding the joint torque by subtraction, the remaining portion of the response was partitioned into an in-phase component (an equivalent stiffness) and a quadrature component (an equivalent viscosity). The design of the experiment allowed both of these components to be measured continuously during passive and voluntary movement of the forearm as well as during the maintenance of a static posture.

With regard to the form of the imposed motion, Lanman selected a high frequency sinusoid so that the impedance could be measured continuously. Based upon the work of several previous authors (Agarwal and Gottlieb 1977; Goodwin et al 1978; Joyce et al. 1974) he used sinusoids above 15 Hz in order to eliminate the contribution of the reflex response. The work of these previous authors showed that muscle tissue cannot contract and release at more than 15 Hz. Consequently, Lanman argued that the resulting force should reflect an ongoing contraction of the muscle and should exclude the contribution of the stretch reflex. Lanman observed elbow impedance under three different conditions: isometric contraction, passive movement, and voluntary movement. The isometric condition was somewhat different from the typical approach used by ergonomists to measure maximum voluntary contraction. A bias load ranging in torque from 2.5 to 40 ft-lbs was placed to pull on the rotating arm-cast system and the subject was instructed to exert sufficient force to maintain a steady position. The small amplitude high

frequency force was then applied to the arm-cast system to generate a displacement. The force of the joint in response to displacement was then computed by subtraction (see below). Since some small displacement must be imposed, the conditions under which the measurements were taken were not truly isometric, but the motion of the arm was small.

Methods of Analysis

In order to remove any contributions from voluntary muscular contractions, the acceleration and the corresponding joint torque were narrow-band filtered (10 Hz) at the drive frequency to remove non-sinusoidal components. The filtered signals were designated $\tau_{j\omega}$ and α_{ω} for the joint torque and angular acceleration respectively. Lanman expressed both the joint torque and the acceleration in terms of the frequency phase of the driving torque.

$$\alpha_{\omega} = A \sin(\omega t) \qquad 4.19$$

$$\tau_{j\omega} = T \sin(\omega t + \phi) \qquad 4.20$$

The equivalent stiffness and viscosity were then computed using equations (5) and (6). The term *T* is the peak amplitude of the filtered joint torque, $\tau_{j\omega}$. The term *A* is the amplitude of the displacement. The equivalent stiffness and viscosity were obtained over the range of the drive frequencies (3-30 Hz) using the following two equations.

$$K_{\omega} = (T \omega^2 \cos \phi)/A \qquad 4.21$$

$$B_{\omega} = (T \omega \sin \phi)/A \qquad 4.22$$

Error analysis of the data. Lanman noted that this method of measuring the equivalent stiffness and viscosity was subject to some constant and some

slowly varying errors. Since the joint torque is computed indirectly by subtraction, it is necessarily determined by a difference in two other terms which are themselves measured. When the actual difference between these two terms is small, the computation of the joint torque will be prone to errors. According to Lanman, small differences between the $I\alpha$ and the τ_s terms are found at the higher frequencies (~30 Hz). Lanman observed that the errors in these terms are due to difficulties in calibrating the equipment. For instance, the electrical output of the strain gauges must be calibrated, but barring drift in the amplifiers, the calibration should remain constant. Similarly, the potentiometer indicating forearm position must be calibrated, but any calibration errors in this part of the apparatus will also be constant.

Lanman apparently did not estimate the moment of inertia of the arm-cast system directly but rather used a different approach in which *changes* in the moment of inertia were related to *changes* in the equivalent stiffness. The approach used was to estimate the moment of inertia of a cast filled with water. The cast was sealed and consequently the water-filled cast constituted a constant purely inertial load. Hence, the joint torque term must be zero under these conditions and the applied torque, τ_S, must equal the product of the moment of inertia and angular acceleration. The applied torque and the angular acceleration can both be measured and the inertia of the water-filled cast may be computed as the quotient of the applied torque divided by the angular acceleration.[1] Lanman reported that by using the precautions mentioned before (concrete footing and rigid shaft between the torque motor and cast) it was possible to reduce the error in the estimated moment of inertia to 0.1%. Consequently, a reliable estimate of the moment of inertia of the

[1] It appears from discussion that the angular acceleration was computed by differentiating the angular position twice. Lanman did not discuss any digital filtering of the position data prior to the computation of the acceleration. While Lanman did note that high resolution potentiometers were used to monitor angular position, the use of some filtering might have proven helpful. Alternatively, the use of accelerometers might have proven to be a better method of measuring the angular acceleration.

water-cast system was found. Lanman then attached small steel weights to the water-cast system at a known distance from the point of rotation by means of an electromagnet. During the course of a perturbation, the current was shut off, causing the weight to drop. The release of the weight created an instantaneous change in the moment of inertia. Lanman observed that the change in the equivalent stiffness is related the change in the moment of inertia by the square of the driving frequency as shown in equation 4.25. Lanman performed this calibration in advance of each trial. Lanman did not discuss the details of how the equivalent viscosity was calibrated, but it was apparently calibrated in relation to the equivalent stiffness.

$$\Delta K_{\omega} = \Delta I \omega^2 \qquad 4.23$$

Discussion of Lanman's findings. For the case of isometric contraction, Lanman found that the calculated impedance increased with increasing bias load. He found that muscle activity as reflected by the iEMGs of the triceps and biceps also increased with increasing loads. Since Lanman made no attempt to calibrate the iEMGs of his subjects, no quantitative statements can be made regarding the relationship between the magnitude of the load, the impedance of the elbow joint, and the force exerted by the triceps and biceps. However, Lanman did note that when subjects were asked to maximally co-contract in the isometric condition, the impedance increased to levels above those found for the 2.5 to 40.0 ft-lbs bias load, primarily due to an increase in the equivalent stiffness. The equivalent stiffness increased several hundred times over the passive condition. Lanman noted that changes on this scale could not result from passive tissues and must therefore be due to muscular contractions.

For the case of passive movement of the forearm, Lanman found a decrease in the stiffness and little change in the viscosity. Lanman attributed

this decrease to a disruption of bond bridges between the actin and the myosin filaments of the muscle. With regard to the speed of the passive movements, Lanman stated that they were all much slower than what was required to elicit a reflex response. Stiffness decreased equally in both directions.

For the condition of voluntary movement, the subject exerted force against a viscous type load[2]. In order to overcome the viscous load characteristics a burst of muscular activity was required. During this burst a large increase in the stiffness was observed. In summary of his results, Lanman noted that the changes in the impedance during voluntary movement could be viewed as the sum of the effects of isometric muscular contraction and passive movement.

Summary

The studies discussed in this chapter reveal several important points. The articles by Hogan (1985) and Mussa-Ivaldi, Hogan and Bizzi (1984) demonstrate that the neuromuscular system can be considered predominantly spring-like in a rigorous general sense. The force generated at the hand in response to an imposed displacement includes a curl force that is small (~10%) in relation to the force produced in the direction of the displacement. The authors also found that the effect of a perturbation immediately prior to the measurement of the stiffness was the increasing of the magnitude of the stiffness in all directions in the transverse plane. This increase in stiffness was accompanied by an increase in the iEMG levels of the biceps and triceps.

The work of Lanman illustrates potential difficulties in obtaining an accurate measurement of the impedance of the elbow joint. The details of the study discussed above indicate the experimental apparatus required to measure the total impedance accurately is difficult to setup and calibrate.

---

[2]The viscous nature of load was generated by feeding back the output of the angular velocity of the arm-cast system to the drive motor providing the resisting torque.

There are also problems of error propagation due to the indirect nature of the impedance measurement. The level of joint stiffness and viscosity were both observed to be monotonically related to levels of iEMG of the biceps and triceps. Due to the fact that Lanman did not calibrate an EMG-Force relation for his subjects, no quantitative statement can be made regarding the correlation between the triceps and biceps muscle forces and the calculated impedance.

If in fact the observed antagonistic co-contraction is attributable to the modulation of impedance during the maintenance of a single posture or during slow movements, then it should be possible to predict some of the variation in the level of co-contraction from observable environmental factors. Among the important variables suggested by the literature review which can alter the level of impedance needed are the inertia of the forearm, the degree of accuracy required, the magnitude and distribution of any disturbing torques, and the amount of information provided about those torques.

CHAPTER 5
EXPERIMENTAL METHOD

Chapter Overview

The study reported here was undertaken to investigate the extent to which antagonistic co-contraction could be predicted from observable variables. Hogan's impedance control theory (discussed in Chapter 3) suggests that the human motor control system should be able to modulate impedance in order to minimize a cost function consisting of position error and energy expenditure. It also suggests that the motor control system might be able to use information about its environment to further reduce this weighted average. That is, if the motor control system knew that perturbations would be smaller in magnitude or less frequent, it could achieve the same error performance with less antagonistic muscle activity. Alternatively, it might improve its accuracy with the same level of performance.

Two experiments were conducted to test the following specific predictions.

1) The level of antagonistic co-contraction increases as the magnitude of the environmental perturbations increases.
2) The level of antagonistic co-contraction increases as the frequency of the environmental perturbations increases.
3) The level of antagonistic co-contraction increases as the information provided about the perturbations decreases.
4) The position error increases as the magnitude of the environmental perturbations increases.
5) The position error increases as the frequency of the environmental perturbations increases.

6) The position error increases as the information provided about the perturbations decreases.

The two experiments conducted employed tracking tasks. Tracking tasks were used in order to give the subjects a target position and to be able to compute a measure of the error from the desired position. Since Hogan (1985c) had hypothesized the body increases the joint impedance in order to reduce the error in the actual or virtual position, it was necessary to specify a desired position over time.

In the first experiment, a zero-order isometric pursuit tracking task was used. The subject exerted force on a wrist brace and the lateral displacement of the icon appearing on a computer monitor was directly proportional to the force exerted. In the second experiment a zero-order position control tracking task was used. This type of tracking task is sometimes referred to as an isotonic tracking task, but as Frost (1972) notes, a true isotonic task is an engineering abstraction, since a real control has both mass and friction. For this reason, the second tracking experiment will be referred to as a position-controlled tracking task and the term "isotonic" will not be used. Details concerning the two tracking tasks are provided below.

Perturbations in the isometric experiment were implemented as sudden changes in the gain. The advantage of using a static tracking task was that the muscle forces could be predicted from the EMG data with good precision. The disadvantage of this approach is that it lacks some of the reality of a dynamic tracking task since no perturbing force is actually applied to the forearm during the tracking task.

Consequently, a dynamic tracking task was employed in a second experiment. Because the two experiments were similar in may respects, they are described together. Differences between the two experiments are noted.

The subjects and the apparatus for the two experiments are described first. The experimental designs used for both experiments are then discussed,

and the experimental procedures that were used are presented. The methods used in collecting and analyzing the EMG data are described only briefly in the body of this chapter. Appendices A and B concern how muscle forces can be estimated from EMG data. These appendices also summarize the literature that served as a basis for selecting these analysis methods.

Subjects

Sixteen male subjects between the ages of 18 and 33 were recruited to participate in the first experiment. Eight different male subjects between the ages of 18 and 28 were recruited to participate in the second experiment. Signs were posted around the Virginia Tech campus soliciting subject participation. The signs indicated that the experiments would require approximately 3 hours and that subjects would be paid $5.00 per hour.

The number of subjects for both experiments was determined by the minimum number needed to counterbalance order across all subjects. Since there were 16 treatment combinations in the first study, 16 subjects were needed to completely counterbalance trial order. Likewise, 8 subjects were needed in the second experiment to counterbalance trial order across the 8 treatment combinations. The subject pool was restricted to males because of the posture constraints described below. The author was concerned that the chest straps used to prevent torso movement during tracking could not be comfortably secured on female subjects. Subjects also completed a screening questionnaire which concerned general health issues and any previous serious injuries. Potential subjects who indicated that they had health problems or serious injuries were not used.

The upper and lower arm lengths of each subject were measured and noted. The experimenter informally evaluated several males before determining a method for measuring upper and lower arm lengths in terms of bony landmarks. In selecting the landmarks to use in the measurement of limb

lengths, the experimenter attempted to locate the centers of rotation of the shoulder and elbow in the postures and motions to be used in experiment. The proximal end of the upper arm was fixed at the point at which the acromion process of the scapula and the clavicle meet. This point appeared to be directly above the point at which the glenoid cavity of the scapula abuts the head of the humerus. The Manual of Structural Kinesiology (Thompson, 1985) shows this point at which the clavicle and scapula connect as being above the point at which the head of the humerus rests against the glenoid cavity.

The center of elbow rotation in the posture of interest was judged to be on the proximal side of the lateral epicondyle. This point was used both as the lower end of the upper arm and the upper end of the forearm. The lower end of the forearm was considered to be the outer surface of the lower end of the radius at the styloid process. These distances were measured using a partial anthropometer.

The pinch width of the subcutaneous body fat on the upper arm of each subject was also noted using spreading calipers. These various anthropometric measures are presented in the Chapters 6 and 8 with the other results.

Experimental Apparatus

EMG measurement system. The electrical activity of the biceps and triceps was measured using bipolar surface silver-silver chloride electrodes with the ground connection placed on the elbow. The individual electrodes were 8 mm in diameter and an array of four electrode pairs were used for each muscle as shown in figure 5.1.

One electrode array was used to monitor the biceps and another was used to monitor the triceps. The electrode pairs on each array were fixed into flexible rubber templates and attached to the skin by using double sided

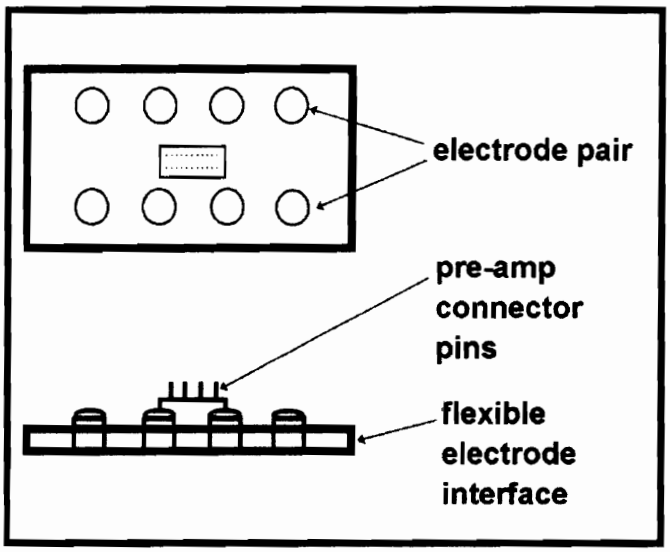

Figure 5.1. Diagram of electrode array.

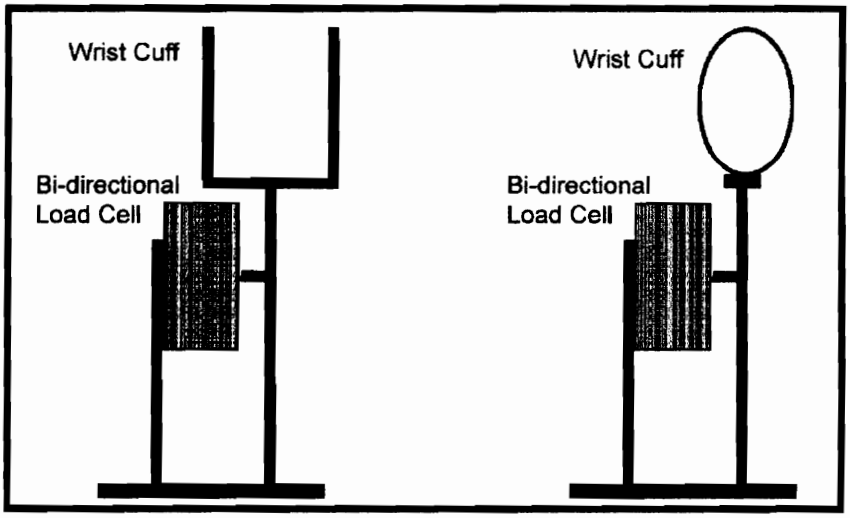

Figure 5.2. Bi-directional load-cell mounted on metal plate with wrist mount and with a wrist cuff.

adhesive electrode washers. The spacing between electrodes of each pair was 1.5 cm apart in accordance with the recommendations of Basmajian and De Luca (1985).

The raw signals from each of the four electrodes were amplified by pre-amplifier (Analog Devices AD624A, 200x) which attached directly to the electrode array. This amplification of the raw signal close to the source was implemented to improve the signal to noise ratio before any additional noise could be introduced. The pre-amplified EMG signals were then amplified again by a second variable gain amplifier (Burr-Brown IN A102KP, 1-1000x). The amplified EMG signals were processed by a root-mean-square estimator (Analog Devices AD536A) with a time constant of 55 msec. The output of the eight RMS estimators were digitally sampled at 100 Hz using an analog-to-digital (A/D) converter (Metrabyte DAS-1602) connected to an 386SX microcomputer.

Force measurement system. A bi-directional load cell was mounted on a metal plate connected to an adjustable wrist mount to detect the force applied laterally to the U-shaped fixture as shown in Figure 5.2 on the preceding page. One side of the U-shaped fixture could be moved laterally to obtain a snug fit against the wrist and then secured by a screw. The wrist of each subject was placed into brace in a neutral position. The neutral position was selected as the preferred position based upon the results of Woldstad (1989). He found slightly better fits of the force-EMG relation in the neutral position as compared to pronated position for the elbow flexors and extensors. The object in using the brace was to eliminate "dead space" between the force applied in one direction and then the other. The adjustable wrist mount was successful at eliminating dead space but several subjects complained of pressure against the wrist while exerting force. Several subjects also showed noticeable drops in hand temperature over the course of testing, indicating diminished blood flow.

As a result of the subject's reported discomfort with the metal wrist brace, a leather wrist cuff was used in the second experiment. This cuff was secured around the subjects wrist with Velcro straps. This alternative still allowed the subject to apply force at the wrist without the discomfort reported by subjects in the static experiment. The main drawback to the use of the wrist cuff was that subjects tended to pronate their wrists from the desired neutral position. Consequently, subjects were permitted to pronate their wrists in the second experiment, but were instructed to keep the variation in forearm twisting to a minimum during and between trials. Subjects' forearm postures were observed and they appeared to settle on a consistent forearm posture during the four preview trials.

In both experiments the plate upon which the load cell was mounted was fixed onto a rotating lever arm. The lever arm position remained fixed during the isometric tracking trial and during the static strength tests for both studies. The lever arm upon which the load cell was mounted rotated freely during the dynamic tracking trials.

The output of the load cell was passed to a variable gain bridge amplifier and then sampled at 100 Hz. This amplifier could be used to adjust the zero position of the load cell and the gain applied to the signal. Tests with the load cell indicated some drift in the zero position load cell or amplifier over time. Such drift in the offset would of course change the force recorded. No discernible change in the gain was detected. In the first experiment, the drift in the offset was addressed by adjusting the zero point between trials as needed. The signal was plotted in real time and the experimenter adjusted the offset to lie along the zero point.

In the second experiment, a slightly different approach was used. All channels were sampled for 4 seconds prior to the start of each trial. Subjects instructed to relax and not exert force to the wrist cuff. The absence of any applied force was verified by observing that the freely-rotating lever arm did

not move during this period. Average readings were computed over the 4 second period and written to a data file. The readings were then used as the zero points in the calibration of the load cell. These baseline readings are reported in Appendix C with the other calibration data. .

The amplifier also incorporated some high frequency noise. This noise was a repeating pattern at approximately 6.25 Hz. The overall pattern also contained some higher frequency components. With some effort, the magnitude of the buzz was been reduced to about 80 analog-to-digital (A/D) units on a scale of ±2048 A/D units or about 2% of the scale but the noise could not be completely eliminated.

Angular position measurement system. The angular position of the lever arm during the dynamic tracking task was measured with a high-resolution Beckman potentiometer (model number 5703-6-1).

Integrated data acquisition system. Figure 5.3 indicates how the different parts of the data collection and storage system were connected. The ISA bus microcomputer was equipped with a 12 bit Analog to Digital and Digital to Analog converter (Metrabyte model DAS-1602). This particular board had 16 channels for input and two variable outputs. It also had a constant 5 volt source that was used as input to the Beckman potentiometer. The microcomputer system was used to collect and store EMG, force and (for the dynamic tracking only) position data. It was also used to control the onset and duration of the Baltimore Therapeutic Equipment (BTE) device which was used to implement the perturbations during the dynamic tracking as described below. Four A/D channels of the A/D board were used to monitor each of the two electrode arrays. Another input channel was used to monitor force applied to the wrist cuff. During the dynamic tracking only, a tenth channel was used to monitor the lever arm position. A sampling rate of 100 Hz was used for all ten channels for all data collection for both experiments.

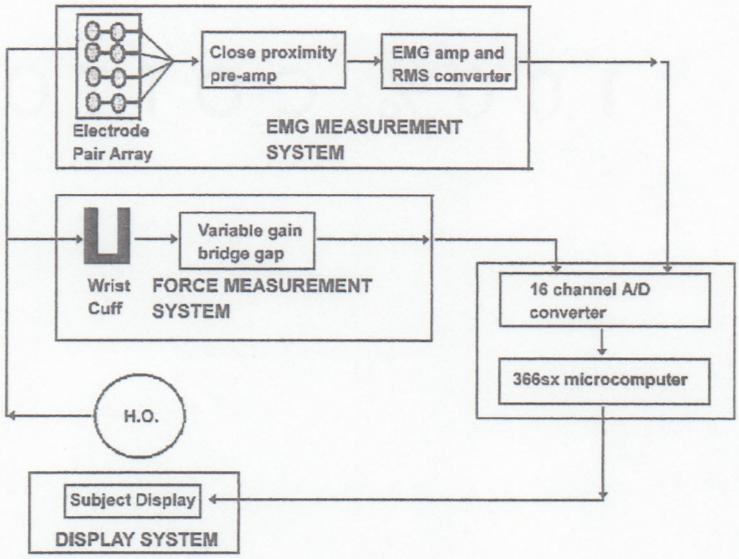

Figure 5.3. Schematic of apparatus components.

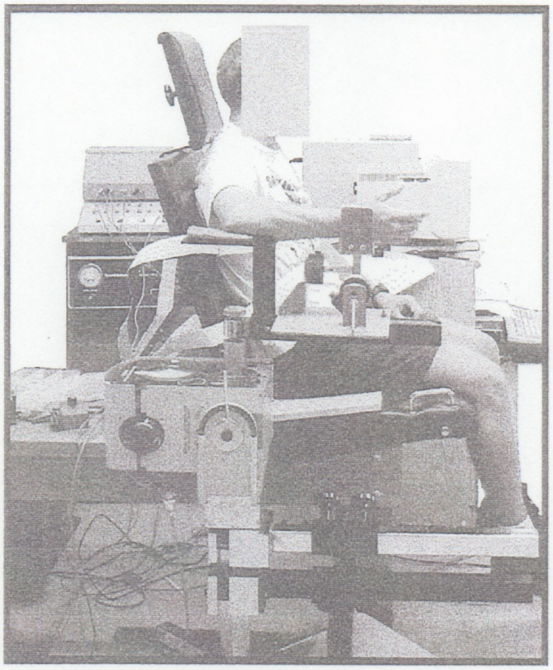

Figure 5.4. Posture support bench.

Posture support bench. The subject was seated on a modified Cybex bench. Pilot tests had indicated that the subject's torso tended to move laterally when pushing and pulling against the wrist cuff. Straps about the waist and chest were added to the bench to restrain this lateral movement. The seat height was adjusted by adding or removing pads on the seat of the Cybex bench. The seat height was adjusted so that the angle of abduction of the upper arm from the body could be adjusted to be between 60 and 80 degrees. The subject's right arm was placed in the adjustable wrist cuff as described above.

Figure 5.4 on the preceding page shows a photograph of the posture support bench with a subject seated in position to perform the tracking task. Note the placement of the subject's wrist in a neutral posture in the wrist fixture. The load cell mounted on the rotating lever arm is also shown.

Baltimore therapeutic equipment device. Perturbations to the static tracking task were implemented in software by momentary changes in the tracking gain as discussed below. The perturbations for the dynamic task were implemented by means of Baltimore Therapeutic Equipment (BTE) device. The lever arm was mounted on the BTE and rotated freely during the trial. The resistance could be continuously selected between freely rotating to a level at which the lever arm was immovable. Perturbations to the tracking task were implemented by using the analog output capability of the Metrabyte Board to turn on and off electrical relays (Aromat relays, model JA1C-TM-DC24V) which turned on and off the BTE. The duration of the "high" digital to analog output from the Metrabyte board was 0.1 seconds. The lever arm could be set to any level of resistance from freely rotating to levels at which it was not possible for the subject to rotate the lever arm. The resistence of the lever arm to rotation during the lower magnitude pertubation was 0.14 newton meters. During the high magnitude perturbation, it was 0.7 Newton meters. The onset and release of the perturbation was essentially instantaneous.

Experimental Design

A 2^5 within-subjects factorial design was used in the isometric experiment. A 2^4 within-subjects factorial design was used in the dynamic tracking experiment. In the both experiments the trial order was completely counterbalanced with a Latin Square. As indicated above, counterbalancing required sixteen subjects in the first study and eight subjects in the second study. Analysis of Covariance (ANCOVA) was also considered for the analysis of the data in which tracking error would have been used as a covariate (1991). However, a proper covariate should not be changed by the treatment. Ideally, it should be measured before the treatment is applied. Otherwise, the ANCOVA may be describing the effect of a variable under physically unrealizable conditions. In this case, an ANCOVA would permit the question of how antagonistic activity is affected if the error rates are held constant. The question assumes that it is possible for subjects to maintain a constant tracking error while characteristics of the tracking task are varied. In an experiment designed to investigate how subjects change their error tolerances and the patterns of muscle activation, it is not appropriate to assume that the tracking error can be held constant. Consequently, the tracking error was treated as a second dependent variable rather than a covariate.

Static experiment. A 2^5 factorial design was used for the first of the two experiments. The independent variables in the static experiment were tracking gain, perturbation frequency, perturbation magnitude, and pre-trial information. A Latin Square blocking design was used to counterbalance order effects between subjects. The levels for the factors are shown in Table 5.1 shown below.

The first factor that was varied was the gain of the isometric control. The force required to move the tracking icon to the point of maximum excursion was either 50% or 70% of the MVC for that direction of motion. Note

that this implies a different gain for the flexion and extension phases of the tracking.

The second variable that was investigated was the effect of perturbation magnitude. The perturbation magnitude was expressed as a percent of the MVC exerted in flexion. Perturbation magnitude was either 15% or 30% of the MVC in flexion. For example, consider a trial with a 70% required tracking force, and a 30% perturbation magnitude. During a "positive" perturbation, the maximum required tracking force would be increased from 70% to 100%. Similarly, during a "negative" perturbation, the maximum required tracking force would be decreased from 70% to 40%.

The levels of the required tracking force and perturbation magnitude were selected together. The experimenter did not want to exceed the maximum required tracking force to exceed the value determined by the MVC procedure. At the same time, it was also important to consider that prior studies had indicated that the fit of the force-EMG relation is generally better at higher levels of exertions (Woldstad, 1989; Redfern, 1988), so it was desired to have levels of maximum required tracking force generally toward the upper end of each subject's capability. The two levels of perturbation magnitude were selected first after some informal testing with several levels of required tracking force. Levels of required tracking force were then selected such that the largest required force during a high magnitude perturbation would not exceed the subject's MVC force. The third variable investigated was the effect of perturbation frequency. Exponentially distributed interarrival times with a mean of five or ten seconds were used. Informal testing of the apparatusindicated that in some trials, one perturbation would follow another so quickly that the subject would not have time to recover from the previous perturbation before the onset of the succeeding one. To account for this occurrence, an additional restriction was placed on the interarrival times. If a

TABLE 5.1 Independent Variables for the Isometric Tracking Task

Variable	Level	
	1	2
Tracking Gain	50%	70%
Perturbation magnitude as a percent of MVC	15%	30%
Mean inter-arrival times	5 seconds	10 seconds
Information about the Perturbation	none	all
Direction of exertion	flexion	extension

perturbation was scheduled less than 3 seconds after a prior perturbation, another exponential variate was added to the next arrival time so that at least three seconds would lapse between perturbations.

The direction of exertion (flexion or extension) was also included as a main effect. Rockwell (1991) found that the direction of exertion affected both the tracking error and the antagonistic muscle force for an unperturbed tracking task. Consequently, the trial data was divided into flexion and exertion phases and the data were analyzed separately.

Perturbations to the static tracking task were implemented by momentarily increasing or decreasing the tracking gain. The gain was increased or decreased randomly so that each "direction" for the simulated perturbation was equally likely. The timing and direction of the perturbations were generated from a pseudo-random string with the same random number seed. Consequently, while all subjects were exposed to the same number of perturbations in the same directions, the method of scheduling the perturbations and their directions was random.

In an effort to minimize learning and also reduce the possibility for differential transfer during the actual testing, the subject performed four practice tracking trials before the actual test trials. On each of these first four trials the subject was informed in advance of the trial the levels of tracking gain, perturbation magnitude and perturbation frequency to expect. On the first trial, the subject saw the higher levels of required force, perturbation magnitude, and perturbation frequency. On the second trial, subjects were shown the lower levels of required force for tracking, perturbation magnitude and perturbation frequency.

On the third and fourth trials, the subject was given tracking trials with no perturbations. On the first of these two trials the subject performed the tracking task with the lower gain. On the second of these two trials, the subject performed the task with the higher level of gain.

Dynamic experiment. A 2^4 factorial design was used in the second of the two experiments. The effects of perturbation frequency, perturbation magnitude, presence or absence of pre-trial information were tested in the second experiment, and direction of exertion were included. The levels used for the main effects of the second experiment are shown in Table 5.2.

Each subject also performed four practice tracking trials before the actual test trials in this second experiment. The subjects were informed in advance of the trial what levels of tracking gain, perturbation magnitude and perturbation frequency to expect on these practice trials. In the first trial, subjects saw the higher level of perturbation magnitude and perturbation frequency. In the second trial, subjects were shown the lower levels of perturbation magnitude and perturbation frequency. In the third and fourth trials, the subject performed the tracking trials without any perturbations.

Experimental Procedures

When the subject first arrived, he first read and signed the informed consent statement and tracking task instructions, which is included as Appendix E. While the subject was reading these items, the experimenter filled the recessed electrodes on each array with electrode gel and applied the double sided adhesive electrode washers.

The subject's skin above the biceps and triceps was prepared for the application of the electrodes by vigorously rubbing the skin with an alcohol-soaked cotton swab. The subject was then seated on the Cybex bench. The height of the seat was adjusted so that the subject's upper arm was abducted away from the body at an included angle of 60 to 80 degrees. The lever arm was fixed in place with an included elbow angle of 100 degrees. The electrodes were then applied to the skin. Medical tape was used to further ensure that the electrode array stayed firmly attached to the skin.

TABLE 5.2 Independent Variables for the Dynamic Tracking Task

Variable	Level	
	1	2
Perturbation magnitude	low	high
Mean inter-arrival times	5 seconds	10 seconds
Direction of exertion	flexion	extension
Information about the Perturbation	none	all

Load cell and potentiometer calibration. The load cell was then calibrated by applying a series of known loads with a Chatillon force gauge against the rigid base of the wrist mount. In the first experiment the load cell was then calibrated with loads of zero force and 100 N force. In the second experiment loads of 0, 50, 100 and 150 N were used. The calibrations of the second experiment confirmed that the response load cell was linearly related to the force applied.

The potentiometer also had to be calibrated during the dynamic experiment. Angles were measured and marked at the base of the rotating lever. The potentiometer was calibrated at included elbow angles of 70, 100, and 135 degrees. Pilot testing had indicated that the potentiometer was linear within the limits of measurement error.

Static strength tests and determination of MVC. A modified version of the Caldwell regimen (Caldwell et al., 1973) was used to used to obtain the maximum voluntary contraction (MVC) in both flexion and extension. Subjects were asked to buildup for two seconds and then maintain a maximal steady application of force for three seconds. Force was plotted against time for the subject in real time so that he could see when he needed to be at his maximum exertion level and how long he had to sustain it. The mean of the three second sample was then computed. If no point during the three seconds of interest lay outside of a range of $\pm 15\%$ of the mean, the trial was deemed acceptable.

These strength trials were also used to adjust the gain on the load cell and EMG amplifiers to a level such that the inputs would use most of the ± 5 volt scale of the Metrabyte A/D board without going off scale.

Static strength tests were also conducted at other fixed positions in the second experiment so that the length-tension relation of the biceps and triceps could later be calibrated. Subjects were asked to exert 50% of the force found for their MVC in flexion at included elbow angle at angles of ± 20, -30, and

$\pm$40 offsets from the 100 degree position. The exertions at -30 degrees was taken because the results of Woldstad (1989) showed substantial nonlinearity for the triceps compensation function between the -20 and -40 angles.

Redfern (1988) and Woldstad (1989) used a different protocol to calibrate the length-tension relation in which subjects very slowly exerted force through a range of motion. The main advantage of the pseudo-static approach is that it provides many more points with which to fit the length-tension relation for each equivalent muscle group. The disadvantage is that there are no truly static measures during the pseudo-static trial.

Tracking Task. The isometric and dynamic tracking tasks used in the two experiments were similar and the common features are described first. The characteristics specific to the two different tracking tasks are then discussed, followed by the particulars of the dynamic task. The display programs developed by Berkowitz (1990) and also used by Rockwell (1992) were adapted for use in both the isometric and position tracking tasks. The pursuit tracking task was displayed on a VGA monitor with a refresh rate of 60 Hz. The target icon moved laterally back and forth across the screen in the manner indicated in the Figure 5.5 below. The tracked symbol was green and tracking symbol was yellow.

The total lateral displacement of the target icon was 10.8 cm on the screen in both experiments. An on-screen message and auditory tone signaled the subjects when a new trial was about to begin.

Following the protocol suggested by Chaffin (1975) a rest period of 180 seconds was observed between each trial for both experiments. The total time for subjects to complete the experiments was approximately three hours with both the static and dynamic experiments. While there were more trials with the static experiment, setup and calibration time was substantially longer for the dynamic tracking experiment. The total trial duration was chosen to be 32.7

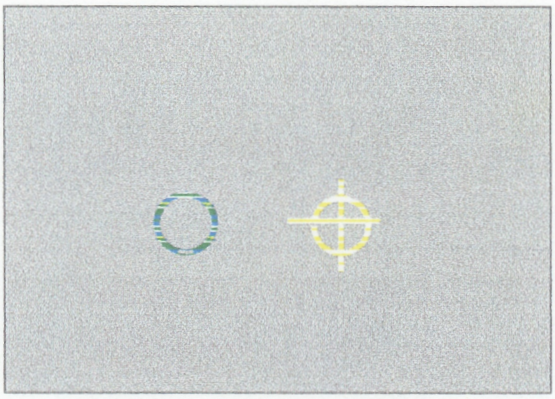

Figure 5.5. Diagram of the tracking screen.

seconds long[1]. No perturbations were scheduled during the first 2.7 seconds of the trial to allow the subject a brief period at the start of each trial to begin tracking. Perturbations were then scheduled during the last 30 seconds of the trial. In both experiments, subjects performed four different practice trials as described previously.

Static tracking task. The lateral position of the target over time varied according a sine function with a frequency of 0.2 Hz. The force applied to the load cell mounted on the lever arm was sampled and the position of the tracking icon corresponded to the amount of force applied to the wrist cuff.

As noted in the previous section, the gain on the static tracking task was such that the subject had to exert either 70% or 50 % of his previously determined MVC to move the tracking icon laterally as far as the target varied.

The electronic buzz in the load cell amplifier resulted in a constantly varying position of the tracking icon that made it very difficult to perform the tracking task. It also made it difficult to determine when an "intended" perturbation was occurring since the icon was so "jumpy" under typical operating conditions. Consequently, the tracking icon actually displayed the moving average of the force over the previous 0.16 seconds immediately preceding each updating of the screen position. This moving average effectively averaged out the noise from the amplifier and resulted in a stable tracking icon.

In order to test the hypothesis that the motor control system would increase the antagonistic co-contraction in an effort to minimize tracking error, it was important that the timing of the perturbations not be predictable.

---

[1] The DMA routines used to collect data in the background while plotting data in the foreground were limited to accessing one "page" of memory under DOS. One page of memory can hold 64 kilobytes of data. Since the integer samples produced by the A/D board each required 2 bytes of data, the data the total number of samples that could be collected in a trial was 32 kilobytes, or 32,768 samples. A sampling frequency of 100 Hz was needed to ensure that the sample rate was at least twice the nyquist frequency for the RMS EMG data. Since there were to be ten channels sampled in the second experiment, the trial duration was limited to 32.7 seconds.

Consequently, the inter-arrival times of the perturbations were exponentially distributed.

The implementation of the perturbation in the isometric tracking task was accomplished by rapidly increasing or decreasing the gain for the duration of the perturbation. The perturbation was chosen to be 0.6 seconds in duration. Pretests of this method of introducing perturbations to the tracking task indicated that instantaneous changes in the gain again resulted in the tracking icon "jumping" from point to point and did not produce the desired effect of simulating a sudden large force "pushing" the tracking icon right or left. The method for correcting this appearance of a "jumping" target icon requires a brief explanation of how perturbations were scheduled during the trial and implemented in software.

The use of the pseudorandom string to generate the exponential inter-arrival times allowed the perturbations to be "scheduled" in advance of the trial. This made it possible to smooth out the transitions in the gain that occurred during the perturbations. An array equal to the length of screen updates during the tracking task was first generated. Since the screen was updated at 50 Hz over the 32.7 second trial, this array consisted of 1635 identical elements (values of 50% or 70% depending of the gain for that trial). Using the pseudorandom string of numbers, perturbations were scheduled to occur during the tracking trial. The points in the array corresponding to the perturbation period were then adjusted up or down 20% or 40% of the MVC depending on the perturbation magnitude for that trial. The numbers in this array containing the gain were then exponentially smoothed with an α of 0.5 to smooth out the jumping appearance of the icon during the transition.

The use of the pseudorandom number generator to determine the exponential inter-arrival times also had another advantage. While the inter-arrival times were random, they were the same for each subject at each treatment combination. Thus, each subject received the same number of

randomly scheduled perturbations at the same time in each treatment combination.

Dynamic tracking task. The gain on the position tracking task was set so that the subject would move the lever arm through an included elbow angle of 70 to 130 degrees in order to track the icon. The lateral position of target over time varied according a sine function with a frequency of 0.4 Hz. The frequency of the target was increased for this second experiment because the slower tracking frequency did not require very much force to move. Prediction of muscle forces at such low levels of exertion is typically poor. Consequently, in order to elicit greater muscle forces, the target frequency was increased. The lateral movement of the icon on screen corresponded to a movement of ± 30 degrees from the center position of 100 degrees included arm angle. The tracking cursor displayed instantaneous position rather than a moving average as in the static task. Because a 5 volt source from the DAS-1602 board was used as the input to the potentiometer, the output did not require any additional amplification. Consequently, the movement of the icon plotted on screen for the subject did not have the "jumpy" appearance associated with the output of the load cell amplifier, and there was no need to plot a moving average of the signal.

Perturbations to the dynamic tracking task were implemented by use of the BTE as described above.

Summary

Two experiments were conducted in which perturbations were incorporated into zero-order tracking tasks. In the first experiment, a force-controlled tracking task was used. In the second experiment, a position-controlled tracking task was used. Varying amounts of information regarding the nature of the perturbation were provided to the subject in advance of each trial.

The details of how the muscle forces can be accurately and precisely estimated using electromyographic methods are included in the appendices. Appendix A addresses the simpler problem of estimating muscle forces from EMG activity under static conditions. Appendix B deals with the more difficult task of obtaining reasonable estimates of muscle force under conditions from EMG data during movement.

CHAPTER 6
RESULTS AND ANALYSIS - EXPERIMENT 1

Overview

The results obtained in the isometric tracking study are presented in this chapter. The anthropometric measures that were measured on each subject are presented first. The results of the EMG-Force modeling are described next. The definitions of the dependent measures used in the Analysis of Variance are then described. The results of tests of normality are presented next. The significant effects are then discussed.

Anthropometric Measures

The pinch width and lower and upper arm lengths were measured as specified in the preceding chapter. These data are shown in Table 6.1 on the following page.

Prediction of Muscle Forces Under Isometric Conditions.

Four channels of the output RMS EMG were sampled from both the biceps and triceps. These channels were filtered with a low-pass FIR filter and then normalized and averaged to produce one estimate of force for each muscle. The EMG data were then cross-correlated with the force data to determine the optimal lag. In each case, a single lag was calculated for both muscles of a particular subject's data.

A quadratic model relating the EMG signals to the observed force was fit to the data. The data were modeled separately for each trial condition resulting in R^2 values from 0.990 to 0.434. The fit of the data of subject 11 proved to be particularly poor. The unscaled EMG and force data had been plotted at the end trial, and reviewed by the experimenter. At the time of collection the data did not appear particularly unusual to the experimenter,

TABLE 6.1 Anthropometric measures for subjects - experiment 1

Subject	Upper Arm (cm)	Lower Arm (cm)	Pinch Width (cm)
1	23.00	27.45	0.80
2	24.45	26.65	0.79
3	26.25	27.35	0.41
4	26.10	27.05	0.15
5	30.08	30.80	0.50
6	24.85	26.75	0.41
7	29.35	28.40	0.11
8	25.60	26.75	0.57
9	28.91	27.00	0.69
10	25.00	26.60	0.42
11	26.70	26.70	0.11
12	27.40	24.70	0.53
13	29.95	29.00	0.50
14	29.70	27.40	0.60
15	29.90	26.10	0.80
16	28.20	26.10	0.60

but post-hoc scaling and filtering of the EMG data showed the data were not well correlated with the force. As Table 6.1 shows, the anthropometric data of subject 11 are well within the range of values noted for other subjects. Excluding the data of Subject 11, the lowest R^2 was 0.852, associated with data of Subject 7. Most of the coefficients of determination were much higher, and the median R^2 was 0.964. In contrast, the median and average coefficients of determination for Subject 11 were 0.725 and 0.715. Given that there was so much more unexplained variance in the estimated muscle forces of Subject 11, it was decided not to include this data in the statistical analysis of the estimated levels of antagonistic co-contraction. Examination of the error data associated with subject 11 also showed irregular values. Consequently, the data associated with subject 11 were excluded from the analysis of error data also. The deletion of the data associated with subject 11 did result in one trial order not being included in the data that were analyzed. However, order effects were minimized by two other factors. First, order effects were minimized by the practice trials conducted before the test trials. Second, 15 of 16 possible orders did appear in the analysis.

Dependent Measures

Tracking error. The Proportional Error was calculated from the data. Berkowitz had noted problems associated with the use of some error measures (such as the root mean square (RMS) and (mean absolute deviation)) in comparing the error from tracking trials with different gains. Since these two measures do not consider the differences in the tracking gain, the measures of error are not comparable. The PE measure explicitly considers the tracking gain and accounts for it in the calculation of the error. The PE error measure was calculated as shown in equations 6.1 and 6.2. As the equations show, separate values of the PE are calculated for the flexion and extension phases.

$$\text{PE Error}_{\text{flexion}} = \frac{\sum \dfrac{\text{ABS(forcing function(N)} - \text{Actual Track(N))}}{\text{Required flexion force for trial: \%MVC}_{\text{flexion}}}}{\text{Number of observations}} \qquad 6.1$$

$$\text{PE Error}_{\text{extension}} = \frac{\sum \dfrac{\text{ABS(forcing function(N)} - \text{Actual Track(N))}}{\text{Required extension force for trial: \%MVC}_{\text{extension}}}}{\text{Number of observations}} \qquad 6.2$$

Antagonistic activity. The absolute antagonistic muscle force (AAF) and the co-contraction ratio (CR) were computed from the estimates of muscle forces. The antagonist muscle force is defined to be the force applied to the wrist brace which opposes the net muscle force. The absolute antagonist force is simply the absolute value of the antagonist muscle force. The co-contraction ratio is defined to be the ratio of antagonist to agonist muscle force.

The period during and immediately following the perturbation was not included in the calculation of the AAF and the CR. Specifically, the CR and AAF data for one half of one period was discarded after a perturbation. This was done to make certain that any difference in antagonistic activity that was observed was due, in fact, to a change in the baseline level of antagonistic activity, and not simply to the immediate response to the perturbation.

Verification of Normality Assumption

One of the assumptions of the ANOVA procedure is that the population from which the sample is drawn is normally distributed. This assumption was verified by testing the error residuals of the three dependent measures for deviations from Normality with the Kolmogorov-Smirnov test.

In testing hypotheses concerning whether the sample data may be said to have come from a particular theoretical distribution, the null hypothesis is always that distribution of the population from which the sample was drawn is the same as the theoretical distribution. The Kolmogorov-Smirnov test allows one to compute the confidence with which this null hypothesis may be rejected. The *D* statistic is maximum of the absolute value of the difference between cumulative relative frequency distribution function of the theoretical distribution and the observed cumulative relative frequency of the sample data. If the distribution from which the sample data were drawn follows the theoretical distribution, we would expect values of *D* to be small. Larger values of D indicate deviations of the sample from the theoretical distribution. The sampling distribution of *D* is known under the null hypothesis and the probability that the population from which the sample was drawn is different than the theoretical one is can be computed. The nonparametric text by Siegel and Castellan (1988) contains a discussion on the Kolmogorov-Smirnov test, as well as references to other sources.

The number of cases, *N*, the *D* statistic and the associated *p* values are given in Table 6.2. The *D* statistic found for each of these tests shows that the null hypothesis of no difference between the population from which the sample was obtained and the normal distribution cannot be rejected at the α = 0.05 level. The *p* values are reported for this test as well as for the ANOVA results, and brief word of explanation is in order concerning *p* values. The α value in a statistical test represents the chance that one is willing to accept that one mistakenly asserts a difference between two populations based on the sample data when none in fact exists. The *p* values correspond to the α level at which the value of the test statistic calculated would just exceed the table value. The *p* value represents the exact probability of falsely asserting that there is a difference based on the data obtained (Winer et al., 1991). Most

TABLE 6.2 Kolmogorov-Smirnov Tests for Dependent Measures

Dependent Measure	N	D	p < D
Absolute Antagonist Force	480	0.9028	0.3888
Co-Contraction Ratio	480	0.8766	0.4258
Proportional Error	480	1.0765	0.1968

popular statistics packages, including SAS and SPSS, specify these *p* values as part of their output.

Proportional Error - Significant Main Effects and Interactions

The Proportional Error (PE) was lower for the flexion phase than for the exertion phase and lower for the 50% of MVC required tracking force. The PE was also lower for the higher magnitude perturbation condition. No other main effects or interactions were significant for this dependent measure. The ANOVA summary table for the significant main effects is shown in Table 6.3. The means and standard errors are plotted by direction of exertion and by perturbation magnitude in figures 6.1 and 6.2. As the graphs show, the proportional error was larger for the extension phase than it was for the flexion phase. It was also larger for the larger perturbation condition as compared to the smaller perturbation condition. The complete ANOVA summary table is shown in Appendix D.

The analyses of variance for this and the other dependent measures are reported without the Greenhouse-Geisser or other corrections sometimes used with repeated measures data. The measure of the departure from circularity, denoted by the letter 'ε', is used to adjust the degrees of freedom for the *F* test. The correction is estimated by the Greenhouse-Geisser formula, but the actual (i.e., population) ε is bracketed by upper and lower bounds as shown in the following equation.

$$\frac{1}{k - 1} \leq \varepsilon \leq 1.0 \qquad 6.1$$

Note that in the case of k = 2, ε = 1, and thus there is no need to apply the correction.

TABLE 6.3 ANOVA summary table for PE - significant effects

Factor	SS	df	MSE	F	p < F
Exertion Direction	87.49	1	87.49	10.5	0.006
Exertion Direction x S	116.39	14	8.31		
Perturbation Magnitude	59.75	1	59.75	7.68	0.015
Perturbation Magnitude x S	108.9	14	7.78		

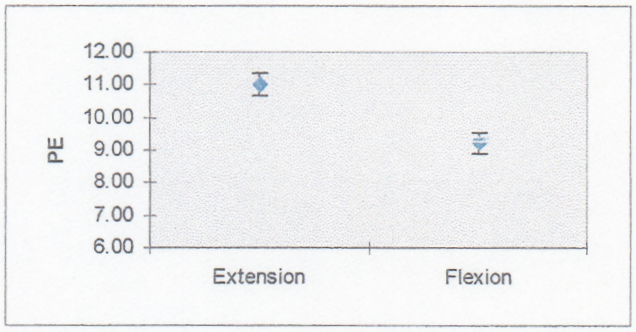

Figure 6.1. PE by direction of exertion.

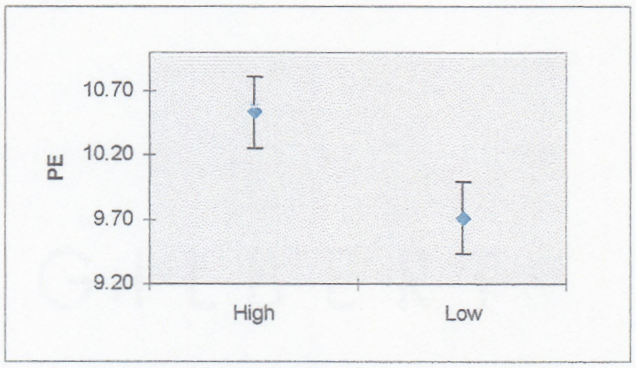

Figure 6.2. PE by perturbation magnitude.

Absolute Antagonistic Muscle Force - Significant Effects

The main effects of tracking phase (flexion or extension) and maximum Required Tracking force (50% or 70%) were significant at the $\alpha = 0.05$ level as shown in Table 6.4. No other main effects or interactions were significant at the $\alpha = 0.05$ level. Figures 6.3 and 6.4 shows the absolute antagonist force by tracking phase and perturbation magnitude.

Co-contraction Ratio - Significant Effects

The CR measure of antagonistic muscle activity was sensitive to the same effects as the AAF measure. The main effects of tracking phase (flexion or extension) and maximum Required Tracking force (50% or 70%) were significant at the $\alpha = 0.05$ level as shown in Table 6.5. No other main effects or interactions were significant at the $\alpha = 0.05$ level.

The average CR for the extension phase was 32.73 N and the average for the flexion phase was 13.04 N. The CR for the lower level of maximum required tracking force (50%) was 27.72 N and the CR for the higher level (70% of MVC) was 18.05 N. Figures 6.3 and 6.4 shows the absolute antagonist force by tracking phase and perturbation magnitude. The results are discussed in the following chapter.

TABLE 6.4 ANOVA summary table for AAF - significant effects

Factor	SS	df	MSE	F	p < F
Exertion Direction	9277	1	9277.1	27.42	0.001
Exertion Direction x S	4737	14	388		
Tracking Gain	134.25	1	134.62	5.32	0.037
Tracking Gain x S	354.25	14	25.3		

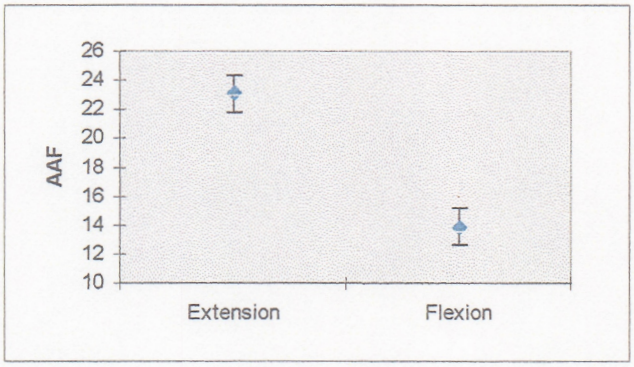

Figure 6.3. AAF by direction of exertion.

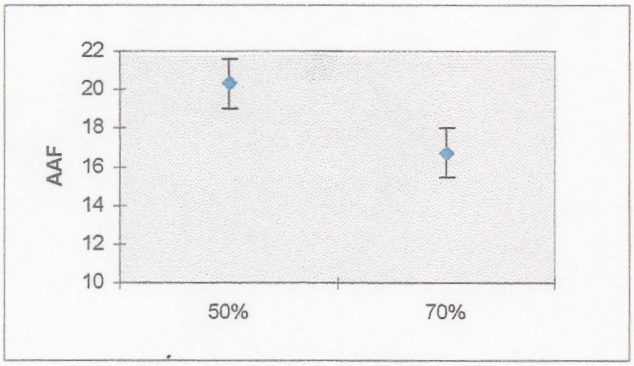

Figure 6.4. AAF by tracking gain.

TABLE 6.5 ANOVA summary for CR - significant effects

Factor	SS	df	MSE	F	p < F
Exertion Direction	43055	1	43055	50.23	0.001
Exertion Direction x S	11928	14	852		
Tracking Gain	1070	1	1070	8.71	0.011
Tracking Gain x S	1720	14	123		

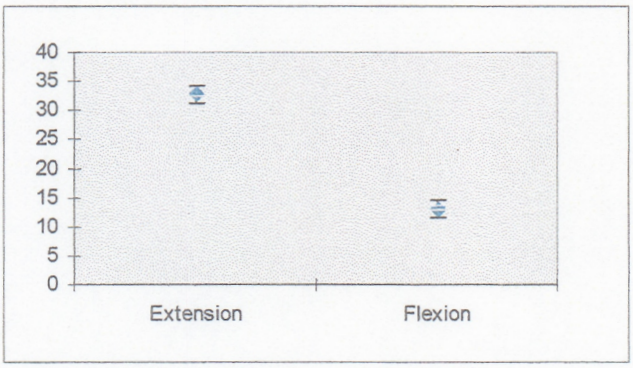

Figure 6.5. CR by exertion direction.

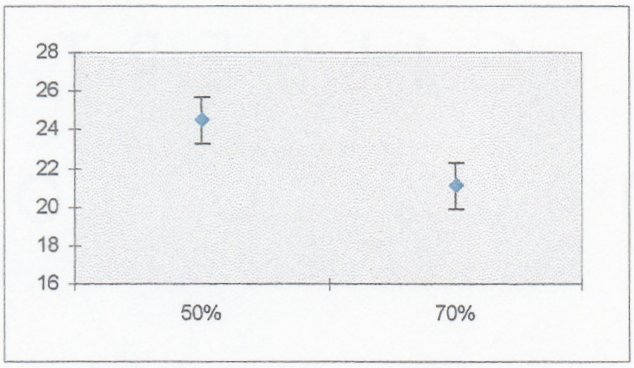

Figure 6.6. CR by tracking gain.

CHAPTER 7
DISCUSSION - EXPERIMENT 1

Overview

The purpose of this research was to investigate the whether and if so, how tracking error and antagonistic muscle force were affected by several factors. As noted earlier, Hogan's formulation impedance-control theory (Hogan, 1985c) predicts that as the magnitude or frequency of environmental perturbations increase, the motor control system would increase the level of antagonistic activity in order to minimize the effects of the perturbations on tracking performance. Hogan's results also suggests that information about any environmental perturbations might be useful in minimizing both the tracking error and antagonistic muscle force used to increase joint impedance. The error data are discussed first, followed by the antagonistic muscle force data.

Proportional Error - Significant Main Effects and Interactions

The current study found a *higher* PE error for the 70% condition than for the 50% condition. This result is somewhat surprising given the findings of other authors in similar studies. Berkowitz (1990) and Rockwell (1991) reported the results of some isometric tracking studies in which target frequency and tracking gain were varied across a range of values. Using data from several different force levels, Berkowitz (1990) and Rockwell (1991) fit quadratic models to the PE-tracking gain relationship. They both found that the PE was predicted to be at a minimum between 60 to 65% of MVC for the 1.0 Hz tracking frequency condition. The increases in the PE were most pronounced at the very low and very high end of the levels tested for required tracking force. Berkowitz argued that neuromuscular "noise" could account for

the increase in the PE at low levels of required tracking force. This constant neuromuscular "noise" would become proportionally larger as the required tracking force declined. Rockwell also adopted this explanation for increased in the PE that he found at the low end of the required tracking force. Consequently, the finding that the PE was actually greater when the maximum required tracking force was at 70% of MVC rather than at 50% of MVC was not anticipated. The procedures in the current study were somewhat different from those used by Berkowitz and Rockwell and those differences may account for the finding of a higher PE at 70% of MVC.

Most notably, the current task included perturbations to the tracking via momentary changes in the gain. Second, and perhaps more important, the current tracking task incorporated a lag to smooth out the position on the CRT of the tracking icon. In Chapter 5 it was noted that the load cell amplifier had a "buzz". The buzz increased when the amplifier gain was increased, but did not seem to be related to the force applied to the load cell. This same amplifier was used by both Berkowitz and Rockwell for their tracking studies. This buzz resulted in a "jittery" tracking icon. Pilot tests indicated that so much noise was present in the load cell output that it was some times hard to perceive an intended perturbation from the background noise while performing the tracking task This "buzz" was smoothed out by using a lag-16 moving average to plot the tracking icon. This change resulted in a stable tracking icon and made the simulated perturbations immediately evident. The incorporation of this lag necessarily changes the calculation of the proportional error (i.e. the PE is calculated using the difference between the target force and the lag-16 moving average of the applied force rather than the difference between the target force and the instantaneous applied force). This change may also have affected the subjects' tracking behavior as well.

There is another reason possible reason for finding a lower PE at the 70% maximum required tracking force. The experimental apparatus and

analysis techniques employed by Berkowitz and Rockwell do not seem able to distinguish between "neuromuscular" noise and that noise introduced by an electronic source such as the load cell amplifier. Consequently, it is possible and indeed likely that at least some of the noise was attributed to the neuromuscular system was in fact introduced by the amplifier buzz. Under anything less than ideal conditions, some amount of random noise will be unintentionally introduced by the equipment into the controlling mechanism of a tracking task. Thus, it is likely that minimum tracking error would occur at some intermediate level of required tracking force. But it is important to consider the frequency and magnitude of any noise and how it might impact the reported error.

Berkowitz argued that the "size principle" (Basmajiian and De Luca, 1985; Henneman, Somjen, and Carpenter, 1965) explained the increases in the PE found at the upper end of the required tracking force levels. This principle states that the smaller motor units are recruited first, at lower force levels, and larger ones are recruited later as the required force increases. The larger units produce proportionally larger increments as the muscle's force output is increased. This in turn means that the ability to finely adjust the output force is diminished. This explanation can also account for the increase in antagonistic muscle force discussed below. This explanation could also account for the finding of a higher PE at 70% of MVC observed in the current study.

Antagonistic Muscle Activity - Significant Effects

This study shows that the both the CR and the AAF declined as the required tracking force increased from 50% of MVC to 70% of MVC. The decline in the AAF and CR indicates that the net force applied to the wrist cuff can be increased by decreasing the antagonistic muscle force. This observation suggests another reason why the increase in error is correlated to

a decrease in antagonistic co-contraction. The net force applied is the algebraic sum of the force applied by the two muscles. At higher levels of exertion, larger motor units are recruited, resulting in larger increments in force output. Antagonistic co-contraction can smooth these increments in force output by pairing increases in the agonist with smaller increases in the antagonist. The data show that as the required tracking force increased from 50% to 70% of MVC, at least some of the additional net force was provided by the cessation of motor units of the antagonist muscle. This reduction in antagonistic activity necessarily results in a more discontinuous output of force, and thus, in more error.

The main effects suggested by the impedance control theory of Hogan (1985d) did not significantly affect the level of observed co-contraction, but one factor, the magnitude of the perturbation, did affect the error. Larger magnitude perturbations were associated with higher PE values. There are several possible reasons that the frequency of the perturbations did not affect the level of error, the most likely being that the choice to use exponentially distributed inter-arrival times resulted in higher within-cell variability. This would have the effect of increasing the standard error of each of the treatment means, which in turn would mean that any significant difference would also have to be proportionately larger.

Preview information also proved to be insignificant with regard to the trial error. The first 2.7 seconds of each trial were not used in calculating the dependent measures in order to exclude any start up effects. Since the period of the target was 2.5 seconds, subjects were exposed to the maximum required tracking force for both directions of exertions by the time the "test" period of the trial started. Subjects also could perceive the magnitude of all the subsequent perturbations from the first perturbation of the trial. Finally, frequency information applied only to the mean interarrival times. Thus, the

preview information provided no measurable utility in reducing the error minimizing the antagonistic co-contraction.

One possible reason that none of these factors affected the level of antagonistic co-contraction is that while the virtual position was changed by the perturbation, the actual tracking task was isometric. Consequently, the proprioceptive feedback that one would receive in a position-controlled tracking task was present in this isometric tracking task. Subjects may have concluded from the practice trials that stiffening the elbow provided no real advantage. Also, when the gain was momentarily changed, an increase or decrease in the required tracking force was equally likely. Thus, the response which would have minimized the error from the perturbation was a decrease in the net force on approximately half of the perturbations and an increase on the other occasions. Finally, stiffening the elbow through antagonistic activity had no impact on the error from the perturbations.

These results demonstrate the difficulty in using an isometric task to simulate the control of a limb position in space. Perturbations were simulated by momentary changes in the required tracking force. At the end of each perturbation, the required tracking force reverted to the prior level. Consequently, the effect was *two* changes in the gain. The alternative was to leave the required tracking force at the "adjusted" level following the perturbation. Prior studies had already shown that both error and antagonistic activity were affected by the level of required tracking force, so simply leaving the required tracking force at the adjusted level following the "perturbation" would have confounded the required tracking force with the occurrence of the perturbations.

This first experiment was not successful in the attempt to demonstrate a change in tracking behavior due to the presence of simulated perturbations. In reviewing the first experiment, the experimental task did not incorporate some key aspects of control of actual limb position in the presence of perturbations.

Most importantly, the position error in this task depended on only the net force applied to the isometric control. Antagonistic activity reduced the error to the extent that it could be used to regulate and smooth out this net force. In this particular task, however, the result which minimized the error was an increase half of the time and decrease half of the time in net force. Thus, there was no consistent error-minimizing response. Finally, recall that an impedance relates a input displacement with a resulting restoring force. The task employed for this experiment attempted to perturb the position of the tracking icon on-screen rather than the actual forearm position. In order to perturb the position of the tracking icon, the magnitude of the perturbation could have been expressed in terms of pixels on screen rather than the percent of MVC, but the effect would still have been a change in the required tracking force.

Thus, it appears that an isometric task cannot adequately capture the important aspects of a movement control task. This is unfortunate because the prediction of muscle forces is substantially better for isometric exertions in comparison to those which actually incorporate movement. The results and discussion of the position-controlled tracking task are presented in the following two chapters.

CHAPTER 8
RESULTS AND ANALYSIS- EXPERIMENT 2

Overview

The results obtained in the dynamic tracking study are presented in this chapter. The anthropometric measures that were measured on each subject are presented first. The next section describes the estimation of muscle forces using a modified version of the sequential parameter estimation process developed by Olney and Winter (1985) and further refined by Redfern (1988) and Woldstad (1989). The dependent measures calculated from the data are described next. The definitions of the dependent measures used in the Analysis of Variance are then described. The results of tests of normality are presented next. The significant effects are then discussed.

Anthropometric Measures

The pinch width and lower and upper arm lengths were measured as specified in Chapter 5. These data are shown in Table 8.1 below. These arm lengths were used to estimate muscle moment arms and distances between points of attachment of the muscles to the bones as described in Appendix B.

Prediction of Muscle Forces Using a Sequential Parameter Estimation Procedure

The literature concerning the estimation of muscle forces with EMGs during movement is described in some detail in appendix B. Olney and Winter (1985) originated a sequential parameter estimation procedure for estimating muscle forces from EMG data during movement. The procedure was based upon the idea that the isometric EMG-Force relation could be multiplied by a length compensation and then by a velocity compensation function to estimate

TABLE 8.1 Anthropometric measures for subjects - experiment 2.

Subject	Upper Arm (cm)	Lower Arm (cm)	Pinch Width (cm)
1	24.6	25.1	0.10
2	32.5	27.8	0.06
3	29.5	24.5	0.08
5	29.4	27.2	0.03
6	27.9	26.6	0.12
7	30.0	28.5	0.09
8	29.5	26.7	0.10

a dynamic EMG -force relation. The general form of this relation is as follows:

$$M(t) = (\sum_{i=1}^{n} K_{li}\, E_i\,(t))\,[1 + K_2\,(\theta(t) - \theta_i) + K_3\,\omega(t)]\;\; d_i$$
$$- (\sum_{i=1}^{n} K_{lj}\, E_j\,(t))\,[1 + K_2\,(\theta(t) - \theta_j) + K_3\,\omega(t)]\; d_i \qquad 8.1$$

The various *K* terms in the model should be understood as compensation functions and not simply constants. The compensation function could be a simple scalar, or it could be a quadratic or other function. The net torque exerted by each muscle is the product of the muscle force, adjusted for length and shortening velocity, multiplied by the corresponding moment arm. The muscle moment arms were estimated using the ball and socket model of the elbow joint developed by Woldstad (1989) described in Appendix B.

The static EMG relation was estimated first in the sequential estimation procedure. The term E_i (t) represents the muscle activity at time *t*. The term K_1 is the isometric force-EMG relation. Based upon the results of Woldstad (1989), a simple linear relation was used in the current study to describe the static force-EMG relation. Woldstad found that the inclusion of a quadratic term in the isometric relation resulted in poor fits of the length compensation function. In particular, he found that the model predicted a decline in muscle force with increasing EMG levels.

Once the isometric relation was determined, the length compensation function, K_2 was estimated by measuring EMG and force data across a range of six different angles. Following the procedures of Woldstad (1989) and Redfern (1988) a quadratic relation was used for the length-compensation function.

The term K_3 is a velocity compensation function, intended to compensate for a decline in muscle force with increasing shortening velocity, first noted by Hill (1938). Redfern (1988) used a quadratic relation to describe

the velocity compensation function while Woldstad (1989) used an exponential velocity compensation function. Woldstad found that fitting the velocity data with the values from the isometric force-EMG relation resulted in a poor prediction of the muscle forces. He noted that some authors had found that muscle fibers react differently when stimulated isometrically as opposed to dynamically (Vander, Sherman, and Luciono, 1970). Consequently, Woldstad re-estimated the basic force-EMG relation using a dynamic calibration. He did this by assuming a particular value for the velocity compensation parameter and then re-estimating the static force-EMG relation using dynamic data. Once he had recalculated the force-EMG parameters, he determined the optimal values for the velocity compensation function.

The approach adopted in the current study was to estimate the isometric force-EMG relation and then the length compensation function. This length-compensated estimate of the force was then scaled by a single constant to account for the non-static exertion. Thus, the approach used here was to scale the isometric length-compensated force-EMG relation by a single constant to account for the muscle shortening velocities.

An effort was made to fit a velocity compensation function to the trial data. The shortening velocities of several subjects, data were regressed against the model residuals and the regressions predicted very little of the remaining error. One possible reason for this finding is that all the tracking trials were conducted with the same frequency of the target, and the movement amplitude was constant across subjects and trials. Once the length-compensated isometric relation was scaled to account for the dynamic nature of the contraction, there remained very little nonrandom error.

The estimation of muscle forces presupposes some knowledge about the moment arms of the muscles around the joint. These moment arms were estimated with anthropometric data from the subject and the ball and socket model of the elbow developed by Woldstad (1989).

Like Redfern (1988), Woldstad (1989) used data from slow pseudo-static exertions to estimate the length tension parameters. This approach is an efficient way to sample points across the entire range of motion. On the other hand, since the muscle shortening velocities are not in fact zero, the approach may also make it difficult to accurately estimate the velocity compensation functions. In contrast, the data used to estimate the length compensation functions in the current study were all collected from static exertions at various included angles. The static exertions (flexion and extension) at the various positions were all sampled three different times during the data collection. These data were measured before the start of the tracking trials, at the half way point, and then again at the end of the data collection. This approach results in fewer data points but the measured values are from static rather than slow dynamic exertions.

The parameters of the length-tension were estimated by calculating the difference between the actual torque and the estimate of the torque from the static EMG data and the muscle moment arm model. The included arm angles were then regressed against the difference between the actual and the estimate of the torque. The estimated torque was then recalculated using the muscle moment arm estimates, the isometric torque-EMG relation and the length compensation. R^2 values for the data ranged from a low of 0.84 for subject 2 to a high of 0.97 for Subject 3. The parameters for each subject are listed in Appendix C.

The isometric relation was then multiplied by the length-tension relation to arrive at an estimate of muscle force. The product of these two functions was then used to estimate a single constant to adjust for the non-static exertion. Parameter estimates and corresponding coefficients of variation (R^2 values) for the length compensation function are given in Appendix C.

A more complex velocity compensation factor was considered but was not used. A second order velocity compensation function was calculated and

the residuals were regressed against the calculated muscle shortening velocity. However, the regressions revealed minimal correlation between the residuals and the muscle shortening velocities. Plots of the residuals against calculated muscle velocities also indicated negligible correlations between the residuals and the estimated muscle shortening velocities. Correlations were uniformly below 0.25 with most less than 0.15. Consequently, a velocity specific compensation function was not used and the length-compensated force-EMG relations were simply scaled by a constant.

The final model employed to estimate the two muscle forces was as follows:

$$T_i = MA_B(\phi) * c_{B1} * E_{B(i-\tau)} * LC_B(\phi) * VC_B - MA_T(\phi) * c_{T1} * E_{T(i-\tau)} * LC_T(\phi) * VC_T \quad 8.2$$

The term $MA_\bullet(\phi)$ is the estimate of the muscle moment arm for each respective muscle, calculated from subject anthropometry and the ball and socket model of the elbow. The "dot" subscript should be understood here to refer to either the biceps or triceps muscle. The term $c_{\bullet 1}$ is the coefficient for or the isometric force-EMG relation. The term $E_{\bullet (i-\tau)}$ is the scaled and normalized EMG for that muscle. $LC_\bullet$ is the length compensation function for each muscle, which is given as:

$$LC_\bullet = 1 + c_{\bullet 1} * (\cos(\phi) - \cos(100)) + c_{\bullet 2} * (\cos^2(\phi) - \cos^2(100)) \quad 8.3$$

The term $VC_\bullet$ is the velocity compensation factor. This term is a single constant used to scale the estimate of the muscle force to account for the effects of movement.

Coefficients of Determination obtained using this model varied substantially between subjects and between trials. The highest R^2 value across subjects and trials was 0.92. Excluding the data of Subject 4, the lowest was 0.53. The mean R^2 across trials and subjects was 0.741 and the median R^2 was 0.742.

Despite a pre-trial examination of EMGs associated with flexion and extension was done for all subjects, the EMG data from Subject 4 was only weakly correlated with the observed force. Coefficients of determination for Subject Four's trial data were uniformly below 0.5. Coefficients of determination and regression coefficients for all trials are provided in Appendix C.

Dependent Measures

Tracking error. The Root Mean Square Error was calculated from the data. Since there were no changes in the gain during or between trials in the dynamic experiment, the problems associated with the RMS measure with regard to isometric tracking noted by Berkowitz (1990) did not apply to this case. The RMS error measure was calculated as shown in equation 8.5. The RMS error was computed using data from the entire 30 second tracking trial.

$$\text{RMS Error} = \sqrt{\frac{\sum(\text{Actual Position} - \text{Desired Position})^2}{\text{Number of observations}}} \qquad 8.4$$

Antagonistic activity. The absolute antagonistic muscle force (AAF) and the co-contraction ratio (CR) were again computed from the estimates of muscle force. Chapter 6 contains definitions of these measures. As with the first experiment, the period during the perturbation and immediately following the perturbation was not included in the calculation of the AAF and the CR.

More specifically, the CR and AAF data for one half of one period was discarded after a perturbation. This was done to make certain that any difference in antagonistic activity that was observed was due to a change in the baseline level of antagonistic activity and not simply to the immediate response to the perturbation.

This approach also deals with the problem of a "missing" antagonistic exertion to which would otherwise occur to brake the forearm movement. During the normal course of a rapid, "ballistic" arm movement, the pattern of muscle activation shows an agonist "burst" which generates the force that puts the arm in motion. This is followed by an antagonist "burst", and then a final smaller agonist burst. This phenomenon was first noted by Wachholder and Altenburger (1928). The ballistic movement refers most specifically to rapid movement of a limb to a stationary target. The task conditions specify the starting and ending points, but the intermediate arm positions are unimportant. While the dynamic tracking task differs from a ballistic arm movement in some important respects, one would certainly expect to observe some antagonistic activity occurring in unperturbed tracking to brake the arm movement as the target position slows and then reverses direction. During one of the larger magnitude perturbations, the subjects' arms were essentially braked by the perturbation. By discarding one-half period of data (0.625 seconds) after the onset of the perturbation in the calculation of the antagonistic activity, the calculation of the dependent measures is resumed at a point 180 degrees out of phase. Deleting a full period (1.25 seconds) of data following a perturbation might be preferable, but because the hardware constraints limited trial duration, deleting a full period would have resulted in a many fewer data points over which to calculate the CR and AAF measures.

Verification of Normality Assumption

The assumption of normality was again verified by testing the error residuals of the three dependent measures for deviations from Normality with the Kolmogorov-Smirnov test.

The number of cases, *N*, the *D* statistic and the associated *p* values are given in Table 8.2. The *D* statistic found for each of these tests shows that the null hypothesis of no difference between the population from which the sample was obtained and the normal distribution cannot be rejected at the α = 0.05 level.

Results

RMS error. The RMS tracking error was analyzed with a within-subjects ANOVA. The main effects included direction of exertion, perturbation magnitude, perturbation frequency, and the absence or presence of preview information. The Root Mean Square Error (RMS) of the difference between the target position on screen and the actual position on screen was calculated from the data. The RMS values were then separated into flexion and extension phases. The flexion phase was specified to be that phase in which the net torque applied to the wrist cuff was positive. The extension phase was considered to be that portion of the track during which the net torque was positive.

The main effects of perturbation magnitude and perturbation frequency were significant at the α = 0.05 level. The RMS error increased as the perturbation magnitude and frequency increased as shown in Table 8.3. The RMS error for the lower magnitude perturbation was 56.7 pixels, while the smaller magnitude perturbation was 59.9 pixels. The RMS error associated with the higher frequency perturbations was 56.9 pixels, and the RMS error for the lower frequency was 59.8. Other main effects were not significant.

TABLE 8.2 Kolmogorov-Smirnov Tests for dependent measures.

Dependent Measure	N	D	p < D
Absolute Antagonist Force	112	1.0604	0.2108
Co-Contraction Ratio	112	0.4347	0.9937
Root Mean Square Error	128	1.2210	0.1014

TABLE 8.3 ANOVA summary table for RMS error - significant effects only.

Source	SS	df	MS	F-Value	P-Value
Perturbation Magnitude	344.61	1	344.61	7.08	0.032
Magnitude x S	330.77	7	7.08		
Perturbation Frequency	268.88	1	267.88	5.76	0.047
Frequency x S	325.59	7	46.51		

The main effects of the tracking phase and absence or presence of preview information were not significant. No interactions were significant at the $\alpha = 0.05$ level. The complete ANOVA summary table is shown in Appendix D. As with the results from the isometric tracking experiment, these statistics are reported without the Greenhouse-Geisser correction sometimes used with repeated measures designs.

The main effects of the tracking phase and absence or presence of preview information were not significant. No interactions were significant at the $\alpha = 0.05$ level. The complete ANOVA summary table is shown in Appendix D. As with the results from the isometric tracking experiment, these statistics are reported without the Greenhouse-Geisser correction sometimes used with repeated measures data. As noted previously, no adjustment of the degrees of freedom is needed since each effect tested has only one degree of freedom.

Measures of antagonistic activity. No main effects or interactions were significant at the $\alpha = 0.5$ level for the Absolute Antagonist Force. The main effect of perturbation magnitude on the co-contraction ratio was significant at the $p = .031$ level as shown in Table 8.4. The CR was higher for the larger perturbation condition. The co-contraction ratio for the lower perturbation magnitude condition was 45.77%, while the CR for the higher magnitude perturbation was 50.82%. No other main effects or interactions were significant. The complete ANOVA summary tables for both the AAF and the CR are shown in Appendix D.

Summary

The sequential parameter estimation procedure was used to estimate the forces generated by the biceps and triceps. Excluding the data of subject

4, the median R^2 value for the prediction of muscle forces was 0.74. The minimum R^2 was 0.53 and the highest observed R^2 was 0.92.

The analysis of the data showed that the RMS error increased as the perturbation magnitude and frequency increased. The analysis also showed that AAF was insensitive to any of the experimental manipulations but the CR was significantly higher for the larger magnitude perturbations. These results are discussed in the following chapter.

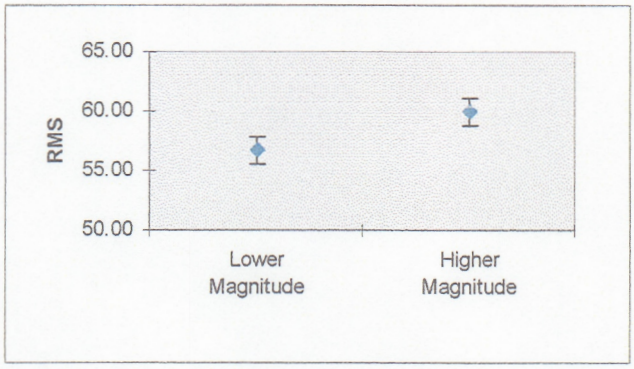

Figure 8.1. RMS by perturbation magnitude.

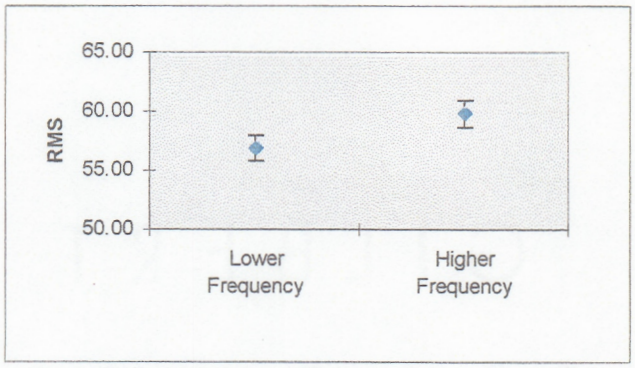

Figure 8.2. RMS by perturbation frequency.

TABLE 8.4 ANOVA summary table for co-contraction ratio - significant effects only

Source	SS	df	MS	F-Value	P-Value
Perturbation Magnitude	713.29	1	713.29	7.93	.031
Magnitude x S	539.94	6	89.99		

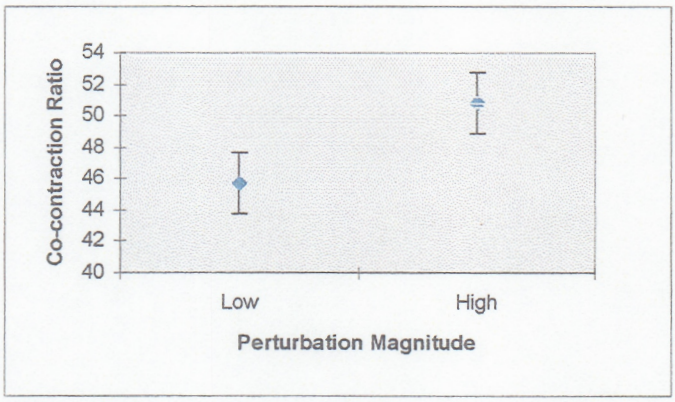

Figure 8.3. Co-Contraction ratio by perturbation frequency.

CHAPTER 9
DISCUSSION - EXPERIMENT 2

Overview

The primary goal of this research was to test the hypothesis that the level of antagonistic co-contraction would increase with increasing perturbation magnitude, perturbation frequency, and task uncertainty. The results of the error data are presented first, followed by the analysis of the antagonistic error data.

Error Data

The RMS measure did increase with increasing perturbation magnitude and frequency, but it was unaffected by task uncertainty and direction of exertion. The fact that RMS error increased with increasing perturbation magnitude and frequency is not surprising. This result is intuitive and indicates that one strategy adopted by the motor control system in the face of larger and more frequent perturbations is simply to allow the position error to increase. It also reveals a statistical difficulty in testing the effect of changes in the perturbations on the antagonistic muscle activity. Ideally, the experimenter would like to hold the error level constant and manipulate the perturbation characteristics to test the effects on the antagonistic muscle force under equivalent conditions. Failing that, one would like to account for changes in the error level using an analysis of covariance. However, as noted in earlier chapters, the use of a covariate that is affected (or in this case, determined) by the treatments presents problems of interpretation.

Antagonistic Muscle Activity

The data showed that the CR increased with increasing perturbation magnitude. No other main affects or interactions were significant. The AAF

was unaffected by any of the independent measures. As predicted, the CR increased with increasing perturbation magnitude. The CR increased from 46% to 51%. However, Table 9.1 shows an interesting feature of the data. It presents the minimum, maximum, and median CR for each subject across all trials, as well as various anthropometric measures. The minimum CR across all subjects and treatment conditions was 15%. This point is important because if one must make an assumption regarding the level of antagonistic co-contraction for a biomechanical model, one should consider the available data indicate in making that estimate. As stated in Chapter 2, the use of optimization-based force-prediction models to determine a unique solution to a linear programming problem require that the lower bound on the antagonist be specified: in most cases, an estimate of zero has been used. The selection of zero for the lower bound is not supported by this study.

The finding of an increased CR for the higher perturbation magnitude is perhaps less remarkable than the fact that the lower of the two numbers is 45%. The lowest CR across all subjects, and trials was 15%, the median CR across trials and subjects was 48%, and the mean CR was 48%.

One important feature to note from this table is that the minimum estimated CR varied substantially by subject. This suggests that individual characteristics may be as important in the level of estimated antagonistic muscle force as movement characteristics or environmental perturbations. Consequently the anthropometric data collected during the study are shown with the estimated co-contraction ratios in Table 9.1. These measures include the upper arm length (UA), the lower arm length (LA), and the pinch width (PW) the measurement of subcutaneous body fat on the upper arm. As the table shows, there were no obvious correlations between these anthropometric

TABLE 9.1 Minimum, Maximum, and Median CR Values for Each Subject

Subject	Minimum	Maximum	Median	UA	LA	PW
1	15	67	54	24.6	25.1	0.10
2	17	43	37	32.5	27.8	0.06
3	44	74	54	29.5	24.5	0.08
5	31	47	41	29.4	27.2	0.03
6	24	63	41	27.9	26.6	0.12
7	39	87	52	30.0	28.5	0.09
8	32	88	59	29.5	26.7	0.10

data and the estimated CR but the wide variation in the minimum estimated CR by subject does suggest that subject characteristics may be an important predictor of antagonistic muscle force.

Estimation of Muscle Forces During Discontinuous Movement

The relation between EMGs and force for an isometric exertion is well described by a linear relationship. The inclusion of a quadratic term typically increases the coefficient of determination, but given the collinearity between the linear and quadratic terms, this is not always advisable. As noted in chapter 6, Woldstad (1989) found that the inclusion of a quadratic term in the isometric relation caused later parameters to be poorly fitted.

A quadratic length compensation function explains a good deal of the variance not explained by the isometric model for data collected at different arm positions. Woldstad (1989) and Redfern (1988) both found that a velocity compensation factor improved the fit of the data enough to justify its inclusion. The final model used in the current study did not include a velocity specific compensation function. Rather, the length-compensated isometric function was scaled by a single constant to account for the fact that the tracking trials involved dynamic contractions. The utility of a velocity-compensation function was explored for some subjects, but these compensation functions predicted very little of the remaining unexplained variance. There are several factors which might contribute to such a finding. One important factor was that all tracking trials involved the same motion at the same tracking frequency with the same inertia. There was of course variation in the velocity of the target (and the shortening velocity of the muscles), but the effects of these changes on the relationship between EMG and muscle force appears to be rather small.

The current study not only involved movement, but also incorporated discontinuous movement due to the perturbations. The original plan was to delete the data corresponding to the time during and immediately after the perturbation before fitting the parameters to describe the force-EMG relation.

Such an approach would yield several discontinuous data segments, but none would include the period during or immediately following the perturbation. However, the force data associated with EMG signals typically lagged the filtered EMG by about 10 milliseconds so that the filtered EMG and force data had to be cross-correlated to obtain the best prediction of muscle forces. Discarding those data associated with the perturbation yielded several different data strings that had to be spliced together. This approach produced much poorer predictions of muscle forces due to the problems of matching spliced sections together.

Consequently, the muscle forces were estimated using all the data, and the "perturbed" sections of the tracking data were deleted before the calculation of the antagonistic measures. The inclusion of the perturbed data during the parameter estimation certainly affected parameter estimates, which is likely reflected in the fit of the models. While the highest R^2 for a tracking trial was 0.92, the median R^2 for the trial data was 0.78 and the minimum was 0.54 (excluding the data of Subject 4). A possible method for dealing with this problem is discussed in the following section.

Experimental Considerations

It should be noted that the hardware limitations restricted the total number of samples per trial to 32,768 (or 2^{15}). The Direct Memory Access (DMA) routines could only access one "page" of memory which contained 2^{16} (64k) bytes. The integers generated by the A/D board each required 2 bytes of memory. Since the data collection rate was 100 Hz and the number of sampled channels was 10, trial duration could be no more than 32.768 seconds.

At some future point, the hardware and software-imposed constraints may be less restrictive so as to permit the collection of more than 64k of data in one trial. The development of such a system would allow trial durations to

be increased. Under such conditions, an experimenter might have periods of tracking with perturbations interspersed with periods without perturbations. For instance, a trial might have an alternating pattern of 20 seconds with perturbations, followed by 20 seconds without. The 20 second periods of perturbed tracking could be discarded. The muscle forces could then be estimated for each of the 20 periods of unperturbed tracking. CR and AAF values could be computed for each of the remaining periods and averaged to arrive at a value for each treatment combination. Subjects might change their tracking behavior between the perturbed and unperturbed phases, but the improvement in the estimation of muscle forces would likely outweigh this concern.

The tracking experiment was specifically designed to avoid some problems noted by Woldstad (1989) in estimating the force-EMG relation. In particular, he found it necessary to incorporate additional compensation functions to account for direction of motion, changes in inertial loading, and elastic effects at the end of the ranges of motion. The tracking trial used here obviously required movement in either direction, but the level of inertial loading was held constant and motion at the extremes was avoided. But the inclusion of perturbations during this tracking task appears to have limited the predictability of the respective muscle forces. Given that perturbations were an integral part of this task, the only alternative appears to be the one outlined in the preceding paragraph.

Summary

Some problems were encountered in accurately estimating the torque-EMG relationship. These problems were likely attributable to the discontinuous nature of the perturbed tracking. The data of subject 4 proved particularly problematic. Given that the R^2 values were uniformly below 0.5, the data of this subject was not used in the statistical analysis of the estimated

co-contraction ratio and the absolute antagonist force. Since there was nothing notably awry with the error data of subject 4, his data was used in the statistical analysis of the RMS error.

The analysis of the RMS data indicated that one strategy adopted by the subjects in the face of increasing perturbation frequency and magnitude was simply to permit more tracking error. The error increased with both increasing perturbation magnitude and increasing perturbation frequency. The RMS error was unaffected by either the tracking phase (flexion or extension) or the absence or presence of pre-trial information.

The analysis of the estimated antagonistic muscle force showed that the only significant effect was the perturbation magnitude. The co-contraction ratio increased with increasing perturbation magnitude. The absolute antagonist force was not affected by the perturbation magnitude or other main effects.

CHAPTER 10
SUMMARY

Overview

Six different hypotheses were set out in the first chapter of this dissertation. These hypotheses are restated here with the results of the data analysis, followed by comments on the frequency effect, and comments on the method of implementing the perturbation and strategies for obtaining interpretable EMG data. The chapter concludes with comments on developing minimum estimates of the CR and suggestions for future studies involving the estimation of muscle forces from EMG data.

Perturbation Magnitude

The first two hypotheses address the effects of perturbation magnitude.

1) **The level of antagonistic co-contraction increases as the perturbation magnitude increases.**
2) **The tracking error increases as the perturbation magnitude increases**

The data from the first experiment indicated that the measures of antagonistic activity were unaffected by the magnitude in the simulated perturbations. Neither the co-contraction ratio or absolute antagonist force were significantly affected by the magnitude of the simulated perturbation. The results of the second experiment showed that the co-contraction ratio increased as the perturbation magnitude increased but the absolute antagonist force was unaffected by perturbation magnitude. The CR increased from 45% to 51%. It should be noted that the static tracking task with simulated

perturbations failed to incorporate some important aspects of movement. While increasing joint stiffness by raising the level of antagonistic activity would tend to reduce the position error during an actual perturbation, increasing the joint stiffness during the simulated perturbation of the static tracking task would not have the same effect.

The second hypothesis concerning the increased error was supported by the data from both the first and second experiment. The difference shows the unsurprising result that tracking performance degrades with increased perturbation magnitude. Stated differently, the subjects were unable to maintain the same error tolerances regardless of the strategies they used to compensate for the stronger perturbations.

Perturbation Frequency

The next two hypotheses address the effects of perturbation frequency.

3) **The level of antagonistic co-contraction increases as the mean number of perturbations per trial increases.**
4) **The tracking error increases as the mean number of perturbations per trial increases.**

The hypothesis that perturbation frequency would increase the level of antagonistic activity was not supported by either of the two experiments. While the mean number of perturbations for a particular frequency (3 per trial or six per trial) were the same (within a level of the treatment effect), the actual number of perturbations varied. This aspect of the frequency effect almost certainly inflated the within-treatment variance, thereby making it more difficult to establish significance for this effect. The variable number of perturbations per trial was a necessary consequence of using exponentially distributed inter-

arrival times. Future research might reconsider the effect of perturbation frequency on antagonistic activity by disregarding the degree of predictability of perturbation timing and specifying a fixed number of perturbations for each treatment condition.

Tracking error increased with increasing perturbation frequency in the dynamic experiment, but not in the static one. The reason for this finding is not clear, but it is likely there are a couple of possible explanations. One reason for the failure to find significance at the at the $\alpha = 0.05$ level for the perturbation frequency effect was discussed in chapter 7. It was noted there that inter-arrival times were exponential random variables. The memoryless property of the exponential distribution was desired so that the subject could not predict the timing of the next perturbation from the last perturbation. This method of selecting the interarrival times would necessarily increase the within-treatment random error over an approach where the interarrival times were fixed and predictable.

Preview Information

The last two hypotheses were as follows:

5) The level of antagonistic co-contraction increases as the information provided about the perturbations decreases.

6) The level of antagonistic co-contraction increases as the information provided about the perturbations decreases.

These hypothesis were not supported by either study. Subjects were unable to use such information to either reduce tracking error or to reduce the energy expenditure due to antagonistic activity. This factor was particularly difficult to test accurately. In the case of the current study, information

concerning the frequency was of limited utility, since the actual number of perturbations was not constant for the low-frequency or high frequency conditions. Information concerning the magnitude of the perturbation was actually useful only for the period of the trial before the first perturbation. Since the levels of perturbation magnitude were so distinctly different, the perturbation magnitude for that trial was after the first perturbation was readily apparent to the subject.

Future Research

Method of implementing the perturbations. Perturbations were implemented in the isometric study by sudden changes in the gain and in the dynamic study by sudden changes in the resistance of the lever arm. The changing of the gain in the first study had no measurable effect on the antagonistic muscle activity. The alternatives for simulating a perturbation to an actual movement using a static task were not very good. It does not appear to be possible to adequately simulate an actual movement with an isometric tracking task.

The dynamic tracking task used a Baltimore Therapeutic Equipment Device to implement the perturbation. As discussed in Chapter 5, consideration was given to perturbing the lever arm by using a torque motor which could actually displace the arm rather than simply impede the movement. However, there were issues of both subject safety and feasibility to consider with this approach. Since the perturbation was to be implemented by momentarily switching the torque motor on, there were substantial concerns for the safety of the subjects if for any reason the motor failed to switch back off. The subject's arm might be severely injured. There were also feasibility problems with getting the sort of pulse profile desired from an electric motor. The torque output of an electric motor is proportional to the rotating angular velocity. Electric motors with the capacity to generate sufficient torque have

substantial inertia and must develop torque slowly. They also spin down slowly. Consequently, for both methodological and safety reasons, the BTE proved to be a superior (but certainly not perfect) means by which to implement the perturbations.

There is a also a third alternative not previously considered. What is needed to generate the perturbations is essentially some sort of device which can apply force briefly to the lever arm. A plot of the applied force over time should resemble a pulse, with a rapid build up, a short duration, and then a rapid decline. Ideally, it should be able either to brake or accelerate a movement. A spring-loaded device might meet these criteria, but such a device would be difficult to reset or reload during a tracking trial. It is also difficult to conceive of how such a spring might be attached to the rotating lever arm assembly. Another method that might satisfy these criteria is the use of small CO_2 cartridges mounted perpendicular to the lever arm. If these could be activated by an electronic switch, the timing could be controlled by the computer using a digital to analog output. When activated, the CO_2 cartridges would produce a force perpendicular to the axis of the lever arm and apply a perturbing force in one direction or the other. The orientation of the cartridges (and thus the direction of the perturbation) would have to be fixed in advance of the trial, but the subject would not necessarily need to be informed of the direction. Cartridges would have to be changed between each trial, but that should not present too great a difficulty. Of course, the force generated by the CO_2 cartridges would have to be small enough to ensure that there was no risk of harm to the subject. Perturbations would likely need to be restricted to the middle of the range of movement to minimize the chance that a perturbation occurring at the extremes of movement might result in injury.

Strategies to obtain interpretable EMG data. While certain features of movement may be interesting, there is little point in measuring the EMGs under conditions where fit of the force-EMG relation is poor. The findings of

Woldstad (1989) indicate that low inertia movements are problematic. This study also indicated that additional compensation factors may be required for movements at the ends of the range of motion to account for viscoelastic properties of the muscles.

The data also show that the basic force-EMG relation for dynamic movements is substantially different from that of static exertions. Thus, a suitable method of estimating the isometric coefficients with data collected during a movement is needed. Neither the approach adopted by Woldstad nor the method used in the current study were entirely satisfactory in this regard. Woldstad had to assume certain values for his velocity compensation parameters in order to re-estimate the basic force-EMG relation. He then recalculated his velocity compensation parameters to best fit the data.

The approach used here was simply to scale the estimate of the trial torque derived from the static torque-EMG relation and the length compensation function by a constant to account for the effects of movement. A more complex second order velocity compensation function was considered, but this function failed to account for much additional variance in the observed torque. Consequently, it was not included in the final model. It is possible and indeed likely that such velocity-specific compensation functions would prove useful for EMG data collected without perturbations. However, the problem regarding how to estimate the basic torque-EMG relation under conditions of movement remains.

This study found that subjects responded to increased perturbation magnitude and increased perturbation frequency by increasing their error tolerance. The increase in perturbation magnitude also resulted in an increase in the co-contraction ratio. Several future studies are suggested by the results presented here. One experiment suggested by these results is essentially a refinement of the current study. Perturbations would be scheduled to occur at a specific point in the movement, and perturbations would be scheduled at that

point during both flexion and extension phases. Perturbations would be implemented by some means similar to the use of compressed CO_2 cartridges suggested above. Perturbation magnitude could be manipulated by changing the point at which the cartridges were attached to the rotating lever arm (i.e., by changing the moment arm through which the force is exerted).

If the hardware and software were sufficiently advanced to permit it, trial duration could be substantially longer. Trials would consist of periods with perturbations (10 to 15 seconds in duration) interspersed with periods with no perturbations (20 to 30 seconds in duration). Muscle forces would be estimated and dependent measures calculated using only the unperturbed segments.

A parallel line of research, suggested by the findings of Woldstad (1989), is an investigation of movement characteristics on the antagonistic activity. The parameters of Fitt's Law, (movement time, movement amplitude, target width) are likely to affect the level of antagonistic muscle activity. Woldstad found that both the active and antagonistic muscle force increased with inertial load and movement amplitude. However, the proportion of co-contractive torque decreased substantially with increased inertial load and increased moderately with movement amplitude. In terms of the measures used in this study, Woldstad found that the CR decreased with increased load but increased with movement amplitude. Since the low inertia condition was associated with poorer estimation of the muscle forces, further investigation of this effect is probably not merited.

A review of the data of this study and previous studies show that subject characteristics and movement characteristics are likely to account for as much of the observed variation in the CR as the characteristics of any perturbations. Future studies should certainly consider subject characteristics and movement characteristics in determining an estimate of the CR.

REFERENCES

Agarwal, G.C., and Gottlieb, G.L. (1977). Oscillation of the human ankle joint in response to applied sinusoidal torque on the foot. *Journal of Physiology (London), 268* 151-176.

Anderson, J.E. (1983). *Grant's atlas of anatomy.* Philadelphia, PA: Lea and Fibiger.

Andersson, B.G.J., Pope, M.H., Frymoyer, J.W., and Snook, S. (1991) Epidemiology and cost. In M.H. Pope, G.B.J. Andersson, and D.B. Chaffin (Eds.) *Occupational low back pain* (pp 95-113). Boston, MA: Mosby Year Book.

Andrews, J.G. and Hay, J.G. (1983). Biomechanical considerations in the modeling of muscular function. *Acta Morphologica. Neer-Scandinavia, 21,* 199-223.

Angel, R.W. (1977). Electromyography during rapid arm movements: Central versus proprioceptive influences. *Journal of Neurology, Neurosurgery, and Psychiatry, 40,* 683-686.

Basmajian, J.V., and De Luca, C.J. (1985). *Muscles alive.* Baltimore, MD: Williams and Wilkins.

Bean, J,.C., and Chaffin, D.B., and Shulz, A.B. (1988). Biomechanical model calculations of muscle contraction forces: A double linear programming method. *Journal of Biomechanics, 21,* 59-66.

Beckett, R and Chang, K. (1968). Analysis of gait using a minimum energy approach. *Journal of Biomechanics, 1,* 147-159.

Berkowitz, J. (1990). *Required force level and isometric tracking.* Unpublished master's thesis, Virginia Polytechnic Institute and State University, Blacksburg, VA.

Bizzi, E., Accornero, N., Chapple, W., and Hogan, N. (1984). Posture control and trajectory formation during arm movement. *Journal of Neuroscience, 5,* 2738-2744.

Bouisset, S., Lestienne, F. (1977). The stability of synergy in agonists during the execution of a simple voluntary movement. *Electroencephagraphy and Clinical Neurophysiology, 42,* 543-551.

Bouisset, S. (1973). EMG and muscle force in normal motor activities. In J.E. Desmedt (Ed.), *New developments in EMG and clinical neurophysiology,* (pp 54-68). Brussels: Karger.

Caldwell, L.S., Chaffin, D.B., Dukes-Dobos, F.N., , Kroemer, K.H.E., Laubach, L.L., Snook, S.H., and Wasserman, D.E. (1974). A proposed standard procedure for static muscle strength testing. *American Industrial Hygiene Association Journal, 35,* 201-206.

Chaffin, D.B. (1975). Ergonomics guide for the assessment of human static strength. *American Industrial Hygiene Association Journal, 36,* 505-511.

Cnockaert, J.C., Lensel, G., and Pertuzon, E. (1975). Relative contributions of individual muscles to the isometric contraction of a muscle group. *Journal of Biomechanics, 8,* 191-197.

Crisco, J.J., and Punjabi, M. (1990). Postural biomechanical stability and gross muscle architecture in the spine. In (Eds.) J.M.Winters and Savio L-Y Woo *Mutliple muscle systems: biomechanics and movement organization.* (pp 438-450). New York: Springer-Verlag.

De Luca, C.J., and Mambrito, B. (1987). Voluntary control of motor units in human antagonist muscles: coactivation and reciprocal activation. *Journal of Neurophysiology, 58,* 525-542.

Ericson, B.E., and Hagberg, M. (1978). EMG signal versus external force: a methodological study on computer aided analysis. In E. Asmussen and K. Jorgensen (Eds.), *Biomechanics VI-A.*, (pp 251-255). Baltimore, MD: Baltimore University Park Press.

Feeman, G.F. (1970). *Linear algebra and multivariable calculus.* New York: McGraw-Hill.

Frost, G. (1972). Man-machine dynamics. In H.P. Van Cott amd R.G. Kinkade (Eds.),, *Human engineering guide to equipment design. (*pp 227-310). New York: John Wiley and Sons.

Gere, J.M., and Timoshenko, S.P. (1984). *Mechanics of materials* (2nd ed.). Boston, MA: PWS Engineering.

Ghez, C. (1987). Contributions of central programs to rapid limb movement in the cat. In H. Asunama and V.J. Wilson (Eds), *Integration in the nervous system (*pp 305-320). Tokyo, Japan: Igaku-Shoin.

Goodwin, G.M., Hoffman, D. and Luschei, E.S. (1978). The strength of the jaw closing in response to sinusoidal stretch of monkey jaw closing muscles during voluntary contraction. *Journal of Physiology (London), 279,* 89-111.

Gordon, A.M., Huxley, A.F., and Julian, F.J. (1966). Variations in isometric tension with sarcomere length in vertebrate muscle fibres. *Journal of Physiology (London), 184,* 170-192.

Hasan, Z. (1986). Optimized movement trajectories and joint stiffness in unperturbed, inertially loaded movements. *Biological Cybernetics 53,* 373-382.

Hill, A.V. (1938). The heat of shortening and dynamic constants of muscle. In *Proceedings of the Royal Society (London)* (pp. 263-274). London: Royal Society.

Hof, A.L., and Van den Berg, J.W. (1981). EMG to force processing parts I-IV. *Journal of Biomechanics, 14* , 747-792.

Hogan, N. and Mann, R.A. (1980). Myoelectric signal processing: optimal estimation applied to electromyography-Part I: derivation of the myoprocessor. *IEEE Transactions on Biomedical Engineering, 27,* 382-395.

Hogan, N. (1984a). Adaptive control of mechanical impedance by coactivation of antagonistic muscles. *IEEE Transactions on Automatic Control, 29,* 681-690.

Hogan, N. (1984b). An organizing principle for a class of voluntary movements. *Journal of Neuroscience, 5,* 2745-27454.

Hogan, N. (1985a). Impedance control: an approach to manipulation: part 1 - theory. *Journal of Dynamic Systems, 107,* 1-7.

Hogan, N. (1985b). Impedance control: an approach to manipulation: part 2 - implementation. *Journal of Dynamic Systems, 107,* 8-16.

Hogan, N. (1985c). Impedance control: an approach to manipulation: part 3 - applications. *Journal of Dynamic Systems, 107,* 17-24.

Hogan, N. (1985d). The mechanics of multi-joint posture and movement control. *Biological Cybernetics, 52,* 315-331.

Hughes, R.E. (1991). *Empirical evaluation of optimizatiion-based lumbar muscle force prediction models.* Unpublished doctoral dissertation, University of Michigan, Ann Arbor, MI.

Ismail, H.M., and Ranatunga, K.W. (1978). Isometric tension development in a human skeletal muscle in relation to its working range of movement: the length tension relation of the biceps brachii muscle. *Experimental Neurology, 62,* 595-604.

Joyce, G.C., Rack, P.M.H., and Ross, H.F. (1974). The forces generated at the human elbow joint in response to imposed sinusoidal movements of the forearm. *Journal of Physiology (London), 240,* 351-374.

Joyce, G.C., Rack, P.M.H. (1969). The mechanical properties of the cat soleus muscle during controlled lengthening and shortening movements. *Journal of Physiology (London), 240,* 351-374.

Kaplan, W. (1984). *Advanced calculus.* Reading, MA: Addison-Wesley.

Karnopp, D., and Rosenberg, R. (1975)., *System dynamics: a unified approach.* New York: Wiley.

Karst,G.M., and Hasan, Z. (1987). Antagonist muscle activity during human forearm movements under varying kinematic and loading conditions. *Experimental Brain Research, 67,* 391-401.

Komi, P.V. (1973). Relationship between muscle tension, EMG and velocity of contraction under concentric and eccentric work. In J.E. Desmedt (Ed.), *New developments in Electromyography and Clinical Neurophysiology (pp.* 596-606). Brussels: Karger.

Komi, P.V., and Vitalaso, J.H.T. (1976). Signal characteristics of EMG at different levels of muscle tension. *Acta Physiologica Scandinavia, 96,* 267-276.

Lacquaniti, F., Licata, F., and Soechting, J.F. (1982). The mechanical behavior of the human forearm in response to transient perturbations. *Biological Cybernetics, 44,* 35-46.

Lanman, J.M. (1980). *Movement and the mechanical properties of the intact human elbow joint.* Unpublished doctoral dissertation, Massachusetts Institute of Technology, Cambridge, MA.

Lawrence, J.H., and De Luca, C.J. (1983). Myoelectric signal versus force relationship in different human muscles. *Journal of Applied Physiology, 54,* 1653-1659.

Lehman, S.L. and Stark, L.W. (1981). Perturbation analysis applied to eye, hand, and arm movements. *IEEE transactions on Systems, Man and Cybernetics, 13*, 927-979.

Lindstrom, L. Magnusson, and Petersen, I. (1970). Muscular fatigue and action potential conduction velocity changes studied with frequency analysis of EMG signals. *Electroencephalography and Clinical Neurophysiology*, *4,* 341-353.

Lippold, O.C.J. (1952). The relation between integrated action potenials in human muscle and its isometric tension. *Journal of Physiology (London), 117,* 492-499.

Marsden C.D., Merton, P.A., and Morton, H.B. (1972). Servo action in human volunatry movement. *Nature, 238,* 140-143.

Marsden C.D., Merton, P.A., and Morton, H.B. (1976). Servo action in the human thumb. *Journal of Physiology (London), 257,* 1-44.

Marsden C.D., Obeso, J.A., Rothwell, J.C. (1983). The function of the antagonist muscle during fast limb movements in man. *Journal of Physiology (London), 335,* 1-13.

Maton, B., and Bouisset, S. (1977). The distribution of activity among the muscles of a single group during isometric contraction. *European Journal of Applied Physiology, 37,* 101-109.

Messier, R.H., Duffy, J., Lichtman, H.M., Paslay, P.R., Soechting, J.F., and Stewart, P.A. (1971). The electromyogram as a measure of tension in the human biceps and triceps muscle. *International Journal of Mechanical. Sciences, 13,* 585-598.

Moritani, T., and Devries, H.A. (1978). Reexamination of the relationship between the surface integrated electromyogram and the force of isometric contraction. *American Journal of Physical Medicine, 57,* 263-277.

Mussa-Ivaldi, F., Hogan, N., and Bizzi, E. (1984). Neural, mechanical, and geometric factors subserving arm posture in humans. *Journal of Neuroscience, 5,* 2732-2743.

Nevins,J. and Whitney, N. (1978). Computer-controlled assembly. *Scientific American, 238,* 62-74.

Niku, S., and Henderson, J.M. (1985). Determination of the parameters for an atheotic arm model. *Journal of Biomechanics, 18,* 209-215.

Nussbaum, M.A., Chaffin, D.B. and Rechtien, C.J. (1995). Muscle lines-of-action affect predicted forces in optimization-based spine muscle modeling. *Journal of Biomechanics, 28,* 401-409.

Nussbaum, M.A. and Chaffin, D.B. (1995). Development and evaluation of a geometric model of the human torso. *Clinical Biomechanics, 11,* 25-34.

Olney, S.J., and Winter, S.J. (1985). Predictions of knee and ankle moments of force in walking from EMG and kinematic data. *Journal of Biomechanics, 18,* 9-20.

Penrod, D.D., Davey, D.T., and Singh, D.P. (1974). An optimization approach to tendon force analysis. *Journal of Biomechanics, 7,* 123-129.

Rack, P.M.H., and Westbury, D.R. (1969). The effects of length and stimulus rate on tension in the isometric cat muscle. *Journal of Physiology (London), 204,* 443-460.

Ralston, H.J. Todd, F.N. and Inman V.T. (1976). Comparison of electrical activity and duration of tension in the human reactus femoris muscle. *Electroencephalography and Clinical Neurophysiology, 16,* 271-279.

Redfern, M.S. (1988). *Electromyographic (EMG) signal processing and biomechanical modeling of the lower leg muscles.* Unpublished doctoral dissertation, University of Michigan, Ann Arbor, MI.

Rockwell, C. (1992). *Characteristics of muscle co-contraction during isometric tracking.* Unpublished master's thesis, Virginia Polytechnic Institute and State University, Blacksburg, VA.

Salas, Saturnino, L. (1986). *Calculus: one and several variables, with analytic geometry.* New York: Wiley.

Schulz, A.B. and Anderson, G. B.J. (1981). Analysis of loads on the lumbar spine. *Spine, 6,* 76-82.

Schmidt. R.A., Zelaznik, H. Hawkins, B., Grant,. J.S., and Quinn, J. T. (1979). Motor output variability: A theory for the accuracy of motor acts, *Psychological Review, 86*, 415-451.

Seigler,S., Hillstrom, H.J., Freedman, W. and Moskowitz, G. (1985). Effect of myoelectric signal processing on the relationship between muscle force and processed EMG. *American Journal of Physical Medicine, 64,* 130-149.

Serig, A., and Avikar, R.J. (1973). A Mathematical model for evaluation of forces in lower extremeties of the musculo-skeletal system. *Journal of Biomechanics, 6,* 313-316.

Sherrington, C.S. (1905). *The integrative action of the nervous system.* New Haven, CT:Yale University Press.

Siegel, S., and Castellan J.N. (1988). *Nonparametric statistics for the behavioral sciences.* New York: McGraw-Hill.

Smith, A.M. (1981). The co-activation of antagonist muscles. *Canadian Journal of Physiology and Pharmacology, 59,* 733-747.

Tinley, F., and Pike. F.H., (1925). Muscular coordination in experimentally studied in relation to the cerebellum. *Archives of Neurology and Psychiatry, 13,* 289-334.

Vander, A.J., Sherman, J.H., and Luciano, D.S. (1970). *Human Phyiology.* New York: McGraw-Hill.

Wachholder, K., and Altenburger, H. (1926). Beitrage Physiologie der willkurlichen Bewegung, IX-X, *Pfluger's Archiv:* 625-66. (As cited by Angel, 1977)

Warfel, J.H. (1985). *The extremities: muscles and motor points.* Baltimore, MD: Williams and Wilkins.

Weineke, G.H., Derneir van der Gon, J.J. (1974). Variations in the output motor impedance of the human motor system. *Kybernetik, 15,* 159-178.

Winer, B.J., Brown, D.R., and Michels, K.M. (1991). *Statistical Principles in Experimental Design.* New York: McGraw-Hill.

Winters, J.M., Stark, L., and Seif-Naraghi, A.H. (1988). An analysis of the sources of musculo-skeletal system impedance. *Journal of Biomechanics, 21,* 1011-1026.

Woldstad, J.C., (1989). *Electromyographic analysis of rapid, accurate elbow movements.* Unpublished doctoral dissertation, University of Michigan Ann Arbor, MI.

Woldstad, J.C., Chaffin, D.B., and Langolf, G.D. (1988). Co-Contraction during isometric elbow exertions. In *The Proceedings of the Twelfth Annual Meeting of the American Society of Biomechanics.* (Available from J.C. Woldstad, Texas Tech University, IE Dept., Mail Stop 3061, Lubbock, Texas 79409)

APPENDIX A

BACKGROUND AND METHODS FOR THE CALIBRATION OF THE STATIC FORCE-EMG RELATION

Electromyography and Estimation of Individual Muscle Forces

The contraction of a muscle is accompanied by electrical activity. The muscle cell membrane is depolarized and repolarized. Small but measurable changes in the potential difference between two points on the skin above the muscle can be observed. The magnitude of these voltage swings observed on the skin reflect the effects both of the *number* of individual motor units that fire and the *rate* at which they fire (Basmajian and De Luca, 1985). A typical EMG trace is shown in figure A.1 below.

Lippold (1952) first observed that the force exerted by muscles was proportional to the integral of the absolute value of the EMG signal (iEMG) as defined in equation A.1. Lippold measured the iEMG activity and attempted to predict the observed torque from the iEMG using the relation shown in equation A.2

$$iEMG(t) = \int_0^t | EMG(t) | \, dt \qquad A.1$$

$$Torque(t) = \beta_0 + B_1 \, iEMG(t) + \varepsilon \qquad A.2$$

In a series of ten experiments Lippold examined the EMG signals of the soleus and gastrocnemius during plantar flexion. He found R^2 values ranging from 0.93 to 0.99 using this linear relation between torque and iEMG. This linear relationship was subsequently confirmed by a number of other

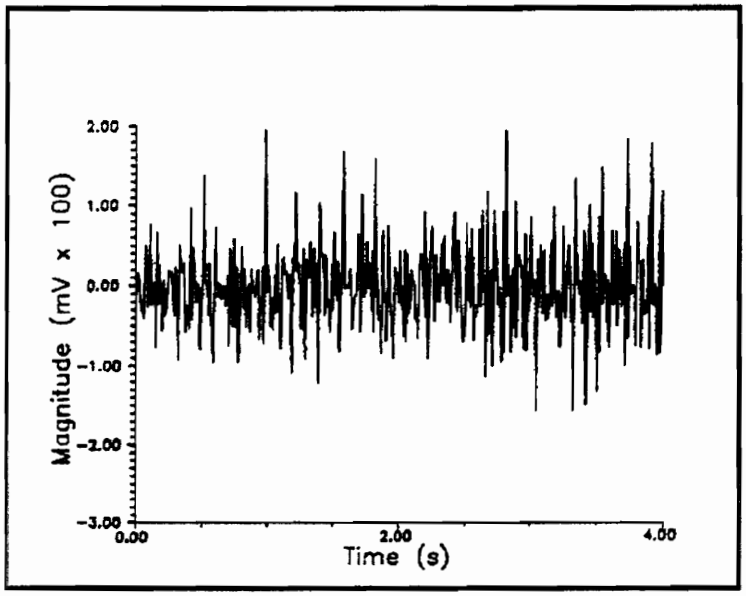

Figure A.1. Raw EMG trace.

researchers (Moritani and Devries, 1978; Ericson and Hagberg, 1978; Hof and Van den Berg, 1981). In contrast, others have found that a quadratic component was necessary to adequately describe the relationship as shown in equation A.3 (Zuniga and Simmons, 1969; Cnockaert, Lensel, and Pertuzon, 1975. Komi and Vitalaso, 1976; Lawrence and DeLuca, 1983; Siegler, Hillstrom, Freedman and Moskovitz; 1985).

$$\text{Torque}(t) = \beta_0 + \beta_1\, \text{iEMG}(t) + \beta_2\, \text{iEMG}^2(t) + \varepsilon \qquad \text{A.3}$$

In a study involving normal subjects, pianists, swimmers, and power lifters, Lawrence and DeLuca (1983) found that the degree to which the relation was nonlinear was apparently dependent on the amount of use of the muscle received. The relation was most nearly linear for swimmers and most nonlinear for normals.

An important result from mathematics should be noted here. Any continuous function can be expressed as a Taylor series expansion about the point on the function. Thus, adding additional terms (quadratic, cubic, etc.) can *only* improve the fit of the torque-EMG relation as measured by the R^2 criterion. On the other hand, as additional terms which are *not* orthogonal to the parameters already in the model are added, the variance of the parameters and the variance of the prediction both increase. Consequently, the improvement in the R^2 criterion must be weighted against the increase in the variance of the parameters.

If the EMG-torque relation is principally linear, then the effect of including a quadratic term would be to substantially increase the variance in the prediction without much improvement in the accuracy. If the relation is truly nonlinear, then a quadratic term will be needed to obtain an accurate prediction. Using methods similar to those of the proposed study, Woldstad

found that the basic torque-EMG relation was well described by a model with only the linear term. The inclusion of the quadratic term did not substantially improve the fit of the model. In contrast, the addition of a quadratic term considerably improved the R^2 criterion for the force-EMG relationship of some subjects in this study. The largest increase in the R^2 was also noted for those subjects for which the fit was the poorest. In order that all subjects' data be treated in the same way, a quadratic model was used for all subjects in the first experiment.

Woldstad (1989) noted an additional problem with the use of a quadratic model for prediction of muscle force from EMG data when different arm positions (i.e. different muscle lengths) were considered. In particular, Woldstad found that increasing EMG values were associated with decreasing levels of force. Woldstad noted that such a relationship is "physically untenable" since muscle force should increase monotonically with increasing EMG activity. The procedure used to account for changes in muscle length is described in appendix B. Consequently, a quadratic model was used for the data from the isometric experiment, but a linear model of the torque-EMG relation was used for the data from the dynamic tracking experiment.

Recent Advances in the Analysis of EMG Data

Several improvements have been made in recent years in the collection, processing, and filtering of EMG signal. The EMG trace shown in Figure 1 is instrumental in understanding the value of these developments. Note that the average value of the voltage difference between the electrode pair is approximately zero.

Lippold (1952) proposed taking the absolute value of the integral of the voltage over time. This operation yields a strictly positive result that is well correlated to the force exerted by the muscle. However, other processing methods such as the root mean square of the voltage also yield a strictly

positive value. One of the questions Redfern (1988) addressed was whether one method could be shown to be superior for theoretical or practical reasons. Redfern's results are discussed below.

A second issue is the placement and spacing of the electrodes on the skin. If one chose a slightly different placement of either or both electrodes, the voltage observed would be different. The activity observed for a single electrode pair reflects the size and firing rate of different motor units as well as each motor unit's proximity to the electrodes. The differences may be (and often are observed to be) substantial. The question then arises of how to determine which electrode placement is best. Alternatively, one might ask if a single pair of electrodes can in fact be representative of the activity of an entire muscle. Consequently, a second question addressed by Redfern concerned how many electrode pairs are needed in order to obtain a representative measure of a muscle's electrical activity.

A third point addressed by Redfern was the use of different filtering techniques. Noise must be expected to be present in any EMG signals obtained for reasons addressed below. Consequently, Redfern (1988) also addressed the question of which filtering method might be the best. Woldstad (1989) also considered this issue. The results of these two authors' work are addresses below.

A few words are needed regarding the terminology used by Redfern (1988) to refer to EMG signals at various stages of processing. Redfern called the time-varying voltage differences between a pair of electrodes on the skin the "raw" signal or "raw" EMG. He termed the output of the iEMG or RMS processors of the raw signal the "physical" signal. As part of his EMG data collection techniques, Redfern developed a method in which the physical signals of several pairs of electrodes over a single muscle were normalized and then averaged. He referred to the result of this operation as the "derived" signals. Finally, Redfern the derived signals are digitally filtered to reduce the

noise in the signal. Redfern called the output of this last step the "processed" signal or the active state (AS). This terminology will be used in the discussions that follow.

Initial EMG processing. Three popular methods of EMG processing were evaluated by Redfern (1988). These techniques included a modified form of the integrated EMG (iEMG) introduced previously, the rectified mean square (RMS) and a modified form of the rectified mean square (mRMS). The modification of the processing technique in both the iEMG and mRMS processors consists of weighting more recent EMG data more heavily. This weighting is accomplished by the convolution of an exponential and the derived signal. The expressions for these three forms are as follows:

$$\text{iEMG}(t) = \frac{1}{\tau}\int_0^t |\,\text{EMG}\,|\, e^{-(t-\theta)/\tau} d\theta \qquad 0 < \theta \le t \qquad \text{A.4}$$

$$\text{RMS}(t) = \sqrt{\frac{1}{\tau}\int_0^t \text{EMG}^2(\theta)\, d\theta} \qquad 0 < \theta \le t \qquad \text{A.5}$$

$$\text{mRMS}(t) = \sqrt{\frac{1}{\tau}\int_0^t \text{EMG}^2(\theta)\, e^{-(t-\theta)/\tau} d\theta} \qquad 0 < \theta \le t \qquad \text{A.6}$$

Redfern noted that the outputs of the three processors were the same under conditions of constant input. However, under conditions of variable input the iEMG signal was smaller by a factor $\sqrt{2/\pi}$. Thus, the iEMG signal is estimated to be approximately 0.80 of the RMS values. Redfern also investigated the response of the three processors to a pulse input. Using digital simulation techniques, Redfern found that all three techniques differed. Specifically, the rise and fall times of the three processors differed. The rise

and fall times of the iEMG technique were nearly equivalent. In contrast, the rise times of the RMS processor were faster than the fall times. In addition, the rise and fall times associated with the true RMS technique were slower than with the mRMS technique.

Redfern tested these predictions in the laboratory. He compared the output of these processors for data collected during a constant isometric contraction and during a pulse contraction. As expected, Redfern found that output of the iEMG processor was about 80% of that of the RMS and mRMS processors for both conditions tested by Redfern. He also found differences between the rise and fall times of the three processors during the pulse contraction as predicted. The rise time of the mRMS technique was the fastest and the iEMG was the slowest. The fall times of the RMS technique were significantly longer than either of the other two processors. Redfern observed that "the rise and fall characteristics of the processor are in effect modeling the time constants of the muscle." He noted that previous authors (Ralston et al., 1976; Redfern, 1984) had found that muscle force rise times are usually faster than the fall times. Redfern found that the RMS and mRMS methods of processing more nearly mimic the muscle force buildup and decline.

The RMS technique was selected over the mRMS technique because of equipment considerations. The EMG amplifier used in this study could also produce a true RMS output through its analog circuitry in addition to the raw EMG signal. If the mRMS signal were used, the raw signal would have to have been sampled and later processed to yield the desired output. In addition to the extra processing, it might have been necessary to sample the signal at a higher rate and shorten the trial duration.

Development of a multi-electrode array. As indicated above, the placement of the individual electrodes affects the raw EMG trace obtained. If one changes the position of one or both electrodes, a different trace is obtained. This change may be attributed to the several factors. The raw EMG

signal really reflects the proximity, size, and firing rate of motor units to the electrode pair as well as the resistance of the skin. This problem of spatial bias was first identified by Lindstrom et al. (1970). These authors found that the gain and the phases of the recorded signal were affected by electrode placement. Hogan and Mann (1980) investigated the possibility that the use of two electrode pairs might reduce this spatial bias. The output of the two electrode pairs could then be averaged to arrive at the estimate of the muscle's activity. They in fact found that the use of two electrode pairs reduced the spatial bias and resulted in a more representative estimate of the muscle activity.

Redfern (1988) evaluated how the reproducibility of EMG data was affected by the use of additional electrode pairs. Redfern constructed an electrode array with four pairs of electrodes. Starting with a single pair, he tested the utility of using the additional pairs by noting the reduction in inter-trial variability by successively using more electrode pairs. To compare how reproducible the EMG signals were between trials, Redfern used the variance ratio proposed by Hershler and Milner specifically for the evaluation of EMG processing methods (1978). This statistic is a measure of how reproducible the data are across trials. A value of 1 indicates that the data are completely irreproducible and a value of zero indicates that the EMG are completely reproducible. Redfern found that the statistic decreased steadily as the number of electrode pairs increased. However, while the reduction in variance was significant as the number of pairs was increased from one to two and two to three, the decrease was not significant for the fourth pair. Thus, there is a point of diminishing returns with additional electrode pairs. While the variance reduction was not statistically significant between three and four electrode pairs, the measured value was still less for the use of four pairs.

EMG filtering techniques. A third improvement in EMG signal processing suggested by Redfern was the introduction of Walsh-Hadamard

Technique (W-H) for the filtering of the derived EMG signals. The W-H method of filtering is based upon square waves rather than sine waves. Previous filtering of EMG had generally been based upon the sinewave-based representation of the actual signal, such as Fourier or Laplace transforms. Redfern noted that several previous researchers (Meyer et al. 1982; Schmidt et al. 1979; Lehman and Stark 1981) had asserted that the neural input to the muscle could be represented as a pulse. Redfern argued that if the derived EMG signal is in fact some combination of pulses and noise, W-H filtering is fundamentally more suited to the processing of the EMG signal.

Redfern tested the use of W-H filtering in an isometric tracking task. Subjects were asked to track a signal by the application of torque to the control. A sine wave and a square wave were used as input. Redfern found that W-H filtering was particularly good at capturing rapid changes in the level of force produced while filtering out noise during the square-wave tracking. Consequently, Redfern adopted and used this method of filtering.

As one might expect from a square-wave based processing technique, the filtered signal was choppy and discontinuous. Consequently, Redfern exponentially smoothed the filtered signal with an α of 0.15 to account for the electromechanical delays in the muscle. This resulted in a signal which still had sharp responses, but not instantaneous increases and decreases in the EMG signal.

As part of a larger study Redfern applied these techniques to the estimation of muscle force in the lower leg during an isometric tracking task. He attempted to predict the net torque about the ankle joint using a geometric model developed for the study and the methods discussed above. The model he used incorporated both linear and quadratic terms of the processed EMG (i.e., the exponentially smoothed AS). It also explicitly accounted for the effect of antagonistic co-contraction on the net torque by calculating the joint torque as the algebraic sum of the opposing muscles' torque. He obtained R^2 values

of 0.97 to 0.99 in eight trials with two different subjects. Thus, Redfern's results indicate that the filtering and smoothing approach worked well with his other methods. However, Redfern did not directly compare his filtering and smoothing procedures with other techniques.

In a later study, Woldstad (1989) applied Redfern's filtering and smoothing techniques to the prediction of torque about the elbow joint from the EMG activity of the biceps and triceps, He obtained generally good results for the prediction of torque at this joint using this approach, but he did note a problem with this approach.

There is a slight delay between the electrical activity associated with a muscular contraction and the actual force resulting from the muscle's shortening. For a single sustained exertion such as a maximum voluntary contraction, the time delay is of little consequence. However, if the muscle force varies over time, systematic errors are introduced into the prediction of muscle force from EMG. In order to obtain the best fit between EMG and muscle force, a slight delay is incorporated. Woldstad noted that the exponential smoothing of the W-H filtered signal introduced some delay by virtue of the smoothing itself. The delay needed for the derived signal to obtain the best correlation with the observed force was therefore confounded with the exponential smoothing of the W-H filtered signal.

Consequently, Woldstad used the more standard filtering technique of a finite-impulse response (FIR) filter. An FIR filter was used in the current study. The filter was generated using the Remez Exchange algorithm.

Summary

This appendix provides an overview of recent advances in the prediction of joint torque from electromyography. It provides a brief summary of the data used to decide how to collect, process, and filter the EMG signals. Figure A.2 shows the processing scheme used in the current study. The raw

signal is amplified by a pre-amplifier fixed onto the EMG array. This pre-amplified signal is passed to another amplifier where it is amplified further. An analog RMS unit then rectifies the signal. This RMS signal is digitally sampled. The data is then filtered and normalized, and then averaged to obtain the estimate of EMG activity. Figure A.2 graphically shows the processing steps used to amplify, filter, normalize and average the EMG data.

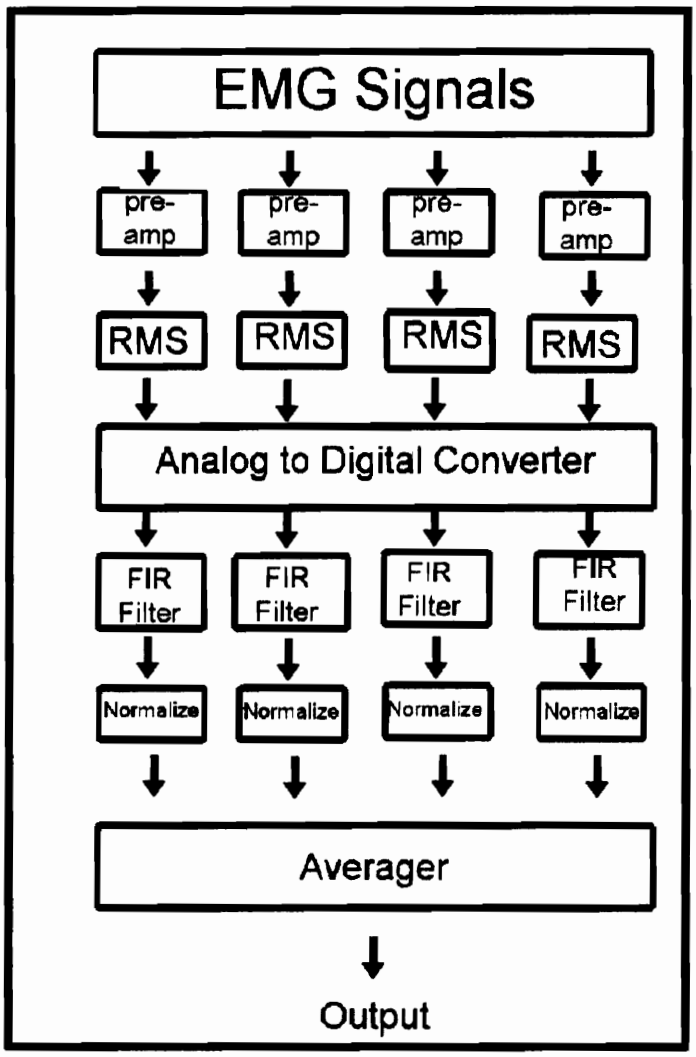

Figure A.2. EMG processing scheme.

REFERENCES

Angel, R.W. (1977). Electromyography during rapid arm movements: Central versus proprioceptive influences. *Journal of Neurololgy, Neurosurgery and Psychiatry, 40,* 683-686.

Basmajian, J.V., and De Luca, C.J. (1985). *Muscles alive.* Baltimore, MD: Williams and Wilkins.

Bouisset, S., Lestienne, F. (1977). *The stability of synergy in agonists during the execution of a simple voluntary movement. Electroencephalagraphy and Clinical Neurophysiology, 42,* 543-551.

Bouisset, S. (1973). EMG and muscle force in normal motor activities. In J.E. Desmedt (Ed.), *New developments in EMG and clinical neurophysiology,* (pp 54-68). Brussels: Karger.

Cnockaert, J.C., Lensel, G., and Pertuzon, E. (1975). Relative contributions of individual muscles to the isometric contraction of a muscle group. *Journal of Biomechanics, 8,* 191-197.

De Luca, C.J., and Mambrito, B. (1987). Voluntary control of motor units in human anatagonist muscles: Coactivation and reciprocal activation. *Journal of Neurophysiology, 58,* 525-542.

Ericson, B.E., and Hagberg, M. (1978). EMG signal versus external force: a methodological study on computer aided analysis. In E. Asmussen and K. Jorgensen (Eds.), *Biomechanics VI-A.*, (pp 251-255). Baltimore, MD: Baltimore University Park Press.

Gordon, A.M., Huxley, A.F., and Julian, F.J. (1966). Variations in isometric tension with sarcomere length in vertebrate muscle fibres. *Journal of Physiology (London), 184,* 170-192.

Hogan, N. and Mann, R.A. (1980). Myoelectric signal processing: optimal estimation applied to electromyography-Part I: derivation of the myoprocessor. *IEEE transactions on Biomedical Engineering, 27,* 382-395.

Hof, A.L., and Van den Berg, J.W. (1981) (1981) EMG to force processing parts I-IV. *Journal of Biomechanics, 14 ,* 747-792.

Ismail, H.M., and Ranatunga, K.W. (1978). Isometric tension development in a human skeletal muscle in relation to its working range of movement: the length tension relation of the biceps brachii muscle. *Experimental Neurology, 62,* 595-604.

Joyce, G.C., Rack, P.M.H., and Ross, H.F. (1974). The forces generated at the human elbow joint in response to imposed sinusoidal movements of the forearm. *Journal of Physiology (London), 240,* 351-374.

Joyce, G.C., Rack, P.M.H. (1969). The mechanical properties of the cat soleus muscle. during controlled lengthening and shortening movements. *Journal of Physiology (London), 193,* 334-357.

Karst, G.M., and Hasan, Z. (1987). Antagonist muscle activity during human forearm movements under varying kinematic and loading conditions. *Experimental Brain Research, 67,* 391-401.

Komi, P.V. (1973). Relationship between muscle tension, EMG and velocity of contraction under concentric and eccentric work. In J.E. Desmedt (Ed.), *New developments in Electromyography and Clinical Neurophysiology* (pp. 596-606). Brussels: Karger.

Komi, P.V., and Vitalaso, J.H.T. (1976). Signal characteristics of EMG at different levels of muscle tension. *Acta Physiologica Scandinavia, 96,* 267-276.

Lawrence, J.H., and De Luca, C.J. (1983). Myoelectric signal versus force relationship in different human muscles. *Journal of Applied Physiology, 54,* 1653-1659.

Lehman, S.L. and Stark, L.W. (1981). Perturbation analysis applied to eye, hand, and arm movements. *IEEE transactions on Systems, Man and Cybernetics, 13,* 927-979.

Lindstrom, L. Magnusson, and Petersen, I. (1970). Muscular fatigue and action potential conduction velocity changes studied with frequency analysis of EMG signals. *Electroencephagraphy and Clinical Neurophysiology, 4,* 341-353.

Lippold, O.C.J. (1952). The relation between integrated action potenials in human muscle and its isometric tension. *Journal of Physiology (London), 117,* 492-499.

Marsden C.D., Merton, P.A., and Morton, H.B. (1972). Servo action in human volunatry movement. *Nature, 238,* 140-143.

Marsden C.D., Merton, P.A., and Morton, H.B., (1976). Servo action in the human thumb. *Journal of Physiology (London), 257,* 1-44.

Marsden C.D., Obeso, J.A., Rothwell, J.C. (1983). The function of the antagonist muscle during fast limb movements in man. *Journal of Physiology (London), 335,* 1-13.

Messier, R.H., Duffy, J., Lichtman, H.M., Paslay, P.R., Soechting, J.F., and Stewart, P.A. (1971). The electromyogram as a measure of tension in the human biceps and triceps muscle. *International Journal of Mechanics and Science, 13,* 585-598.

Meyer, D.E., Smith, J.E.K., and Wright, C.E. (1982). Models for the speed and accuracy of aimed movements. *Psychological Review., 89,* 449-482.

Moritani, T., and Devries, H.A. (1978). Reexamination of the relationship between the surface integrated electromyogram and the force of isometric contraction. *American Journal of Physical Medicine, 57*, 263-277.

Olney, S.J., and Winter, D. (1985). Predictions of knee and ankle moments of force in walking from EMG and kinematic data. *Journal of Biomechanics, 18*, 9-20.

Ralston, H.J. Todd, F.N. and Inman, V.T. (1976). Comparison of electrical activity and duration of tension in the human reactus femoris muscle. *Electroencephagraphy and Clinical Neurophysiology, 16,* 271-279.

Redfern, M.S. (1984). *Time delays between the onset of the EMG and tension in the triceps brachii.* (Tech. Report), Ann Arbor: University of Michigan, The Center for Ergonomics.

Redfern, M.S. (1988). *Electromyographic (EMG) signal processing and biomechanical modeling of the lower leg muscles.* Unpublished doctoral dissertation, University of Michigan Ann Arbor, MI.

Schmidt. R.A., Zelaznik, H. Hawkins, B., Grant,. J.S., and Quinn, J. T. (1979). Motor output variability: A theory for the accuracy of motor acts, *Psychological Review, 86*, 415-451.

Seigler,S., Hillstrom, H.J., Freedman, W. and Moskowitz, G. (1985). Effect of myoelectric signal processing on the relationship between muscle force and processed EMG. *American Journal of Physical Medicine, 64,* 130-149.

Woldstad, J.C. (1989). *Electromyographic analysis of rapid, accurate elbow movements.* Unpublished doctoral dissertation, University of Michigan Ann Arbor, MI.

Zuniga, H.N., and Simmons, D.G. (1969). Nonlinear relationship between averaged electromyogram and muscle tension in normal subjects. *Archives of Physical Medicine, 50,* 613-620.

APPENDIX B

ADJUSTMENTS TO THE TORQUE-EMG RELATION NEEDED TO ACCOUNT FOR MUSCLE LENGTH, SHORTENING VELOCITY, AND MOMENT ARM EFFECTS

Introduction

The EMG-torque relation is affected both by changes in the limb position and the velocity of movement. Specifically, the tension produced by the muscle is a function of both muscle length and the muscle's velocity of shortening. The moment arms of each muscle about a joint also vary with joint position. In order to estimate muscle torques during movement, these effects must be taken into account. A sequential approach originated by Olney and Winter (1985) and further refined by Redfern (1988) and Woldstad (1989) was used in the current study. In this approach, the parameters of the force-EMG relation are first estimated for a single position. A suitable geometric model of the joint under study is used to calculate the force required to produce the predicted torque. Measurements of torque and EMG activity are then taken across a range of other positions and the original estimate of the force of each muscle is adjusted by multiplying the estimated force by a length compensation function. After compensating for muscle lengths, torque and EMG activity are measured with several different velocities. Using these data, the parameters of the force-EMG relation are then adjusted for muscle shortening velocities. Using this approach, previous authors (Redfern, 1988; Woldstad, 1989) have demonstrated that muscle forces can be estimated with a reasonable degree of precision under *some* conditions. Conditions for which the procedure yielded poor parameter estimates and poor predictive capability include high velocity movements and movement near the extreme ranges of joint motion. Additional corrections were also required to account for changes in the direction of movement and changes in the moment of inertia.

An important preliminary to the discussion of the compensation functions is the consideration of an appropriate geometric model. Muscle lengths, muscle shortening velocities, and muscle moment arms cannot be

measured *in vivo* and must be estimated from joint angles. Woldstad (1989) developed two different geometric models of the elbow for these purposes which are described below.

Geometric Models Used to Estimate Moment Arms, Muscle Lengths, and Shortening Velocities

Woldstad (1989) used a ball-and-cup model of the elbow to estimate the muscle moment arms and a simple hinge model to estimate the muscle lengths. Woldstad noted that the ball-and-cup model significantly improved the prediction of muscle moment arms, but did not substantially affect the muscle lengths and shortening velocities. As a result, Woldstad used a standard parallel hinge model to calculate changes in muscle lengths and shortening velocities.

Estimation of moment arms. Woldstad (1989) used the two-dimensional ball-and cup model of the elbow shown in Figure B.1 to calculate the muscle moment arms of the biceps and triceps.

The moment arm of the biceps is calculated as a function of the included elbow angle, ϕ, as shown in equation B.1.

$$MA_B(\phi) = MAX\{b_{90} * \cos(\phi), b_{min}\} \qquad B.1$$

The term b_{90} is the moment arm of the biceps at 90 degrees. The term b_{min} is the minimum possible moment arm of the biceps given the diameter of the distal head of the humerus. Based upon the work of Niku and Henderson (1985), Woldstad estimated the value of b_{90} for each subject to be 15% of the lower arm length. Based upon an examination of human humerus bones, the value of b_{min} was estimated by Woldstad to be 1 cm for all subjects.

The moment arms of the triceps at an included elbow angle of ϕ were estimated by Woldstad as follows:

$$MA_T(\phi) = \begin{cases} MAX\{t_{135} * \cos\phi, t_{min}\} & \text{if } 0^\circ \le \phi \le 135^\circ \\ t_{135} & \text{if } 135^\circ \le \phi \le 180^\circ \end{cases} \qquad B.2$$

Based upon the work of Messier, (1971), the moment arm of the triceps at an included angle of 135 degrees, t_{135}, was estimated by Woldstad to be 10.1 % of the lower arm length. The value t_{min} was again estimated to be 1 cm.

Estimation of muscle lengths, and shortening velocities. Woldstad (1989) adopted a slightly different model of the elbow in the calculation of the muscle length and velocity changes. Specifically, Woldstad neglected the two-dimensional nature of the joint. He noted that while the ball-and-cup model significantly enhanced the accuracy of the moment arm calculations, the incorporation of this feature did not substantially affect the calculation of muscle lengths or velocities. The assumption of a standard parallel hinge model of the joint greatly simplifies the derivation of muscle lengths and velocities. Using this model, Woldstad noted that the muscle lengths for the biceps and triceps can be calculated as a function of upper arm length and joint angle as shown in the following two equations.

$$L_B(\phi) = UA - b_{90} * \cos(\phi) \qquad \text{B.3}$$

$$L_T(\phi) = UA + t_{90} * \cos(\phi) \qquad \text{B.4}$$

The term *UA* is the upper arm length and L_B and L_T are the estimated biceps and triceps lengths respectively. The terms b_{90} and t_{90} are the biceps and triceps moment arms at 90 degrees.

The shortening velocities are estimated by differentiating the muscle lengths with respect to time. Since the lengths are expressed as functions of included muscle angle, the chain rule is used to obtain the shortening velocities for each muscle. The resulting equations are shown below.

$$V_B(\phi) = b_{90} * \sin(\phi) * \frac{d\phi}{dt} \qquad \text{B.5}$$

$$V_T(\phi) = - t_{90} * \sin(\phi) * \frac{d\phi}{dt} \qquad \text{B.6}$$

Since the differentiation of the length estimates to obtain shortening velocities necessarily amplifies the noise in the data, some filtering of the shortening velocity was needed. Woldstad employed a nearly-equal-ripple derivative

(NERD) finite-impulse-response filter to filter the shortening velocity estimates. A in the current study a Parks-McClellan optimal derivative filter was designed using the Remez exchange algorithm.

Use of the equivalent muscle group assumption. Both the ball-and-socket model and the parallel hinge model of the elbow employ the assumption that the flexion and extension of the forearm is controlled by two antagonistic "equivalent muscle" groups. There are three different primary elbow flexors: biceps brachii, brachialis, brachioradialis, each with different origins and insertions. In addition, there are two primary elbow extensors: the triceps brachii and the Anconeus (Warfel, 1985; Anderson, 1983). Consequently, a realistic model of muscle torques about the elbow would include many muscles.

The basic premise of the equivalent muscle group assumption is that the EMG activity of one flexor and one extensor can be considered representative of all the flexors and all the extensors for this particular motion. This eliminates the need to obtain the EMG signals from each muscle and each branch of a muscle. The activity of the biceps brachii was assumed to be representative of flexor activity. The EMG activity of the triceps brachii was assumed to be representative of the extensor activity. The validity of the equivalent muscle group assumption is supported by the work of Bouisset et al. (1977) and Maton and Bouisset. (1977).

Bouisset and his co-workers examined the degree to which elbow flexor muscles were activated independently or in concert during dynamic flexions using a range of velocities. They found that the time of onset and cessation of EMG activity within each of the three flexors was almost identical, and this finding held over all the levels of inertial loads or velocities employed. They also found that the level of EMG activity with each of the flexors was highly correlated. Consequently, the activity of the biceps could be reasonably taken to be representative of the EMG activity of the entire equivalent muscle group.

There are also statistical reasons for employing the assumption of equivalent muscle groups. If one attempted to measure the activity of each muscle's EMG activity and use these EMG signals in a regression equation to predict the net torque, one would find that the collinearity of the regressors

would lead to poor parameter estimation and very wide prediction intervals. Consequently, there are both practical and theoretical reasons for employing the equivalent muscle group assumption.

A Sequential Method for Estimating Muscle Forces During Movement

Olney and Winter (1985) developed a sequential method of incorporating the effects of muscle length and the velocity of shortening into the basic torque-EMG relationship. They proposed the model shown in equation B.7.

$$M(t) = (\sum_{i=1}^{n} K_{fi}\, E_i\,(t))\,[1 + K_2\,(\theta(t) - \theta_i) + K_3\,\omega(t)] - (\sum_{i=1}^{n} K_{ij}\, E_j\,(t))\,[1 + K_2\,(\theta(t) - \theta_j) + K_3\,\omega(t)] \qquad \text{B.7}$$

The terms $E_i\,(t)$ and $E_i\,(t)$ are the amplitudes of the iEMGs of the agonist and antagonist muscle at time *t*. The terms $\theta(t)$ and $\omega(t)$ represent the angular position and velocity of the limb respectively. The various *K* terms are all experimentally derived constants. Thus, the torque for each muscle was estimated as a function of the iEMG, the iEMG-joint angle interaction, and the iEMG-angular velocity interaction.

In practice, the slope of the torque-EMG relation was first estimated for each muscle. The effects of muscle length were then incorporated through the joint angle term. Finally, the effects of muscle shortening velocity were incorporated through the angular velocity term. Note that this model assumes that the joint angle and the muscle length differ only by a constant. The same assumption is made for the muscle shortening velocity and the angular velocity. The validity of these assumptions is addressed below.

The model proposed by these authors explicitly incorporated the effects of co-contraction by asserting that the net torque about a joint was the algebraic sum of the torque of the antagonistic muscles. That is, the contribution of the muscles opposing the motion is not arbitrarily assumed to be zero. The effects of changes in the moment arms of the muscles are implicitly incorporated into the model through the muscle length factor. The

isometric torque-iEMG relation, the muscle length-torque relation, and the torque-shortening velocity were all assumed to be linear in the model statement.

Redfern (1988) and Woldstad (1989) investigated two possible improvements to this basic formulation. They considered the use of higher order terms in the length-tension relation and the velocity of shortening-tension relation. Second, they formulated geometric models of the joints under study so that the effect of changing moment arm lengths could be considered separately from the length-tension relation. Redfern (1988) developed a model for the prediction of torque about the ankle and Woldstad formulated a model to predict the torque about the elbow. The general form of this revised model is shown in equation B.8.

$$T_m = \sum_{all\,m} MA_m * (IF_m * LC_m * VC_m) \qquad B.8$$

According to this model, the torque due to each muscle is the product of the moment arm of the muscle and the estimated isometric force, IF_m, of muscle *m*, compensated for the muscle length, LC_m, and the velocity of shortening, VC_m. However, the LC and VC compensation "factors" shown here are in fact *functions* describing the required adjustment to the basic torque-EMG relation and not merely constants. In the sections that follow, some of the previous studies concerning the effects of muscle length and shortening velocity are reviewed. These studies form the basis for selecting the compensation functions used.

Accounting for the Effects of Muscle Length

Gordon, Huxley, and Julian (1966) first established that the efficiency of the muscle depends on its length. In particular, they examined the isometric tension produced by the individual fibers isolated from striated frog muscle. They carefully controlled the changes in sarcomere length and observed the change in the tension with the sarcomere. The authors noted that the maximum tension occurred at some intermediate sarcomere length. On the basis of these results they proposed the now familiar sliding filament theory of

muscle contraction. According to this theory, the amount of muscle force generated is determined in part by the ability or inability of the muscle proteins to interact. If the muscle is stretched too much, thereby elongating the sarcomere, then the tension produced will be limited by the small number of available cross-bridges between the actin and myosin. Alternatively, if the sarcomere length is too short, the ability of the muscle to produce tension is limited by the fact that the fibers interfere with one another, and further shortening is not possible. Consequently, there is some intermediate sarcomere length at which the capacity to produce tension is a maximum.

On a more macroscopic scale, this effect is reflected in the length-tension relation of the muscle. Rack and Westbury (1969) showed that force produced by an isolated cat soleus muscle varied with the muscle's length. Thus, the effects of muscle length on the force produced by a muscle must be considered in any model of the torque-EMG relation during movement.

Both Olney and Winter (1985) assumed that muscle force could be related to muscle length by a single constant. Citing the work of several previous authors (Gordon, Huxley, and Julian, 1966; Rack and Westbury, 1969; Ismail and Ranatunga, 1978) which indicated a quadratic term was needed, Redfern (1988) and Woldstad (1989) adopted the quadratic length compensation function shown below.

$$LC = \beta_0 + \beta_1 L + \beta_2 L^2 \qquad \text{B.12}$$

Using the geometric model discussed previously, Woldstad (1989) showed that the muscle length compensation functions for both the biceps and triceps could be rewritten in terms of the included elbow angle, ϕ:

$$LC = \beta_0 + \beta_1 * \cos(\phi) + \beta_2 \cos^2(\phi) \qquad \text{B.13}$$

In order to scale the length compensation function to appropriately adjust the isometric EMG-torque relation, Woldstad imposed the additional constraint that the length compensation should be unity at an included elbow angle of 100

degrees and less than one everywhere else. The resulting compensation function is shown in equation B.14

$$LC = 1 + \beta_1 * [\cos(\phi) - \cos(100)] + \beta_2 * [\cos^2(\phi) - \cos^2(100)] \qquad B.14$$

This quadratic length compensation function was used in the current study.

Accounting for the Effect of Movement Velocity

Another factor which must be considered in a dynamic torque-EMG relation is the effect of the muscle shortening velocity. Hill (1938) first established that the ability of a muscle to produce tension is dependent upon the muscle shortening velocity. Hill assumed that all the energy consumed by the muscle was expended either as heat or in performing work. He then examined the effect of velocity and load on the heat released during shortening. From his work he derived the relation now popularly known as Hill's equation shown in equation B.15. The relation indicates that a decrease in muscle force per unit of heat generated will be observed with an increase in shortening velocity (i.e., the muscle will be less efficient as it contracts more rapidly).

$$(P+a)(V+b) = (P_0+a)b = \text{constant} \qquad B.15$$

The terms are as follows: *P* is the load placed upon the muscle, *a* is shortening heat per unit distance shortened, V is the velocity of the muscle during the shortening, P_0 is the maximum isometric tension of the muscle, and *b* is the increase in energy rate per unit distance shortened. A more common form of Hill's equation is the re-arranged version shown in equation B.16:

$$(P+a)V = (P_0 - P)b. \qquad B.16$$

Thus, as the shortening velocity increases, there is more heat produced per unit distance shortened. The electrical analog to Hill's "heat of shortening"

is the EMG activity. Consequently, there is more EMG activity per unit of shortening at higher velocities. Stated another way, the same EMG activity at faster shortening velocities represents less muscle tension.

Three recent authors (Olney and Winter, 1985; Redfern, 1988; Woldstad 1989) have each used different adjustments to the torque EMG-relation to account for the effects of movement velocity. Olney and Winter (1985) assumed a linear decline in the force with increasing shortening velocity as shown in equation B.17. Redfern included a quadratic term in the velocity compensation function (VC) as shown in equation B.18. In both cases, the term *V* represents the estimated shortening velocity. The velocity compensation functions are scaled to unity either for muscle lengthening or for no change in muscle length.

$$VC = 1 + \beta_1 * V \qquad \text{B.17}$$

$$VC = 1 + \beta_1 * V + \beta_2 * V^2 \qquad \text{B.18}$$

These two velocity compensation functions are both empirically derived. Consequently, the derived velocity compensation function should be considered valid only over the range of the velocities investigated. Any extrapolation beyond the range of the velocities examined would be improper. Woldstad (1989) adopted a somewhat different procedure to adjust the force for the shortening velocity. He derived the velocity compensation function shown in equation B.19 from Hill's equation. The equation predicts that the force produced by each muscle should fall off exponentially as the shortening velocity increases.

$$VC = \beta_1^{-|V|} \qquad \text{B.19}$$

Woldstad collected force data across a range of velocities and then estimated the β_1 parameter for each muscle using a quasi-Newton nonlinear estimation package. The approach of Woldstad is clearly the most general of the three authors. However, it is also more difficult to use. This study involved the prediction of muscle force only within the range of the velocities over which

the model will be calibrated. Consequently, the quadratic relation previously employed by Redfern was used here.

The question of whether the force exerted by the muscle is affected by the speed of lengthening during an eccentric contraction is still a matter of some debate. Zahalak et al (1976) found that the muscle force was independent of the speed of lengthening. However, Redfern (1988) noted that several authors (Joyce and Rack, 1969; Komi, 1973; and Bouisset, 1973) have found slight increases in the force exerted during eccentric contractions.

As noted in chapter 8, velocity compensation functions were calculated for several of the subjects, but the functions failed to predict much of the unexplained variance. Consequently, the EMG-derived estimate of the muscle force was scaled to account for movement, but no other velocity compensation was applied

Criticisms of the Sequential Parameter Estimation Process

The sequential parameter estimation approach involves estimating the parameters of these compensation factors in succession. The length parameter estimates depend on the calibration of the isometric torque-EMG relation. Likewise, the velocity parameter estimates depend on both the isometric and length calibration. Woldstad (1989) noted that there are some substantial drawbacks to this approach. This sequential or piece-wise approach is "a relatively inefficient iterative approach to the solution of a very complex nonlinear optimization problem." He further states that parameter estimates obtained with this approach are not even necessarily local optima. He notes that the use of more sophisticated optimization techniques could be expected to improve the model accuracy.

One additional problem with using the sequential procedure is that several assumptions involved in the traditional measures of goodness of fit such as R^2 do not hold. In particular, while the upper bound of R^2 is one, (all the variance in the observed torque is explained) it is possible to obtain values of the statistic less than zero (i.e., it is possible to obtain parameter estimates that result in a worse fit than just predicting the mean). Woldstad (1989) noted that the sequential parameter estimation procedure could result in SS_E values

larger than the SS_T because the later parameters are based upon *different* data from those used in the later calibrations. For instance, the velocity compensation function parameters are calculated using the data during the velocity compensation calibration trials. However, they also depend upon the isometric calibration and the length calibration trials. The usual rule that the SS_E and the SS_{Reg} must equal the SS_T holds only if all parameters are fitted at once.

Consequently, Woldstad reported his results in terms of a measure he called R^2_{Equiv} shown in the following equation. This measure is similar to the traditional R^2 statistic in that it provided a measure of the goodness of fit, but is not R^2 as traditionally defined.

$$R^2_{equiv[\hat{t}_i, t_i]} = 1 - L_{[\hat{t}_i, t_i]} = 1 - \frac{\sum_1^n (\hat{t}_i - t_i)^2}{\sum_1^n (\bar{t}_i - t_i)^2} \qquad \text{B.11}$$

Alternatives to the Sequential Parameter Estimation Approach

It should be noted that some attempts have been made to estimate the parameters of the force-EMG relation simultaneously without much success. Hof and Van den Berg (1981 a, b, c, d) attempted to independently estimate the parameters for a model with six parameters based upon the Hill muscle model. The parameters in the model included the following terms:

1) a linear EMG-force function.
2) an exponential filter to account for electromechanical delays between the electrical activity of the muscle and the force produced.
3) a logarithmic function compensating for the contributions of the series elastic component to the total force.
4) an exponential function compensating for the parallel elastic components.
5) a linear length-tension compensation factor.
6) an exponential function of angular velocity to compensate for velocity of shortening effects.

Woldstad (1989) observed that this calibration procedure yielded poor parameter estimates and poor predictive capability.

Thus, while the sequential parameter estimation procedure does have significant drawbacks, it appears to be the best method yet developed to predict the muscle force from EMG data during dynamic exertions. Consequently, the sequential parameter estimation procedure originated by Olney and Winter (1985) and further developed by Redfern (1988) and Woldstad (1989) was adopted here.

Summary

This appendix describes the methods and procedures that were used in estimating the length and velocity compensation function in sequence. The methods for obtaining the estimates of isometric muscle force are described. The procedure for estimating the length compensation factor is described. Finally, the adjustment for shortening velocity is described.

This review was included to describe how muscle forces can be estimated from EMG data during movement. The point of the current study was to examine the effects of certain factors upon the level of co-contraction observed. This necessarily requires that the muscle forces be estimated as accurately as possible. Based upon the work of Woldstad (1989), certain candidate task conditions were excluded due to poor estimation in these circumstances. Specifically, high-velocity movements, low inertia movements, and movements near the extremes were excluded.

References

Basmajian, J.V., and De Luca,C.J. (1985). *Muscles alive.* Baltimore, MD: Williams and Wilkins.

Bouisset, S., Lestienne, F. (1977). *The stability of synergy in agonists during the execution of a simple voluntary movement. Electroencephagraphy and Clinical Neurophysiology, 42,* 543-551.

Bouisset, S. (1973). EMG and muscle force in normal motor activities. In J.E. Desmedt (Ed.), *New developments in EMG and clinical neurophysiology,* (pp 54-68). Brussels: Karger.

Gordon, A.M., Huxley, A.F., and Julian, F.J. (1966). Variations in isometric tension with sarcomere length in vertebrate muscle fibres. *Journal of Physiology (London), 184,* 170-192.

Hof, A.L., and Van den Berg, J.W. (1981). EMG to force processing parts I-IV. *Journal of Biomechanics, 14* , 747-792.

Ismail, H.M., and Ranatunga, K.W. (1978). Isometric tension development in a human skeletal muscle in relation to its working range of movement: the length tension relation of the biceps brachii muscle. *Experimental Neurology, 62,* 595-604.

Joyce, G.C., Rack, P.M.H., and Ross, H.F. (1974). The forces generated at the human elbow joint in response to imposed sinusoidal movements of the forearm. *Journal of Physiology (London), 240,* 351-374.

Joyce, G.C., Rack, P.M.H. (1969). The mechanical properties of the cat soleus muscle. during controlled lengthening and shortening movements. *Journal of Physiology (London), 193,* 334-357.

Komi, P.V. (1973). Relationship between muscle tension, EMG and velocity of contraction under concentric and eccentric work. *New developments in EMG and clinical neurophysiology* (pp 596-606). Brussels: Karger.

Maton, B., and Bouisset, S. (1977). The distribution of activity among the muscles of a single group during isometric contraction. *European Journal of Applied Physiology, 37,* 101-109.

Messier, R.H., Duffy, J., Lichtman, H.M., Paslay, P.R., Soechting, J.F., and Stewart, P.A. (1971). The electromyogram as a measure of tension in the human biceps and triceps muscle. *International Journal of Mechanics and Science, 13,* 585-598.

Olney, S.J., and Winter, D.A., (1985). Predictions of knee and ankle moments of force in walking from EMG and kinematic data. *Journal of Biomechanics, 18*, 9-20.

Rack, P.M. H., and Westbury, D.R. (1969). The effect of length ans stimulus rate on tension in the isometretric cat muscle. *Journal of Physiology (London), 204,* 443-460.

Redfern, M.S. (1984). *Time delays between the onset of the EMG and tension in the triceps brachii.* (Tech. Report), Ann Arbor: University of Michigan, The Center for Ergonomics.

Redfern, M.S. (1988). *Electromyographic (EMG) signal processing and biomechanical modeling of the lower leg muscles.* Unpublished doctoral dissertation, University of Michigan, Ann Arbor, MI.

Woldstad, J.C. (1989). *Electromyographic analysis of rapid, accurate elbow movements.* Unpublished doctoral dissertation, University of Michigan, Ann Arbor, MI.

Zahalak, G.I., Duffy, J., Stewart, P.A., Lichtman, H.M., Hawley, R.H., and Paslay, P.R. (1976). Partially activated human skeletal muscle: an experimental investigation of force, velocity, and EMG. *Journal of Applied Mechanics. 98,* 81-86.

APPENDIX C

EMG-FORCE PARAMETERS AND CALIBRATION DATA

Parameters for Static Tracking Experiment

Parameters for each trial for the fit of the EMG-Force relation are given below. The B_1 and T_1 terms are the linear terms for the biceps and triceps respectively. The B_2 and T_2 terms are the corresponding quadratic terms.

Table C.1 Static tracking parameters.

Subject Number	Trial Number	B_1	T_1	B_2	T_2	R^2
1	1	388.385	-261.404	-134.137	34.8993	0.975131
1	2	453.665	-288.241	-186.865	16.794	0.972933
1	3	477.709	-326.875	-191.607	67.7781	0.980695
1	4	367.488	-251.781	-137.349	35.6682	0.973464
1	5	412.068	-248.028	-196.426	76.2948	0.981256
1	6	393.762	-220.902	-226.717	92.4076	0.975351
1	7	365.331	-254.295	-75.1537	-57.8008	0.964467
1	8	321.572	-247.403	-69.5092	-54.2204	0.950619
1	9	392.778	-336.169	-122.297	17.8571	0.957389
1	10	362.319	-264.1	-92.2358	-5.40424	0.954096
1	11	495.342	-378.465	-220.702	127.482	0.963638
1	12	403.375	-259.786	-265.882	136.279	0.965655
1	13	291.367	-179.662	-221.392	113.087	0.940757
1	14	363.337	-200.873	-269.87	158.017	0.974546
1	15	438.896	-263.194	-203.563	26.7114	0.92632
1	16	242.833	-108.534	-183.907	89.2844	0.933136
2	1	178.021	-11.4243	-158.553	90.4125	0.950051
2	2	196.092	-115.265	-119.038	40.4379	0.918517
2	3	209.856	-74.1446	-149.656	62.5773	0.962922
2	4	171.429	-20.3984	-145.141	64.6069	0.951017
2	5	142.432	-26.9799	-106.245	28.1652	0.937794
2	6	124.154	-15.0048	-95.1507	35.7309	0.918465
2	7	161.199	-53.0677	-97.4601	35.2106	0.960134
2	8	177.239	-62.9415	-166.666	88.6167	0.967336
2	9	173.756	-56.866	-159.483	64.7462	0.977454
2	10	146.609	-70.2443	-100.378	35.0051	0.945013
2	11	112.114	-37.9534	-95.0976	32.9122	0.918302
2	12	99.588	-13.12	-138.533	82.0015	0.889029
2	13	219.873	-101.29	-155.075	62.6069	0.961816
2	14	162.839	-49.237	-175.047	70.7399	0.971488
2	15	174.295	-80.2085	-118.179	31.7819	0.903418
2	16	212.01	-110.413	-220.275	100.711	0.935327

Table C.1 Static tracking parameters. (continued)

Subject Number	Trial Number	B_1	T_1	B_1	T_1	R^2
3	1	189.167	-13.9305	-150.933	84.6969	0.979049
3	2	151.647	26.1204	-148.805	87.0973	0.980147
3	3	84.9879	57.7118	-85.8137	42.4374	0.96928
3	4	124.993	52.5597	-105.514	64.7504	0.974473
3	5	150.254	10.2018	-113.246	69.0091	0.959517
3	6	152.529	48.6283	-125.896	61.3831	0.977279
3	7	159.837	45.5319	-126.296	60.5293	0.976397
3	8	72.7563	30.3447	-92.469	49.968	0.964979
3	9	83.0382	25.5019	-93.0471	60.8578	0.973339
3	10	122.273	10.4882	-114.012	56.7972	0.980773
3	11	128.226	39.8683	-107.75	53.4934	0.982897
3	12	74.5841	30.4714	-80.8579	46.8752	0.968552
3	13	70.393	27.9477	-77.3322	36.8803	0.96683
3	14	66.0402	37.6165	-100.216	53.9718	0.967613
3	15	123.063	19.4071	-107.381	57.3705	0.983994
3	16	130.417	25.5587	-136.279	89.0641	0.982671
4	1	198.492	-81.4764	-135.396	48.8572	0.967778
4	2	252.441	-92.6776	-187.043	93.1885	0.97724
4	3	184.161	-80.8692	-133.994	59.6421	0.977332
4	4	287.887	-90.5624	-172.034	75.3097	0.980713
4	5	249.922	-74.5864	-181.569	92.1809	0.983012
4	6	226.241	-104.002	-139.865	66.9465	0.965591
4	7	247.903	-157.131	-110.262	38.8793	0.970326
4	8	367.706	-178.576	-128.503	47.0646	0.974208
4	9	318.627	-151.057	-118.116	45.3862	0.973664
4	10	223.302	-105.182	-100.868	37.7881	0.975182
4	11	180.087	-61.5002	-126.728	64.6731	0.971494
4	12	333.164	-158.819	-151.844	79.2982	0.97524
4	13	316.275	-102.759	-191.517	105.8	0.979157
4	14	201.462	-81.6971	-108.361	44.4611	0.959666
4	15	339.764	-160.899	-123.723	46.4035	0.972136
4	16	269.464	-155.752	-105.337	43.2501	0.980823

Table C.1 Static tracking parameters. (continued)

Subject Number	Trial Number	B_1	T_1	B_1	T_1	R^2
5	1	330.499	-157.836	-217.172	103.25	0.975534
5	2	517.558	-282.115	-272.344	125.379	0.990283
5	3	432.081	-181.388	-278.91	144.838	0.987411
5	4	599.292	-393.633	-298.679	157.154	0.987167
5	5	334.724	-170.89	-205.46	87.5558	0.980538
5	6	543.733	-332.396	-272.03	124.722	0.983459
5	7	527.021	-308.888	-241.955	84.6341	0.98443
5	8	228.645	-53.1589	-171.496	54.2785	0.977199
5	9	281.324	-83.0326	-151.659	35.7691	0.978936
5	10	379.086	-147.755	-247.418	107.558	0.981442
5	11	413.045	-207.042	-263.771	127.832	0.980635
5	12	285.611	-101.54	-175.765	39.8355	0.969027
5	13	553.395	-378.591	-310.649	181.404	0.980707
5	14	386.682	-161.86	-278.74	135.283	0.975633
5	15	321.175	-163.835	-162.88	40.1518	0.971498
5	16	209.146	-31.3525	-191.163	80.5864	0.976343
6	1	290.349	-181.504	-130.398	66.9987	0.963032
6	2	265.843	-178.719	-108.009	61.3756	0.919088
6	3	291.788	-220.479	-114.211	72.2707	0.952626
6	4	285.81	-208.634	-128.386	98.1962	0.930166
6	5	396.018	-315.053	-146.132	83.0266	0.947178
6	6	230.786	-92.7989	-146.511	85.7851	0.934659
6	7	278.148	-185.873	-142.079	100.771	0.918077
6	8	329.64	-253.139	-153.58	91.7487	0.947532
6	9	382.436	-358.798	-133.089	73.7504	0.929998
6	10	121.217	-24.7469	-112.69	73.2478	0.941092
6	11	251.511	-156.906	-132.911	80.052	0.954341
6	12	248.816	-148.749	-193.961	132.038	0.943436
6	13	191.192	-115.132	-100.106	48.4448	0.922669
6	14	191.75	-117.671	-111.833	68.0351	0.928337
6	15	201.352	-121.686	-136.55	98.9288	0.882856
6	16	236.04	-125.998	-144.327	86.9427	0.951124

Table C.1 Static tracking parameters. (continued)

Subject Number	Trial Number	B_1	T_1	B_1	T_1	R^2
7	1	202.367	-83.3357	-152.141	77.7675	0.890778
7	2	328.879	-206.175	-140.546	26.3028	0.941641
7	3	370.23	-254.006	-168.373	85.9922	0.923098
7	4	326.222	-188.243	-138.763	50.9945	0.880399
7	5	188.62	-95.287	-154.902	60.9348	0.871073
7	6	232.431	-119.429	-114.901	42.6738	0.879176
7	7	271.795	-120.533	-190.955	102.302	0.925919
7	8	206.689	-123.276	-112.181	14.3398	0.879064
7	9	265.55	-106.838	-175.028	75.6694	0.945478
7	10	247.443	-91.2727	-139.364	46.1152	0.923822
7	11	159.599	-53.8968	-134.91	55.4752	0.902757
7	12	190.239	-91.5123	-134.906	52.8483	0.887034
7	13	205.223	-125.346	-114.898	9.6845	0.907018
7	14	372.468	-266.102	-137.837	21.7659	0.932436
7	15	360.117	-226.709	-140.266	32.6571	0.938312
7	16	242.096	-156.075	-120.366	45.1182	0.890296
8	1	205.374	-150.658	-180.453	80.4061	0.939987
8	2	121.908	-59.1295	-121.415	49.3651	0.891704
8	3	121.763	-63.1312	-129.207	65.8242	0.938318
8	4	160.838	-69.4431	-173.32	85.0527	0.971993
8	5	203.855	-117.2	-161.613	82.4151	0.966048
8	6	141.016	-86.9001	-109.294	55.7156	0.967962
8	7	202.658	-125.902	-155.875	69.6865	0.977336
8	8	160.116	-72.8163	-145.168	80.2467	0.981126
8	9	160.4	-80.3104	-142.44	72.5725	0.963774
8	10	273.872	-154.191	-193.348	90.9621	0.967575
8	11	218.1	-134.71	-142.352	60.9268	0.970437
8	12	246.828	-114.3	-131.595	25.3114	0.969151
8	13	239.453	-118.956	-158.445	57.8646	0.977758
8	14	153.109	-63.8898	-98.7243	-2.9436	0.951801
8	15	268.857	-170.754	-125.632	29.4472	0.930489
8	16	188.976	-27.3631	-122.738	5.74065	0.952816

Table C.1 Static tracking parameters. (continued)

Subject Number	Trial Number	B_1	T_1	B_1	T_1	R^2
9	1	218.471	-62.0782	-243.277	167.167	0.942045
9	2	430.754	-263.819	-279.965	151.683	0.965234
9	3	421.463	-257.402	-237.265	90.3728	0.975823
9	4	286.287	-142.089	-222.976	117.79	0.957656
9	5	440.034	-281.128	-307.988	160.78	0.978221
9	6	485.573	-341.503	-287.844	155.891	0.975027
9	7	365.504	-240.138	-218	100.392	0.967414
9	8	229.246	-108.097	-203.388	102.677	0.933466
9	9	239.986	-101.228	-199.14	102.098	0.93907
9	10	279.313	-150.978	-225.997	121.845	0.954091
9	11	374.489	-239.187	-282.37	174.82	0.954489
9	12	343.693	-198.791	-259.037	129.013	0.974524
9	13	264.884	-131.886	-234.537	123.665	0.954359
9	14	430.007	-303.047	-240.215	114.539	0.965699
9	15	364.321	-215.855	-281.57	164.682	0.950688
9	16	298.581	-170.543	-224.766	143.331	0.919054
10	1	320.396	-165.583	-239.42	71.9305	0.966008
10	2	335.611	-240.793	-211.733	46.8125	0.920925
10	3	367.496	-217.038	-293.705	130.224	0.965551
10	4	354.696	-197.211	-278.538	102.459	0.946352
10	5	281.268	-164.652	-263.755	101.096	0.950343
10	6	285.282	-174.892	-302.996	146.159	0.962553
10	7	244.184	-129.849	-213.113	45.0367	0.952438
10	8	320.995	-175.813	-304.033	114.473	0.963363
10	9	374.525	-241.887	-289.255	94.0325	0.960938
10	10	320.383	-228.173	-302.76	118.535	0.930897
10	11	266.284	-151.126	-213.662	45.2932	0.939291
10	12	331.617	-255.416	-238.736	63.6712	0.931932
10	13	375.821	-233.419	-267.979	79.7691	0.979047
10	14	375.715	-230.318	-281.461	99.1108	0.969731
10	15	324.16	-235.173	-262.22	106.844	0.956376
10	16	345.47	-209.867	-299.25	99.0662	0.945673

Table C.1 Static tracking parameters. (continued)

Subject Number	Trial Number	B_1	T_1	B_1	T_1	R^2
11	1	184.55	8.36852	-350.807	201.978	0.846965
11	2	302.787	-240.216	-376.866	272.57	0.655244
11	3	195.034	-43.0372	-240.09	113.436	0.726048
11	4	223.35	-75.2701	-227.489	77.7049	0.687418
11	5	269.899	-173.89	-160.463	3.27908	0.52317
11	6	212.672	-64.1838	-131.811	-18.7056	0.849528
11	7	178.977	-7.60369	-189.448	36.0552	0.755006
11	8	292.738	-105.534	-205.687	106.04	0.761907
11	9	390.55	-232.107	-140.539	-8.82428	0.71005
11	10	260.505	-63.0061	-225.265	66.9148	0.792257
11	11	417.57	-255.358	-202.427	45.4911	0.688178
11	12	267.206	-89.0541	-206.347	76.0571	0.793305
11	13	283.83	-131.453	-147.965	67.9824	0.723121
11	14	278.073	-232.958	-152.493	11.3619	0.434719
11	15	410.688	-246.264	-491.107	313.682	0.723706
11	16	348.515	-136.426	-237.811	60.5035	0.770675
12	1	285.398	-149.28	-183.897	87.0039	0.983572
12	2	344.43	-147.104	-291.813	173.144	0.985786
12	3	278.483	-138.143	-217.517	120.12	0.978227
12	4	431.982	-260.672	-282.013	165.712	0.988301
12	5	419.183	-264.463	-337.46	163.344	0.973771
12	6	209.049	-61.4917	-191.652	89.8445	0.97948
12	7	334.234	-208.54	-179.847	87.0465	0.978855
12	8	388.982	-214.896	-414.368	263.187	0.984107
12	9	376.576	-207.484	-349.362	204.91	0.984644
12	10	303.486	-189.579	-250.948	144.434	0.976884
12	11	230.792	-114.321	-205.916	106.63	0.988058
12	12	429.29	-270.678	-419.292	282.317	0.98563
12	13	440.254	-295.041	-347.404	191.974	0.983577
12	14	217.305	-94.9782	-273.776	155.778	0.967928
12	15	459.512	-282.925	-353.255	215.476	0.978303
12	16	183.986	-48.9544	-236.298	139.815	0.98466

Table C.1 Static tracking parameters. (continued)

Subject Number	Trial Number	B_1	T_1	B_1	T_1	R^2
13	1	183.506	-81.7668	-189.687	105.575	0.959359
13	2	248.414	-122.348	-165.45	73.5773	0.960708
13	3	204.111	-51.853	-197.201	93.9541	0.967287
13	4	290.94	-126.824	-226.598	118.243	0.972329
13	5	189.968	-60.3207	-182.294	90.2688	0.968178
13	6	226.577	-70.9769	-191.807	76.1977	0.96749
13	7	262.95	-117.707	-202.247	87.1404	0.966244
13	8	192.906	-87.7311	-178.005	97.3335	0.944555
13	9	176.088	-79.6457	-169.973	91.5482	0.937485
13	10	167.769	-33.5518	-207.762	108.657	0.952092
13	11	252.242	-135.728	-222.751	121.849	0.970086
13	12	157.556	-49.016	-142.381	60.0985	0.960098
13	13	203.797	-62.7586	-227.722	112.529	0.964102
13	14	237.564	-117.541	-287.301	175.112	0.951549
13	15	173.725	-62.6683	-169.135	88.1791	0.93862
13	16	207.413	-83.3007	-217.735	142.948	0.929659
14	1	171.827	-61.0953	-235.289	120.016	0.95988
14	2	133.815	-45.9769	-159.243	63.9758	0.932901
14	3	140.844	-63.2441	-176.606	85.3435	0.934106
14	4	169.144	-105.507	-209.072	113.288	0.931985
14	5	232.323	-112.746	-230.47	118.955	0.944004
14	6	227.969	-105.523	-325.793	221.748	0.945664
14	7	135.16	-51.6542	-177.063	86.9469	0.928587
14	8	207.39	-88.0274	-272.537	163.135	0.9644
14	9	252.005	-123.863	-278.296	169.259	0.965623
14	10	116.53	-21.8417	-211.023	143.487	0.96762
14	11	201.714	-76.8206	-314.114	220.283	0.967982
14	12	329.68	-220.526	-283.765	185.488	0.966805
14	13	185.129	-102.938	-236.751	147.694	0.942058
14	14	194.315	-101.922	-213.673	130.139	0.953759
14	15	146.39	-45.1254	-174.436	102.589	0.973394
14	16	235.978	-111.448	-271.485	178.413	0.977117

Table C.1 Static tracking parameters. (continued)

Subject Number	Trial Number	B_1	T_1	B_1	T_1	R^2
15	1	158.775	-33.8473	-156.172	67.3899	0.972513
15	2	300.214	-115.738	-255.022	129.555	0.968349
15	3	256.156	-75.7159	-246.916	126.254	0.97107
15	4	193.461	-32.4006	-170.032	75.3093	0.957922
15	5	191.965	-78.2886	-184.495	76.3302	0.957528
15	6	161.917	-34.2905	-150.553	55.3391	0.962889
15	7	309.745	-134.599	-282.697	152.976	0.969151
15	8	117.587	74.4357	-322.145	228.772	0.852542
15	9	88.9537	92.6057	-292.341	175.995	0.879201
15	10	331.431	-207.576	-260.584	169.847	0.874944
15	11	77.3132	92.4267	-245.954	182.973	0.883598
15	12	36.5375	138.968	-185.677	107.519	0.874446
15	13	96.9623	46.7931	-242.153	165.085	0.892697
15	14	59.6257	146.049	-354.631	267.375	0.903694
15	15	208.558	55.4055	-236.757	139.335	0.937925
15	16	220.25	-91.8387	-189.78	120.133	0.920135
16	1	445.325	-227.458	-346.728	207.835	0.984489
16	2	377.11	-205.01	-228.922	88.5098	0.950391
16	3	387.582	-231.299	-271.738	141.236	0.972659
16	4	548.53	-345.647	-324.299	167.081	0.985007
16	5	474.064	-269.434	-403.654	257.206	0.984713
16	6	367.484	-208.693	-244.913	112.045	0.970622
16	7	475.406	-261.969	-356.304	205.172	0.984633
16	8	251.125	-89.8706	-210.076	99.2697	0.964412
16	9	255.886	-96.4319	-273.938	172.941	0.954298
16	10	475.56	-282.891	-272.703	129.338	0.981245
16	11	379.144	-226.214	-250.568	125.881	0.940188
16	12	415.651	-219.271	-313.751	163.918	0.964067
16	13	396.966	-198.342	-354.567	219.024	0.980201
16	14	273.348	-88.1006	-247.815	114.666	0.958866
16	15	246.369	-77.9744	-233.656	104.483	0.957596
16	16	409.649	-217.972	-324.39	174.901	0.970128

Parameters for Dynamic Tracking Experiment

Table C.2 Isometric EMG-torque parameters for the dynamic tracking study

Subject Number	Biceps	Triceps	R^2
1	1917.35	-1097.79	0.928
2	1518.42	-2560.27	0983
3	4391.84	-4383.68	0.987
4	2619.09	-3884.76	0.948
5	964.27	-1417.95	0.931
6	1680.47	-1599.67	0.924
7	450.05	-412.50	0.959
8	1215.42	-2684.74	0.921

Table C.3 Length-compensation parameters for the dynamic tracking study

Subject Number	Biceps	Triceps	Biceps	Triceps	R^{2*}
1	0.2306	0.2741	-0.0587	0.9885	0.9515
2	0.4330	-0.2761	-0.4345	-0.3791	0.9653
3	0.3718	0.2495	-0.2088	-0.8239	0.9837
4	-0.6331	-2.7116	-0.4075	-0.3392	0.8764
5	0.4641	1.1081	-0.2879	0.9286	0.9506
6	1.0486	-2.2201	-0.3731	-1.5205	0.8643
7	0.1225	-0.4356	0.5896	1.5721	0.9078
8	0.1880	0.2776	0.2021	-0.0349	0.9306

Table C.4 Velocity compensation scaling factors

Subject Number	Trial Number	Biceps Velocity Parameter	Triceps Velocity Parameter	R^2
1	1	0.87361	0.14747	0.77058
1	2	0.90758	0.21141	0.72932
1	3	0.92879	0.11071	0.67362
1	4	0.80000	0.09263	0.69733
1	5	0.88593	0.20584	0.72547
1	6	0.86485	0.10301	0.73947
1	7	0.86230	0.13420	0.76659
1	8	0.82832	0.18771	0.76751
2	1	0.96039	0.96977	0.90126
2	2	0.90882	0.96908	0.85304
2	3	0.89057	0.88075	0.83468
2	4	1.08555	0.92823	0.85326
2	5	1.06448	0.95942	0.84992
2	6	0.98578	0.92664	0.92301
2	7	0.93249	0.93946	0.86093
2	8	0.98404	0.99561	0.85581
3	1	0.27229	0.37325	0.75394
3	2	0.25522	0.41702	0.74513
3	3	0.26597	0.48370	0.74711
3	4	0.37576	0.41231	0.74421
3	5	0.39516	0.38164	0.80199
3	6	0.34927	0.49707	0.82284
3	7	0.34352	0.36325	0.79594
3	8	0.35471	0.37657	0.80243
4	1	0.34327	0.14484	0.46744
4	2	0.69102	0.39538	0.36261
4	3	0.33976	0.22815	0.40264
4	4	0.16240	0.26966	0.42998
4	5	0.24711	0.17867	0.39691
4	6	0.13901	0.28753	0.40443
4	7	0.14674	0.24151	0.47868
4	8	0.05067	0.15575	0.43530

Table C.4 Velocity compensation scaling factors (continued)

Subject Number	Trial Number	Biceps Velocity Parameter	Triceps Velocity Parameter	R^2
5	1	0.28789	0.3861	0.6311
5	2	0.29626	0.43176	0.79460
5	3	0.25443	0.41071	0.69962
5	4	0.37860	0.51739	0.73995
5	5	0.21817	0.36958	0.69063
5	6	0.33552	0.58730	0.81781
5	7	0.31871	0.48723	0.7031
5	8	0.24829	0.44655	0.74350
6	1	0.84409	0.82792	0.53900
6	2	1.01839	1.20031	0.67938
6	3	1.08190	0.8963	0.88837
6	4	1.20021	0.99885	0.82426
6	5	1.08557	1.0885	0.6220
6	6	1.23736	1.1457	0.72994
6	7	0.89176	0.90629	0.63980
6	8	1.14311	1.08644	0.75342
7	1	0.92207	0.5545	0.75394
7	2	0.87350	0.58917	0.74513
7	3	0.94499	0.65531	0.74711
7	4	0.94912	0.32302	0.74421
7	5	0.70244	0.46576	0.80199
7	6	0.811	0.54140	0.82284
7	7	0.79737	0.52161	0.79594
7	8	0.92827	0.7936	0.80243
8	1	0.8127	0.33096	0.63905
8	2	0.5950	0.32664	0.67313
8	3	0.66916	0.3829	0.6910
8	4	0.98901	0.2170	0.5801
8	5	1.02056	0.26014	0.68262
8	6	0.91062	0.39934	0.60973
8	7	0.96761	0.28652	0.69120
8	8	0.97250	0.51160	0.80776

Table C.5 Pre-trial zero force readings for the second experiment.

	Subject Number							
Trial Number	1	2	3	4	5	6	7	8
1	82.0	46.3	20.2	74.4	55.7	82.9	140.6	-76.5
2	17.6	32.4	66.1	78.5	43.8	82.3	94.6	-71.4
3	16.8	20.6	55.7	84.7	63.8	72.8	93.1	-88.7
4	12.4	11.8	71.5	86.87	59.9	88.4	104.9	-91.5
5	11.0	34.6	73.5	76.25	42.0	16.3	71.3	-109.0
6	25.6	24.9	27.91	84.01	53.6	33.4	112.6	-106.7
7	24.2	16.8	103.7	70.64	58.6	48.9	98.4	-188.9
8	-3.33	32.1	62.1	33.72	44.3	13.0	90.8	-110.6

APPENDIX D

ANOVA SUMMARY TABLES

ANOVA Summary Tables for the Isometric Tracking Study

The complete ANOVA summary tables for each of the dependent measures in the isometric study is given below. The data are coded as follows.

A - Direction of exertion
B - Required Tracking Force
C - Perturbation Magnitude
D - Perturbation Frequency
E - Preview information

Table D.1 Anova summary table - PE: static experiment

Factor	SS	df	MS	F	p < F
A	87.49	1	116.59	10.5	0.006
AxS	116.39	14	8.31		
B	48.63	1	48.63	3.21	0.095
BxS	211.8	14	15.13		
C	59.75	1	59.75	7.68	0.015
CxS	108.90	14	7.78		
D	27.05	1	27.05	3.28	0.092
DxS	115.59	14	8.26		
E	1.50	1	1.50	0.18	0.674
ExS	113.98	14	8.14		
AxB	0.81	1	0.81	0.12	0.730
AxBxS	91.65	14	6.55		
AxC	11.72	1	11.72	1.46	0.247
AxCxS	112.489	14	8.04		
AxD	14.61	1	14.61	2.19	0.161
AxDxS	93.27	14	6.66		
AxE	8.84	1	8.84	0.95	0.345
AxExS	129.58	14	9.26		
BxC	22.79	1	22.79	3.78	0.071
BxCxS	90.34	14	6.02		
BxD	8.53	1	8.53	0.58	0.459
BxDxS	221.87	14	14.79		
BxE	11.35	1	11.35	1.50	0.241
BxExS	105.97	14	7.57		
CxD	170.79	1	1.55	0.13	0.727
CxDxS	170.79	14	12.20		
CxE	2.54	1	2.54	0.22	0.643
CxExS	170.59	14	11.37		
DxE	0.8	1	0.8	0.07	0.794
DxExS	170.35	14	11.36		

Table D.1 Anova summary table - PE: static experiment (continued)

Factor	SS	df	MS	F	p < F
AxBxC	1.91	1	1.91	0.64	0.438
AxBxCxS	45.21	14	3.01		
AxBxD	18.22	1	18.22	2.80	0.117
AxBxDxS	91.16	14	6.51		
AxBxE	1.82	1	1.82	0.88	0.362
AxBXExS	30.87	14	2.06		
AxCxD	4.38	1	4.38	0.41	0.532
AxCxDxS	149.33	14	10.66		
AxCxE	5.03	1	5.03	0.45	0.513
AxCxExS	156.64	14	11.19		
AxDxE	0.49	1	0.49	0.07	0.789
AxDxExS	92.10	14	6.58		
BxCxE	6.53	1	6.53	0.98	0.339
BxCxExS	93.32	14	6.67		
BxDxE	27.70	1	27.70	3.64	0.077
BxDxExS	106.41	14	7.60		
BxDxE	35.62	1	35.62	3.71	0.075
BxDxExS	134.48	14	9.61		
CxDxE	0.5	1	0.5	0.06	0.809
CxDxExS	123.98	14	8.27		
AxBxCxD	16.67	1	16.67	2.15	0.165
AxBxCxDxS	108.71	14	7.76		
AxBxCxE	4.57	1	4.57	3.34	0.089
AxBxCxExS	63.96	14	4.57		
AxCxDxE	7.04	1	7.04	0.74	0.404
AxCxDxExS	133.36	14	9.53		
AxBxDxE	11.89	1	11.89	1.73	0.209
AxBxDxExS	103.3	14	6.89		
BxCxDxE	31.04	1	31.04	1.9	0.188
BxCxDxExS	244.89	14	16.33		
AxBxCxDxE	66.61	1	66.61	9.95	
AxBxCxDxExS	100.42	14	6.69		

Table D.2 Anova summary table - CR: static experiment

Factor	SS	df	MS	F	p < F
A	43055.0	1	43055.0	50.53	0.001
AxS	1720.38	14	122.88		
B	1070.47	1	1070.47	8.71	0.011
BxS	633.39	14	45.24		
C	45.54	1	45.54	1.01	0.333
CxS	378.86	14	27.06		
D	4.55	1	4.55	0.17	0.688
DxS	197.54	14	14.11		
E	27.78	1	27.78	1.97	0.182
ExS	615.86	14	43.99		
AxB	132.5	1	132.5	3.01	0.105
AxBxS	370.37	14	26.45		
AxC	1.41	1	1.41	0.05	0.821
AxCxS	380.94	14	27.21		
AxD	40.55	1	40.55	1.49	0.242
AxDxS	171.32	14	12.24		
AxE	41.62	1	41.62	3.40	0.086
AxExS	800.75	14	57.2		
BxC	12.10	1	12.10	0.21	0.653
BxCxS	348.32	14	24.88		
BxD	71.46	1	71.46	2.87	0.112
BxDxS	295.86	14	21.13		
BxE	15.31	1	15.31	0.72	0.409
BxExS	265.86	14	18.94		
CxD	12.89	1	12.89	0.68	0.423
CxDxS	265.19	14	29.70		
CxE	4.91	1	4.91	0.17	0.690
CxExS	415.76	14	99.04		
DxE	10.95	1	10.95	0.11	0.744
DxExS	1386.54	14	34.14		

Table D.2 Anova summary table - CR: static experiment (continued)

Factor	SS	df	MS	F	p < F
AxBxC	10.19	1	10.19	0.30	0.593
AxBxCxS	1386.54	14	29.57		
AxBxD	33.64	1	33.64	1.14	0.304
AxBxDxS	477.98	14	13.83		
AxBxE	7.80	1	7.80	0.49	0.494
AxBXExS	414.05	14	16.78		
AxCxD	34.03	1	34.03	2.03	0.176
AxCxDxS	221.61	14	15.56		
AxCxE	1.03	1	1.03	0.07	0.801
AxCxExS	234.87	14	33.22		
AxDxE	217.83	1	111.22	3.35	0.089
AxDxExS	465.08	14	32.99		
BxCxE	008	1	0.08	00	0.963
BxCxExS	461.83	14	25.77		
BxDxE	0.06	1	0.06	00	0962
BxDxExS	360.78	14	25.77		
BxDxE	12.52	1	12.52	1.19	0293
BxDxExS	146.69	14	10.48		
CxDxE	40.48	1	40.48	1.58	0.229
CxDxExS	357.66	14	25.55		
AxBxCxD	46.33	1	46.33	1.16	0.299
AxBxCxDxS	557.4	14	39.81		
AxBxCxE	5.46	1	5.46	0.35	0.563
AxBxCxExS	217.34	14	15.52		
AxCxDxE	0.01	1	0.01	00	0.983
AxCxDxExS	256.10	14	18.29		
AxBxDxE	17.91	1	17.91	0.70	0.416
AxBxDxExS	356.68	14	25.48		
BxCxDxE	0.93	1	0.93	0.03	0.862
BxCxDxExS	416.67	14	29.76		
AxBxCxDxE	8.20	1	8.20	0.45	0.513
AxBxCxDxExS	254.72	14	18.19		

Table D.3 Anova summary table - AAF: static experiment

Factor	SS	df	MS	F	p < F
A	9277.13	1	9277.13	27.42	0.001
AxS	4736.99	14	338.36		
B	134.62	1	134.62	5.32	0.037
BxS	354.25	14	354.25		
C	84.90	1	84.90	.95	.347
CxS	1253.87	14	89.56		
D	7.83	1	7.83	0.15	0.704
DxS	726.29	14	51.88		
E	41.31	1	41.31	1.31	0.272
ExS	443.10	14	31.65		
AxB	103.09	1	103.09	1.08	0.316
AxBxS	1331.75	14	95.12		
AxC	78.05	1	78.05	1.73	0.210
AxCxS	631.63	14	45.12		
AxD	94.93	1	94.93	3.27	0.092
AxDxS	406.63	14	29.05		
AxE	64.05	1	64.05	3.19	0.096
AxExS	280.87	14	20.06		
BxC	0.82	1	0.82	0.01	0.907
BxCxS	822.64	14	58.76		
BxD	137.89	1	137.89	2.35	0.147
BxDxS	820.02	14	58.57		
BxE	0.18	1	0.18	0.01	0.942
BxExS	475.66	14	33.98		
CxD	0.12	1	0.12	0.01	0.944
CxDxS	319.31	14	22.81		
CxE	4.79	1	4.79	0.31	0.586
CxExS	215.87	14	15.42		
DxE	9.92	1	9.92	0.62	0.446
DxExS	225.82	14	16.13		

Table D.4 Anova summary table - AAF: static experiment (continued)

Factor	SS	df	MS	F	p < F
AxBxC	50.25	1	50.25	1.46	0.247
AxBxCxS	482.02	14	34.43		
AxBxD	18.08	1	18.08	0.56	0.467
AxBxDxS	452.37	14	32.31		
AxBxE	8.18	1	8.18	0.41	0.535
AxBXExS	282.43	14	20.17		
AxCxD	83.87	1	83.87	3.15	0.098
AxCxDxS	372.62	14	26.62		
AxCxE	1.21	1	1.21	0.19	0.672
AxCxExS	90.46	14	6.46		
AxDxE	18.60	1	18.60	2.00	0.179
AxDxExS	130.05	14	9.29		
BxCxE	159.35	1	159.35	7.71	0.15
BxCxExS	289.28	14	20.66		
BxDxE	1.44	1	1.44	0.06	0.805
BxDxExS	319.93	14	22.85		
BxDxE	7.45	1	7.45	0.36	0.556
BxDxExS	286.54	14	20.47		
CxDxE	24.96	1	24.96	0.97	0.342
CxDxExS	361.28	14	25.81		
AxBxCxD	75.72	1	75.72	2.81	0.116
AxBxCxDxS	377.89	14	26.99		
AxBxCxE	1.01	1	1.01	0.18	0.679
AxBxCxExS	78.97	14	5.64		
AxCxDxE	0.20	1	0.20	0.02	0.899
AxCxDxExS	170.29	14	12.16		
AxBxDxE	52.94	1	52.94	1.95	0.185
AxBxDxExS	380.91	14	27.21		
BxCxDxE	27.20	1	27.20	0.73	0.408
BxCxDxExS	522.92	14	37.35		
AxBxCxDxE	25.23	1	25.23	1.11	0.310
AxBxCxDxExS	318.89	14	22.78		

ANOVA Summary Tables for the Dynamic Tracking Study

The complete ANOVA summary tables for each of the dependent measures are given below. The data are coded as follows.

A - Direction of exertion
B - Perturbation Magnitude
C - Preview information
D - Perturbation Frequency

Table D.4 Anova summary table - PE: dynamic experiment

Factor	SS	df	MS	F	p < F
A	136.19	1	136.19	2.06	0.194
AxS	461.93	7	65.99		
B	334.61	1	334.61	7.08	0.032
BxS	330.77	7	47.25		
C	206.7	1	206.7	1.43	0.270
CxS	1009.46	7	144.21		
D	267.88	1	267.88	5.76	0.047
DxS	325.59	7	46.51		
E	39.63	1	39.63	0.96	0.359
ExS	288.51	7	41.22		
AxB	7.44	1	7.44	0.12	0.735
AxBxS	418.94	7	59.85		
AxC	14.77	1	7.77	3.64	0.098
AxCxS	28.44	7	4.06		
AxD	191.06	1	191.06	1.73	0.230
AxDxS	774.48	7	110.64		
BxC	429.42	1	429.42	4.62	0.069
BxCxS	651.07	7	93.01		
BxD	16.44	1	16.44	0.24	0.640
BxDxS	482.29	7	68.90		
CxD	85.69	1	85.69	2.56	0.154
CxDxS	234.44	7	33.49		
AxBxC	30.19	1	30.19	0.76	0.412
AxBxCxS	278.04	7	39.72		
AxBxD	4.05	1	4.05	0.13	0.725
AxBxDxS	210.70	7	30.10		
AxCxD	280.18	1	280.18	2.11	0.189
AxCxDxS	928.44	7	132.63		
BxCxD	120.49	1	120.49	3.04	0.125
BxCxDxS	277.26	7	39.63		

Table D.5 Anova summary table - CR: dynamic experiment

Factor	SS	df	MS	F	p < F
A	181.94	1	181.94	0.70	0.436
AxS	1568.75	6			
B	713.29	1	713.29	7.93	0.031
BxS	539.94	6			
C	20.88	1	20.88	0.50	0.506
CxS	250.14	6			
D	99.95	1	99.95	1.55	0.260
DxS	387.05	6			
AxB	6.60	1	6.60	0.07	0.794
AxBxS	531.8	6			
AxC	29.65	1	29.65	0.13	0.729
AxCxS	1346.71	6			
AxD	3.28	1	3.28	0.02	0.886
AxDxS	886.31	6			
BxC	1.41	1	1.41	0.04	0.852
BxCxS	223.47	6			
BxD	104.69	1	104.69	0.75	0.420
BxDxS	839.53	6			
CxD	42.88	1	42.88	0.58	0.476
CxDxS	445.07	6			
AxBxC	40.57	1	40.57	0.17	0.695
AxBxCxS	1433.46	6			
AxBxD	250.16	1	250.16	0.62	0.462
AxBxDxS	2435.06	6			
AxCxD	0.10	1	0.10	0.01	0.987
AxCxDxS	1914.99	6			
BxCxD	66.59	1	66.59	1.30	0.298
BxCxDxS	768.81	6			
BxCxD	0.01	1	0.01	0.01	0.994
BxCxDxS		6			

Table D.6 Anova summary table - AAF: dynamic experiment

Factor	SS	df	MS	F	p < F
A	1.18	1	1.18	0.3	0.606
AxS	23.87	6	3.98		
B	3.48	1	3.48	1.29	0.3
BxS	16.23	6	2.7		
C	0.02	1	0.02	0.04	0.857
CxS	3.5	6	0.58		
D	0.33	1	0.33	0.26	0.63
DxS	7.79	6	1.3		
AxB	1.6	1	1.6	3.3	0.119
AxBxS	2.91	6	0.49		
AxC	0.56	1	0.56	0.32	0.59
AxCxS	10.4	6	1.73		
AxD	0.03	1	0.03	0.04	0.843
AxDxS	4.57	6	0.76		
BxC	0.66	1	0.66	0.57	0.479
BxCxS	6.91	6	1.15		
BxD	0.38	1	0.38	0.78	0.411
BxDxS	2.92	6	0.49		
CxD	1.2	1	1.2	0.55	0.486
CxDxS	13.14	6	2.19		
AxBxC	1.14	1	1.14	0.47	0.518
AxBxCxS	14.54	6	2.42		
AxBxD	0.02	1	0.02	0.15	0.711
AxBxDxS	0.68	6	0.11		
AxCxD	1.85	1	1.85	5.23	0.062
AxCxDxS	2.13	6	0.35		
BxCxD	0.49	1	0.49	0.44	0.53
BxCxDxS	6.64	6	1.11		
BxCxD	0.64	1	0.64	0.5	0.508
BxCxDxS	7.7	6	1.28		

APPENDIX E

Informed Consent for Participants of Investigative Projects

Title of Project: The Effects of Perturbation Frequency, Magnitude, and Uncertainty on the Estimated Level of Muscle Co-Contraction During Static and Dynamic Tracking

Principal Investigator: Jerry P. Purswell

I. THE PURPOSE OF THIS RESEARCH/PROJECT

You are invited to participate in a study about position tracking of a target in the presence of perturbations. You will track a green circle on a computer screen which moves horizontally by moving a lever arm. When you rotate the arm, the yellow circle will move in the direction of the corresponding direction. You will be presented with two practice trials to familiarize you with the experiment.

At random intervals *within* each trial the lever arm will momentarily require more force to move it. The intended effect is to simulate what it might be like if you were to try to track an actual moving object with your forearm while your arm was periodically bumped. The frequency and magnitude of these "simulated perturbations" will vary across trials. On some trials you will be shown in advance what levels of each variable will be used and on others you will not be given any advance information.

The electrical activity of your upper arm muscles will be monitored during the task so that we can observe how and when you activate your arm muscles.

We are researching how accurately you can track the target in the presence of the simulated perturbations and what effect changing the magnitude and frequency of the simulated perturbations has on the tracking performance and on the way in which you activate your muscles. We are also interested in determining if changes in the tracking gain changes your tracking performance. Finally we are also interested in determining if you can use information about

these other variables to reduce your tracking error or if it changes the way you activate your muscles. This study involves seven subjects in addition to yourself.

II. PROCEDURES

The procedures to be used in this research are tracking an icon on a computer screen by rotating a lever arm. The time required to complete this experiment is approximately three hours. The possible risks and discomfort are fatigued upper arm and shoulder muscles. Safeguards that will be used to minimize your risk or discomfort are one minute rest periods between each thirty-second trial.

III. BENEFITS OF THIS PROJECT

Your participation in this project will provide the following information that may be helpful. The results of this study will indicate how a person activates his muscles during a position tracking task.

IV. EXTENT OF ANONYMITY AND CONFIDENTIALITY

The results of this study will be kept strictly confidential. At no time will the researchers release the results of the study to anyone other than the individuals working on the project without your written consent. The information you provide will have your name removed and only a subject number will identify you during analyses and any written reports of the research.

V. COMPENSATION

For participate in this project you will receive $5.00 for each hour completed for a total of $15.00

VI. FREEDOM TO WITHDRAW

You are free to withdraw from this study at any time without penalty. If you choose to withdraw, you will be compensated for the portion of the time you participated in the study.

There may be the following circumstances under which the investigator may determine that you should not continue as a subject of this project: error in the functioning of the computerized data collection system. You will be compensated for the portion of the project completed.

VII. APPROVAL OF RESEARCH

This research project has been approved, as required, by the Institutional Review Board for projects involving human subjects at Virginia Polytechnic and State University, by the Department of Industrial and Systems Engineering.

VIII. SUBJECT'S RESPONSIBILITIES

I know of no reason I cannot participate in this study.

_____

Signature

IX. SUBJECT'S PERMISSION

I have read and understand the informed consent and conditions of this project. I have had all my questions answered. I hereby acknowledge the above and give my voluntary consent for participation in this project.

If I participate, I may withdraw at anytime without penalty. I agree to abide by the rules of this project.

Should I have any questions about this research or its conduct, I will contact:

Jerry P. Purswell Graduate Student	(703) 231-5359 Phone
Dr. Jeffrey Woldstad Faculty Advisor	(703) 231-4927 Phone
Earnest R. Stout Chair, IRB Research Division	(703) 231-9359 Phone

Tracking Task Instructions

Thank you for participating in this experiment. In the first part of the experiment the amount of subcutaneous body fat on your upper right arm will be measured using spreading calipers. The experimenter will then prepare your upper arm for electrode placement by rubbing it with an cotton swab soaked with alcohol. One electrode array will then be placed over your biceps brachii and another will be placed over your triceps. These electrode arrays will then be used to monitor the electrical activity of your muscles during the trials. The design of the EMG arrays is such that there is no way current flow can be reversed. Consequently, there is no possibility of an electric shock.

The experimenter will then seat you in the apparatus. Your torso position will be held fixed with straps around your chest. You will place your forearm in the wrist cuff. The experimenter will then perform calibrations of the equipment. As a part of the calibration you will be asked to perform a maximum voluntary contraction (MVC) in flexion (i.e. toward your left). You will also be asked to perform a maximum voluntary contraction in extension (i.e. toward your right).

Following the calibration of the equipment you will be asked to perform 12 tracking trials. The first two will be practice trials which will illustrate the different levels of tracking gain, perturbation frequency, perturbation magnitude, and perturbation direction. You will then be asked to perform two tracking trials without perturbations present. You will then perform 8 test trials. You will then perform two additional trials without perturbations. During each trial you should track the target (the green circle) as closely as possible. Do this by applying force to the wrist cuff to displace the yellow circle to the left or the right. You will be given a one minute rest period between each trial. We are interested in how information about the tracking task may affect the way in which your arm muscles are controlled. Consequently, on some trials you will be presented with information about the levels of the different variables but on others you will not receive any preview of the trial.

Thank you for your participation in this study. If you have any questions please ask the experimenter now.

Experimental Protocol and Justification

Justification of the Project

The purpose of this project is test the hypothesis that antagonistic muscle co-contraction about the elbow during a static tracking task can be quantitatively predicted from perturbation magnitude, perturbation frequency, tracking gain, and task uncertainty. Antagonistic co-contraction is a situation in which muscles on opposite sides of a joint are active at the same time. The torque contributions of the opposing muscles cancel each other but a metabolic cost is incurred. Consequently, antagonistic co-contraction is assumed absent in many optimization-based models of the lower back. However, electromyographic recordings often indicate that opposing muscles are indeed active. Previous authors have shown that if antagonistic co-contraction is present when it is assumed absent, the muscle force of the agonist and the spinal compression are seriously underestimated. The problem then is to determine why antagonistic activity occurs and how to obtain a reasonable estimate what the antagonistic co-contraction might be. It is hypothesized that certain task characteristics affect the level of antagonistic activity observed. Antagonism around the elbow rather than at the lower back is studied because of the difficulty in quantitatively estimating muscle forces at the lower back.

The object of the current study is to quantitatively predict the level of estimated co-contraction from task characteristics. If the current study is successful, we will find what a reasonable estimate of antagonistic co-contraction is for a given set of task characteristics.

Procedures

Eight male subjects between the ages of 19 and 40 will be recruited for the study. Only subjects whose dominant hand is their right hand will be used. Each subject will be seated and then will place his right wrist in a U-shaped wrist cuff. The elbow will rest on a padded fixture. The position of the subject's torso will be fixed by velcro-secured straps at the waist and the chest. Nothing in the posture constraint system will prevent the subject from releasing himself.

A measure of subcutaneous body fat on the upper arm will be taken using standard anthropometric equipment. Electrode arrays will then be placed over the biceps brachii and the triceps to monitor each muscle's electrical activity.

Each subject will perform twenty-two four-second trials in which he will be asked to exert force in flexion and then in extension. One of these trials will be a maximum voluntary contraction (MVC) in flexion and one will be an MVC exertion in extension. The remaining trials will be submaximal exertions The subjects will then perform a series of twelve tracking trials. Each trial will last 32.6 seconds and then a rest period of three minutes will be observed.

Risks and Benefits

One potential risk to the subject is muscle fatigue of the upper arm. The risk of muscle fatigue has been addressed by providing rest periods between each trial. A second possibility is that some failure of the EMG amplifier could cause current to be applied to the electrodes on arm. This risk has been eliminated by incorporating diodes in the amplifier circuitry. These diodes prevent current from flowing to the person.

There is no particular benefit to the subject (aside from the monetary compensation) for his participation.

Confidentiality and Anonymity

Each subject will be assigned a subject number when he arrives. All data collected will be identified only by subject number. There will be no means of associating the subject with his data subsequent to the data collection.

Informed Consent - Dynamic Experiment

Informed Consent for Participants of Investigative Projects

Title of Project: The Effects of Perturbation Frequency, Magnitude, and Uncertainty on the Estimated Level of Muscle Co-Contraction During Static and Dynamic Tracking

Principal Investigator: Jerry P. Purswell

I. THE PURPOSE OF THIS RESEARCH/PROJECT

You are invited to participate in a study about position tracking of a target in the presence of perturbations. You will track a green circle on a computer screen which moves horizontally by moving a lever arm. When you rotate the arm, the yellow circle will move in the direction of the corresponding direction. You will be presented with two practice trials to familiarize you with the experiment.

At random intervals *within* each trial the lever arm will momentarily require more force to move it. The intended effect is to simulate what it might be like if you were to try to track an actual moving object with your forearm while your arm was periodically bumped. The frequency and magnitude of these "simulated perturbations" will vary across trials. On some trials you will be shown in advance what levels of each variable will be used and on others you will not be given any advance information.

The electrical activity of your upper arm muscles will be monitored during the task so that we can observe how and when you activate your arm muscles.

We are researching how accurately you can track the target in the presence of the simulated perturbations and what effect changing the magnitude and frequency of the simulated perturbations has on the tracking performance and on the way in which you activate your muscles. We are also interested in determining if changes in the tracking gain changes your tracking performance. Finally we are also interested in determining if you can use information about

these other variables to reduce your tracking error or if it changes the way you activate your muscles. This study involves seven subjects in addition to yourself.

II. PROCEDURES

The procedures to be used in this research are tracking an icon on a computer screen by rotating a lever arm. The time required to complete this experiment is approximately three hours. The possible risks and discomfort are fatigued upper arm and shoulder muscles. Safeguards that will be used to minimize your risk or discomfort are one minute rest periods between each thirty-second trial.

III. BENEFITS OF THIS PROJECT

Your participation in this project will provide the following information that may be helpful. The results of this study will indicate how a person activates his muscles during a position tracking task.

IV. EXTENT OF ANONYMITY AND CONFIDENTIALITY

The results of this study will be kept strictly confidential. At no time will the researchers release the results of the study to anyone other than the individuals working on the project without your written consent. The information you provide will have your name removed and only a subject number will identify you during analyses and any written reports of the research.

V. COMPENSATION

For participate in this project you will receive $5.00 for each hour completed for a total of $15.00

VI. FREEDOM TO WITHDRAW

You are free to withdraw from this study at any time without penalty. If you choose to withdraw, you will be compensated for the portion of the time you participated in the study.

There may be the following circumstances under which the investigator may determine that you should not continue as a subject of this project: error in the functioning of the computerized data collection system. You will be compensated for the portion of the project completed.

VII. APPROVAL OF RESEARCH

This research project has been approved, as required, by the Institutional Review Board for projects involving human subjects at Virginia Polytechnic and State University, by the Department of Industrial and Systems Engineering.

VIII. SUBJECT'S RESPONSIBILITIES

I know of no reason I cannot participate in this study.

_____

Signature

IX. SUBJECT'S PERMISSION

I have read and understand the informed consent and conditions of this project. I have had all my questions answered. I hereby acknowledge the above and give my voluntary consent for participation in this project.

If I participate, I may withdraw at anytime without penalty. I agree to abide by the rules of this project.

Should I have any questions about this research or its conduct, I will contact:

Jerry P. Purswell Graduate Student	(703) 231-5359 Phone
Dr. Jeffrey Woldstad Faculty Advisor	(703) 231-4927 Phone
Earnest R. Stout Chair, IRB Research Division	(703) 231-9359 Phone

Tracking Task Instructions -Dynamic Experiment

Thank you for participating in this experiment. In the first part of the experiment the amount of subcutaneous body fat on your upper right arm will be measured using spreading calipers. The experimenter will then prepare your upper arm for electrode placement by rubbing it with an cotton swab soaked with alcohol. One electrode array will then be placed over your biceps brachii and another will be placed over your triceps. These electrode arrays will then be used to monitor the electrical activity of your muscles during the trials. The design of the EMG arrays is such that there is no way current flow can be reversed. Consequently, there is no possibility of an electric shock.

The experimenter will then seat you in the apparatus. Your torso position will be held fixed with straps around your chest. You will place your forearm in the wrist cuff. The experimenter will then perform calibrations of the equipment. As a part of the calibration you will be asked to perform a maximum voluntary contraction (MVC) in flexion (i.e. toward your left). You will also be asked to perform a maximum voluntary contraction in extension (i.e. toward your right).

Following the calibration of the equipment you will be asked to perform 12 tracking trials. The first two will be practice trials which will illustrate the different levels of tracking gain, perturbation frequency, perturbation magnitude, and perturbation direction. You will then be asked to perform two tracking trials without perturbations present. You will then perform 8 test trials. You will then perform two additional trials without perturbations. During each trial you should track the target (the green circle) as closely as possible. Do this by applying force to the wrist cuff to displace the yellow circle to the left or the right. You will be given a one minute rest period between each trial. We are interested in how information about the tracking task may affect the way in which your arm muscles are controlled. Consequently, on some trials you will be presented with information about the levels of the different variables but on others you will not receive any preview of the trial.

Thank you for your participation in this study. If you have any questions please ask the experimenter now.

Experimental Protocol and Justification

Justification of the Project

The purpose of this project is test the hypothesis that antagonistic muscle co-contraction about the elbow during a static tracking task can be quantitatively predicted from perturbation magnitude, perturbation frequency, tracking gain, and task uncertainty. Antagonistic co-contraction is a situation in which muscles on opposite sides of a joint are active at the same time. The torque contributions of the opposing muscles cancel each other but a metabolic cost is incurred. Consequently, antagonistic co-contraction is assumed absent in many optimization-based models of the lower back. However, electromyographic recordings often indicate that opposing muscles are indeed active. Previous authors have shown that if antagonistic co-contraction is present when it is assumed absent, the muscle force of the agonist and the spinal compression are seriously underestimated. The problem then is to determine why antagonistic activity occurs and how to obtain a reasonable estimate what the antagonistic co-contraction might be. It is hypothesized that certain task characteristics affect the level of antagonistic activity observed. Antagonism around the elbow rather than at the lower back is studied because of the difficulty in quantitatively estimating muscle forces at the lower back.

The object of the current study is to quantitatively predict the level of estimated co-contraction from task characteristics. If the current study is successful, we will find what a reasonable estimate of antagonistic co-contraction is for a given set of task characteristics.

Procedures

Eight male subjects between the ages of 19 and 40 will be recruited for the study. Only subjects whose dominant hand is their right hand will be used. Each subject will be seated and then will place his right wrist in a U-shaped wrist cuff. The elbow will rest on a padded fixture. The position of the subject's torso will be fixed by velcro-secured straps at the waist and the chest. Nothing in the posture constraint system will prevent the subject from releasing himself.

A measure of subcutaneous body fat on the upper arm will be taken using standard anthropometric equipment. Electrode arrays will then be placed over the biceps brachii and the triceps to monitor each muscle's electrical activity.

Each subject will perform twenty-two four-second trials in which he will be asked to exert force in flexion and then in extension. One of these trials will be a maximum voluntary contraction (MVC) in flexion and one will be an MVC exertion in extension. The remaining trials will be submaximal exertions The subjects will then perform a series of twelve tracking trials. Each trial will last 32.6 seconds and then a rest period of three minutes will be observed.

Risks and Benefits

One potential risk to the subject is muscle fatigue of the upper arm. The risk of muscle fatigue has been addressed by providing rest periods between each trial. A second possibility is that some failure of the EMG amplifier could cause current to be applied to the electrodes on arm. This risk has been eliminated by incorporating diodes in the amplifier circuitry. These diodes prevent current from flowing to the person.

There is no particular benefit to the subject (aside from the monetary compensation) for his participation.

Confidentiality and Anonymity

Each subject will be assigned a subject number when he arrives. All data collected will be identified only by subject number. There will be no means of associating the subject with his data subsequent to the data collection.

VITA

Jerry P. Purswell was born August 11, 1964 in Dallas Texas. He received a B.S. in Chemistry and Biology from Oklahoma Baptist University in 1986. He completed an M.S. in Industrial Engineering in 1989 from the University of Oklahoma. While working in the Industrial Ergonomics laboratory at Virginia Tech, he conducted research on finger strength in typing and tapping motions. He also performed an ergonomic and safety analysis of the activities of the trackmen for the Association of American Railroads.
He is a member of the Institute of Industrial Engineers and Alpha Pi Mu, the National Industrial Engineering Honor Society. He is a also member of the Human Factors and Ergonomics Society and currently serves as one of the editors for Safety News, the newsletter of the Safety Technical Group of the Human Factors and Ergonomics Society. He is currently employed by Purswell and Associates, an ergonomics and safety consulting firm.

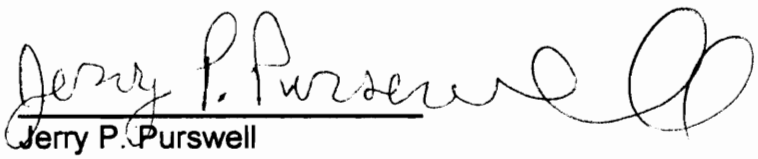

Jerry P. Purswell